

POLYMERIC SCAFFOLDS FOR BIOACTIVE AGENT DELIVERY  
IN BONE TISSUE ENGINEERING

A THESIS SUBMITTED TO  
THE GRADUATE SCHOOL OF NATURAL AND APPLIED SCIENCES  
OF  
MIDDLE EAST TECHNICAL UNIVERSITY

BY

ŞENİZ UÇAR

IN PARTIAL FULFILLMENT OF THE REQUIREMENTS  
FOR  
THE DEGREE OF MASTER OF SCIENCE  
IN  
CHEMISTRY

OCTOBER 2012

Approval of the thesis:

**POLYMERIC SCAFFOLDS FOR BIOACTIVE AGENT DELIVERY  
IN BONE TISSUE ENGINEERING**

submitted by **ŞENİZ UÇAR** in partial fulfillment of the requirements for the degree of **Master of Science in Chemistry Department, Middle East Technical University** by,

Prof. Dr. Canan Özgen  
Dean, Graduate School of **Natural and Applied Sciences**

Prof. Dr. İlker Özkan  
Head of Department, **Chemistry**

Prof. Dr. Nesrin Hasırcı  
Supervisor, **Chemistry Dept., METU**

Assist. Prof. Dr. Pınar Yılgör  
Co-Supervisor, **Biomedical Eng. Dept., Çukurova Uni.**

**Examining Committee Members:**

Prof. Dr. Serpil Aksoy  
Chemistry Dept., Gazi University

Prof. Dr. Nesrin Hasırcı  
Chemistry Dept., METU

Prof. Dr. Teoman Tinçer  
Chemistry Dept., METU

Prof. Dr. Erdal Bayramlı  
Chemistry Dept., METU

Prof. Dr. Levent Toppare  
Chemistry Dept., METU

**Date:** 05.10.2012

**I hereby declare that all information in this document has been obtained and presented in accordance with academic rules and ethical conduct. I also declare that, as required by these rules and conduct, I have fully cited and referenced all material and results that are not original to this work.**

Name, Last name: Şeniz Uçar

Signature:

## **ABSTRACT**

# **POLYMERIC SCAFFOLDS FOR BIOACTIVE AGENT DELIVERY IN BONE TISSUE ENGINEERING**

Uçar, Şeniz

M.Sc., Department of Chemistry

Supervisor : Prof. Dr. Nesrin Hasırcı

Co-Supervisor: Assist. Prof. Dr. Pınar Yılğör

October 2012, 139 pages

Tissue engineering is a multidisciplinary field that is rapidly emerging as a promising new approach in the restoration and reconstruction of tissues. In this approach, three dimensional (3D) scaffolds are of great importance. Scaffolds function both as supports for cell growth and depot for sustained release of required active agents (e.g. enzymes, genes, antibiotics, growth factors). Scaffolds should possess certain properties in accordance with usage conditions. Wet-spinning is a simple technique that has been widely used for the fabrication of porous scaffolds for tissue engineering applications. Natural polymers can effectively be used in scaffold fabrication due to their biocharacteristics. Among natural polymers, chitosan and alginate are two of the most studied ones in tissue engineering and drug delivery fields because of being biologically renewable, biodegradable, biocompatible, non-

antigenic, non-toxic and biofunctional. In this study, two kinds of porous scaffolds were produced as chitosan and alginate coated chitosan fibrous scaffolds by wet-spinning technique. In order to investigate the delivery characteristics of the scaffolds, loading of gentamicin as a model antibiotic and bovine serum albumin (BSA) as a model protein was carried out in different loading models. Resultant scaffolds were characterized in terms of their structural formation, biodegradation, biomineralization, water uptake and retention ability and mechanical properties. Additionally, release kinetics of gentamicin and BSA were examined. Efficiency of gentamicin on *Escherichia coli* (E.coli) was examined. Characterization of scaffolds revealed their adequacy to be used in bone tissue engineering applications and capability to be employed as bioactive agent delivery systems.

**Keywords:** Bone Tissue Engineering, Scaffolds, Wet Spinning, Bioactive Agent Delivery.

## ÖZ

# KEMİK DOKU MÜHENDİSLİĞİNDE BİYOAKTİF MADDE SAĞLAYAN POLİMER YAPI İSKELELERİ

Uçar, Şeniz

Yüksek Lisans, Kimya Bölümü

Tez Yöneticisi : Prof. Dr. Nesrin Hasırcı

Ortak Tez Yöneticisi :Yar. Doç. Dr. Pınar Yılgör

Ekim 2012, 139 sayfa

Doku mühendisliği, dokuların yenilenmesi ve yeniden yapılanması konusunda umut vadeden bir yaklaşım sunan, çok disiplinli bir alandır. Bu yaklaşımda üç boyutlu yapı iskeleleri büyük önem taşır. Yapı iskeleleri hücrelerin büyümesi için destek ve gerekli aktif maddelerin (örneğin, enzimler, genler, antibiyotikler ve büyüme faktörleri) salımı için depo görevi görür. İskele yapıların, kullanım şartlarına göre bir takım özellikler taşıması gerekir. Islak döndürme, doku mühendisliğine yönelik gözenekli yapı iskelelerinin oluşturulmasında kullanılan bir yöntemdir. Doğal polimerler biyolojik özelliklerinden dolayı iskele yapımında sıklıkla kullanılır. Bunlar arasında kitosan ve aljinat, biyolojik olarak yenilenebilirlik, biyobozunurluk, biyoyumluluk, antijenik ve toksik olmayan biyoişlevsel özelliklerinden dolayı doku mühendisliğinde ve ilaç salımı alanında sıklıkla çalışılan

dođal polimerlerden ikisidir. Bu alıřmada, ıslak dndrme tekniđi kullanılarak gzenekli fiber kitosan ve aljinat kaplı fiber kitosan yapı iskeleleri retilmiřtir. Yapı iskelelerinin salım zelliklerini incelemek iin iskelelere model antibiyotik olarak gentamisin ve model protein olarak sıđır serumu albmini (BSA) deđiřik ykleme modelleri ile eklenmiřtir. Elde edilen yapı iskeleleri yapısal oluřumları, biyobozunurlukları, biyomineralleřmeleri, su alma ve tutma yeterlikleri ve mekanik zellikleri bakımlarından incelenmiřtir. Ayrıca, gentamisin ve BSA iin salım kinetikleri alıřılmıřtır. Salınan gentamisinin Escherichia coli (E.coli) zerindeki etkinliđi arařtırılmıřtır. İncelenen yapı iskelelerinin kemik doku mhendisliđine ynelik kullanımlar iin uygun olduđu ve biyoaktif madde salımı amacıyla da kullanılabilecekleri grlmřtir.

**Anahtar Kelimeler:** Kemik Doku Mhendisliđi, Yapı İskeleleri, Islak Dndrme, Biyoaktif Madde Sađlanması

*Dedicated to my family...*

## ACKNOWLEDGEMENTS

I would like to express my special thanks to my supervisor Prof. Dr. Nesrin Hasırcı for her continuous guidance and support throughout my thesis. I am grateful for the time and effort she has spent to improve my scientific experience during my graduate years.

I am thankful to my co-supervisor Assist. Prof. Dr. Pınar Yılgör for her helps and Prof. Dr. Vasıf Hasırcı for the guidance he has provided in my experiments. I would like to express my special gratitude to Dr. Aysel Kızıltay for her continuous help, support and motivation throughout my graduate studies. I was very fortunate to have her as an accessible source of knowledge and experienced coworker.

I wish to express my appreciation to my dear lab mates Tuğba Endođan, Aysun Güney, Filiz Kara, Özge Özgen, Ümran Aydemir, Gülçin Çiçek and Shahla Bagheri for the fun and friendly environment, continuous support and valuable coffee times. I am also thankful to Aysu Küçükturhan for her kind helps in my experiments and our worth to remember brain storming meetings.

I would like to thank to my tatami friends, especially to Köksal Muş and Cavid Musayev, for their endless patience and precious friendship. Also, I am deeply grateful to the ‘oldies but goldies’, ‘girls and Gökhan’ and ‘my ecury’ for simply always being there.

TUBITAK is gratefully acknowledged for the financial support throughout my graduate studies.

Last but not least, I would like to express my deepest appreciation to my family for their splendid love, care, courage, support and guidance throughout my entire life.

# TABLE OF CONTENTS

ABSTRACT.....	iv
ÖZ .....	vi
ACKNOWLEDGEMENTS .....	ix
TABLE OF CONTENTS.....	x
LIST OF TABLES .....	xiii
LIST OF FIGURES .....	xiv
LIST OF ABBREVIATIONS .....	xix
CHAPTERS .....	1
1. INTRODUCTION .....	1
1.1. Bone.....	1
1.1.1. Bone Structure .....	1
1.1.2. Bone Repair .....	7
1.2. Approaches in Bone Repair and Regeneration.....	8
1.3. Bone Tissue Engineering.....	11
1.3.1. Scaffolds in Bone Tissue Engineering.....	12
1.3.1.1. Materials Used in Scaffold Production .....	16
1.3.1.1.1. Chitosan.....	26
1.3.1.1.2. Alginate .....	29
1.3.1.2. Methods Used in Scaffold Production .....	32
1.3.1.2.1. A Comprehensive Technique for Scaffold Production: Wet Spinning.....	37

1.3.2. Controlled Delivery of Bioactive Agents in Bone Tissue Engineering ....	39
1.3.2.1. Antibiotic Delivery in Bone Tissue Engineering .....	43
1.3.2.2. Protein Delivery in Bone Tissue Engineering.....	45
1.4. Aim, Novelty and Approach of the Thesis .....	47
2. MATERIALS AND METHODS .....	49
2.1. Materials .....	49
2.2. Methods .....	50
2.2.1. Preparation of Scaffolds.....	50
2.2.1.1. Production of Fibrous Chitosan Scaffolds by Wet Spinning .....	50
2.2.1.2. Alginate Coated Fibrous Chitosan Scaffolds .....	51
2.2.2. Structural Characterization of Scaffolds.....	52
2.2.2.1. Determination of Fiber Thickness.....	52
2.2.2.2. Structure Analysis of Coated Scaffolds .....	52
2.2.3. Water Uptake and Retention Capacities of Scaffolds.....	53
2.2.4. Degradation of Scaffolds .....	53
2.2.5. Determination of Bioactivity .....	54
2.2.6. Mechanical Analysis of Scaffolds .....	55
2.2.7. Release Studies .....	56
2.2.7.1. BSA Release from Scaffolds.....	56
2.2.7.2. Gentamicin Release from Scaffolds.....	59
2.2.7.3. Antibacterial Tests .....	61
3. RESULTS AND DISCUSSION .....	62
3.1. Preparation of Scaffolds .....	62
3.2. Characterization of Scaffold Properties.....	64
3.2.1. Structural Characterization .....	64

3.2.2. Water Uptake and Retention Capacities of Scaffolds.....	69
3.2.3. Degradation Behavior of Scaffolds.....	73
3.2.4. Determination of Bioactivity .....	77
3.2.5. Mechanical Properties.....	84
3.3. Release Studies.....	86
3.3.1. BSA Release from Scaffolds .....	86
3.3.2. Gentamicin Release from Scaffolds .....	92
3.3.2.1. Antibacterial Effect of Released Gentamicin.....	94
4. CONCLUSION.....	96
REFERENCES.....	99
APPENDICES .....	127
A. Calibration Curves.....	127
B. EDX Analyses of Scaffolds Incubated in SBF Solution .....	129
C. Compressive Stress-Strain Curves of Scaffolds Incubated in Culture Medium .	136
D. Compressive Stress-Strain Curves of Scaffolds Incubated in SBF Solution .....	138

## LIST OF TABLES

### TABLES

<b>Table 2.1</b>	Composition of 1 L SBF-5 solution prepared in distilled water...	55
<b>Table 3.1</b>	Atomic Ca:P ratio of deposited minerals on scaffolds.....	82
<b>Table 3.2</b>	Compression modulus values for scaffolds.....	84

## LIST OF FIGURES

### FIGURES

<b>Figure 1.1</b>	Representations of (a) primary structure of collagen chain and (b) chemical structures of constituent amino acids.....	2
<b>Figure 1.2</b>	Illustration of hierarchical structure of collagen fiber.....	3
<b>Figure 1.3</b>	Crystal structure of hydroxyapatite mineral.....	4
<b>Figure 1.4</b>	Schematic representation of bone structure.....	5
<b>Figure 1.5</b>	Compressive modulus of cancellous bone as a function of apparent density.....	7
<b>Figure 1.6</b>	Scaffold based tissue engineering approach.....	12
<b>Figure 1.7</b>	Chemical structure of chitosan.....	26
<b>Figure 1.8</b>	Chemical structure of alginate composed of G and M units.....	29
<b>Figure 1.9</b>	Reaction mechanism for dissolution of chitosan in acetic acid (1) and coagulation in sodium hydroxide bath as a result of proton exchange (2).....	38
<b>Figure 1.10</b>	Representative release curves for continuous and pulsatile delivery.....	42
<b>Figure 2.1</b>	Schematic representation for the preparation of fibrous chitosan scaffolds by wet spinning technique.....	51

<b>Figure 2.2</b>	Schematic representation of four different BSA loading models as (A) Ch-ON; (B) Ch-ON/Alg; (C) Ch-IN/Alg and (D) Ch/Alg-IN.....	57
<b>Figure 2.3</b>	Schematic representation of loading models with vacuum crosslinked alginate layer.....	58
<b>Figure 2.4</b>	Schematic representation of three different gentamicin loading models as (A) Ch-ON; (B) Ch-ON/Alg and (C) Ch-IN/Alg.....	60
<b>Figure 3.1</b>	SEM images of (a) chitosan scaffold and (b) alginate coated chitosan scaffold (x50 magnification).....	65
<b>Figure 3.2</b>	ATR-FTIR spectra of alginate coated and uncoated chitosan filaments.....	66
<b>Figure 3.3</b>	Cross section SEM images of alginate coated scaffold (a) x100, (b) x1000 and (c) x8000.....	68
<b>Figure 3.4</b>	Light microscopy images of (a) uncoated and (b) coated filaments.....	69
<b>Figure 3.5</b>	Percent uptake values for uncoated (ch) and alginate coated (ch/alg) scaffolds examined in distilled water and culture medium.....	71
<b>Figure 3.6</b>	Percent retention values for uncoated (ch) and alginate coated (ch/alg) scaffolds examined in distilled water and culture medium.....	72
<b>Figure 3.7</b>	Degradation graphs of both chitosan (red lines) and alginate coated chitosan (black lines) scaffolds in PBS (dashed lines) or 1mg/mL lysozyme solution (solid lines).....	74

<b>Figure 3.8</b>	SEM images of (a,b) chitosan and (c,d) alginate coated chitosan scaffolds on 3rd d of incubation in enzyme solution at (a,c) x30 and (b,d) x500 magnifications.....	75
<b>Figure 3.9</b>	SEM images of (a,b,c) chitosan and (d,e,f) alginate coated chitosan scaffolds from upperview and (g,h,i) chitosan scaffolds from cross section at (a,d,g) x30, (b,e,h) x100 and (c,f,i) x500.....	76
<b>Figure 3.10</b>	SEM images of uncoated scaffolds at (a) x30, (b) x100 and alginate coated scaffolds at (c) x30, (d) x100 magnifications incubated for 48 h.....	78
<b>Figure 3.11</b>	SEM images of uncoated scaffolds at (a) x30, (b) x100 and alginate coated scaffolds at (c,e) x30, (d,f) x100 magnifications incubated for 7 d in (c,d) same solution and (e,f) refreshed solution.....	79
<b>Figure 3.12</b>	SEM images of uncoated scaffolds at (a) x30, (b) x100 and alginate coated scaffolds at (c,e) x30, (d,f) x100 magnifications incubated for 14 d in (c,d) same solution and (e,f) refreshed solution.....	81
<b>Figure 3.13</b>	Release of BSA from scaffolds in 7 d period.....	87
<b>Figure 3.14</b>	Release of BSA from Ch-ON/Alg model prepared by crosslinking of alginate layer via either vacuum crosslink or incubation crosslink.....	89
<b>Figure 3.15</b>	Cumulative release profiles of BSA from Ch-ON and vacuum crosslinked Ch-ON/Alg models.....	90
<b>Figure 3.16</b>	Release of BSA from Ch/Alg-IN model prepared by crosslinking of alginate layer via either vacuum crosslink or incubation crosslink.....	91

<b>Figure 3.17</b>	Release profiles of gentamicin from scaffolds.....	92
<b>Figure 3.18</b>	Photograph of E.coli spreaded agar plate after incubation at 37°C for 24 h; (a) chitosan, (b) Ch-ON, (c) Ch-ON biom mineralized, (d) Ch-ON/Alg scaffolds and (e) gentamicin tablet.....	95
<b>Figure A.1</b>	Calibration curve of BSA concentration for Bradford Assay, microplate protocol at 595 nm.....	127
<b>Figure A.2</b>	Calibration curve of gentamicin concentration for UV-vis spectrometry at 256 nm.....	128
<b>Figure B.1</b>	EDX spectrum of chitosan scaffold incubated in SBF solution for 48 h.....	129
<b>Figure B.2</b>	EDX spectrum of chitosan scaffold incubated in SBF solution for 7 d.....	130
<b>Figure B.3</b>	EDX spectrum of chitosan scaffold incubated in SBF solution for 14 d.....	131
<b>Figure B.4</b>	EDX spectrum of alginate coated chitosan scaffold incubated in same SBF solution for 7 d.....	132
<b>Figure B.5</b>	EDX spectrum of alginate coated chitosan scaffold incubated in refreshed SBF solution for 7 d.....	133
<b>Figure B.6</b>	EDX spectrum of alginate coated chitosan scaffold incubated in same SBF solution for 14 d.....	134
<b>Figure B.7</b>	EDX spectrum of alginate coated chitosan scaffold incubated in refreshed SBF solution for 14 d.....	135

<b>Figure C.1</b>	Stress-strain curves of chitosan scaffolds incubated in DMEM, high glucose medium for 24 h.....	136
<b>Figure C.2</b>	Stress-strain curves of alginate coated chitosan scaffolds incubated in DMEM, high glucose medium for 24 h.....	137
<b>Figure D.1</b>	Stress-strain curves of (a,b) chitosan and (c,d,e) alginate coated chitosan scaffolds incubated in SBF-5 solution for 48 h.....	138
<b>Figure D.2</b>	Stress-strain curves of (a,b) chitosan and (c,d,e) alginate coated chitosan scaffolds incubated in SBF solution for 7 d.....	139

## LIST OF ABBREVIATIONS

3D	3 Dimensional
ALP	Alkaline Phosphatase
BM	Biomaterialized
BMP	Bone Morphogenetic Protein
BSA	Bovine Serum Albumin
CAD	Computer Aided Design
dH <sub>2</sub> O	Distilled Water
DMEM	Dulbecco's Modified Eagle Medium
ECM	Extracellular Matrix
EDX	Energy Dispersive X-ray
FGF	Fibroblast Growth Factor
GAG	Glycosamine Glycan
GH	Growth Hormone
hBMSC	Human Bone Marrow Stromal Cell
hMSC	Human Mesenchymal Stem Cell
IGF	Insulin-like Growth Factor
mRNA	Messenger Ribonucleic Acid
MSC	Mesenchymal Stem Cell
PBS	Phosphate Buffered Saline
PCL	Polycaprolactone
PDGF	Platelet Derived Growth Factor
PDLA	Poly(d-lactic acid)
PDTE	Poly(desaminotyrosyl-tyrosine-ethyl ester)
PEC	Polyelectrolyte Complex
PEG	Poly(ethylene glycol)
PHBV	Poly(3-hydroxybutyrate-co-3-hydroxyvalerate)

PLA	Poly(lactic acid)
PLGA	Poly(lactic acid-co-glycolic acid)
PLLA	Poly(L-lactic acid)
PU	Polyurethane
PVA	Polyvinylalcohol
RGD	Arginine-Glycine-Aspartic Acid
SBF	Simulated Body Fluid
SEM	Scanning Electron Microscope
TGF- $\beta$	Transforming Growth Factor-Beta
VEGF	Vascular Endothelial Growth Factor

# CHAPTER 1

## INTRODUCTION

### 1.1. Bone

Bone is a dense, porous and semi rigid connective tissue forming the endoskeleton of human body with the main functions of structural support, organ protection, mineral storage, locomotion and production of red and white blood cells. Bone is a dynamic tissue with a high capacity of self healing and remodeling but with a slow rate of regeneration.

#### 1.1.1. Bone Structure

Bone is mainly composed of an organic phase of type I collagen, an inorganic phase of carbonated apatite and water in varying proportions based on bone types (Skedros *et. al.*, 1993).

The organic matrix accounts for 20% of the wet weight of bone and it is mainly comprised of type I collagen constituting 90% of the organic phase in bone tissue. The polypeptide chains of collagen have the primary structure (Gly – X – Y) where generally X and Y define proline and hydroxyproline respectively as given in Figure 1.1. Three strands of collagen come together and generate a triple helix structure called tropocollagen which is stabilized through hydrogen bonding. Self assembling of those tropocollagen molecules in a parallel orientation forms collagen

fibrils which finally bundle together and result in collagen fibers as demonstrated in Figure 1.2. (Olszta *et. al.*, 2007). Besides collagen, 10% of organic matrix is composed of noncollagenous proteins and proteoglycans that serve crucial functions in mineralization and remodeling of bone, cell attachment and differentiation.

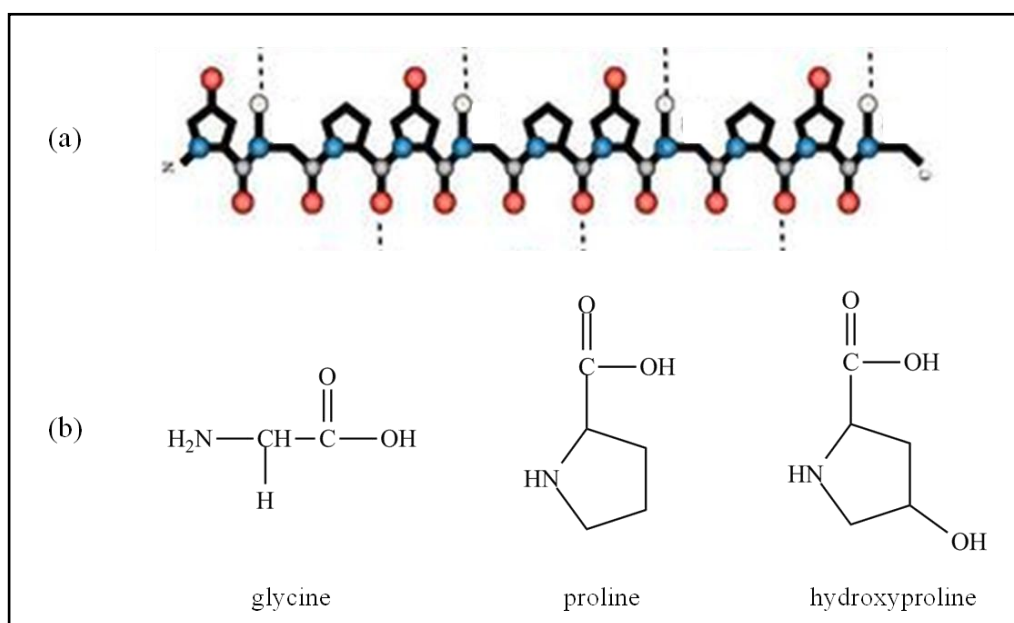


**Figure 1.1.** Representations of (a) primary structure of collagen chain and (b) chemical structures of constituent amino acids.

The inorganic phase of bone tissue contributes 65-70% of the wet weight of bone and is dominantly composed of carbonated apatite, an analogue of hydroxyapatite,  $\text{Ca}_{10}(\text{PO}_4)_6(\text{OH})_2$ , found both on the surface of and embedded in the collagen fibrils. Crystal structure of hydroxyapatite is shown in Figure 1.3. The inorganic content gives hardness and stiffness to the bone so that it demonstrates unique biomechanical properties. Additionally bone minerals are the primary ion

reservoirs of the body storing nearly 99% of calcium, 85% of phosphorus and 40-60% of sodium and magnesium totally found in the body.

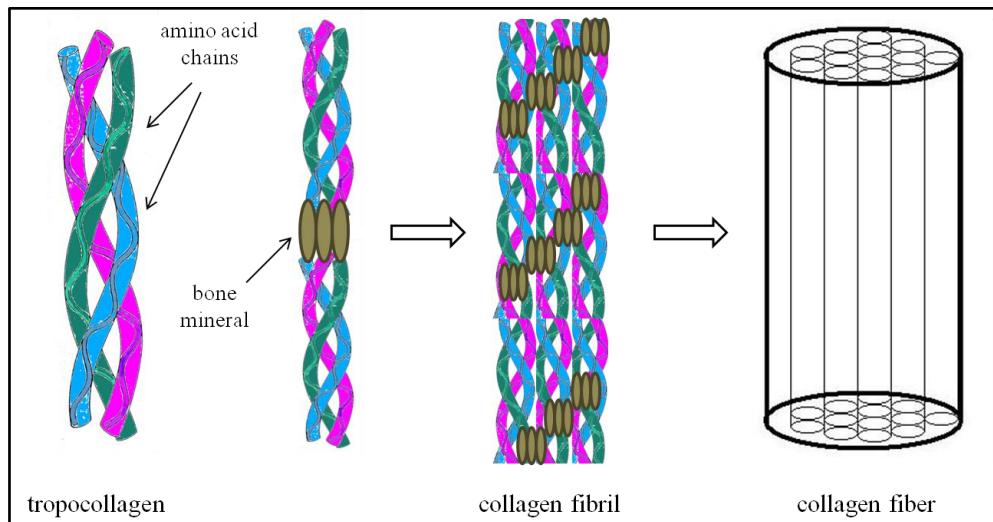


**Figure 1.2.** Illustration of hierarchical structure of collagen fiber.

Water is another major component of bone that exists within the fibrils, in the gaps and in between the tropocollagen molecules. Interstitial water is responsible for the stabilization of collagen and mineral contents of bone tissue through hydrogen bonding so that it plays a major role in maintaining the biomechanical functions of the bone (Weiner and Wagner, 1998).

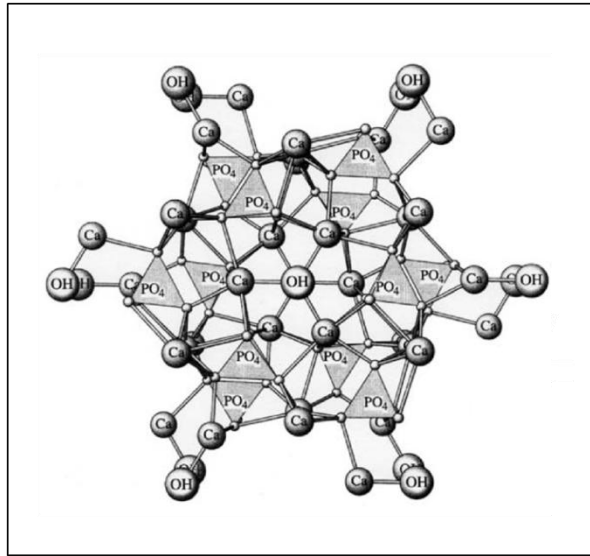


**Figure 1.3.** Crystal structure of hydroxyapatite mineral (Skinner, 2005).

Cellular components of bone represent only a small percentage of total mass and composed of osteoprogenitor cells, osteoclasts, osteoblasts, osteocytes and bone lining cells which are derived from either hematopoietic stem cells or mesenchymal stem cells (Clarke, 2008). Osteoblasts function for bone formation whereas osteoclasts mediate bone resorption. Osteocytes are numerous most found cells in bone and act as mechanosensors.

The mature adult bone has a highly hierarchical structure and mainly divided into two parts as cortical (compact) bone and cancellous (trabecular) bone. Skeletal mass of human adult skeleton is composed of approximately 80% of cortical bone and 20% of cancellous bone with varying proportions between individual bones. Cortical bone generates the dense outer layer of bone coated with periosteum which is a fibrous connective tissue. It consists of closely packed osteons also referred as Haversian systems. Osteon is the basic structural unit of cortical bone formed by bundles of collagen fibers with bone minerals and bone cells embedded in. Each

osteon has a central Haversian canal containing blood vessels and nerves enveloped in bone tissue lamellae which are formed by parallel alignment of collagen into sheets. Haversian canals of osteons are connected to each other by Volkmann's canals. Cortical bone withstands the compressive forces and gives bone its strong mechanical properties. Cancellous bone fills the interior part of the bone and it is composed of stacks of layers of lamellae. Throughout cancellous bone there exists small cavities named as lacunae between lamellae and they are connected by tubular canals called canaliculi. Cancellous bone provides space for bone marrow, where blood cells are produced, blood vessels and connective tissues. Therefore, it provides support on functioning of bone in hematopoiesis and mineral homeostasis. In addition, cancellous bone provides internal support to the bone so that it also contributes to the mechanical properties (Fuchs *et. al.*, 2009). A schematic representation of hierarchical bone structure is given in Figure 1.4.

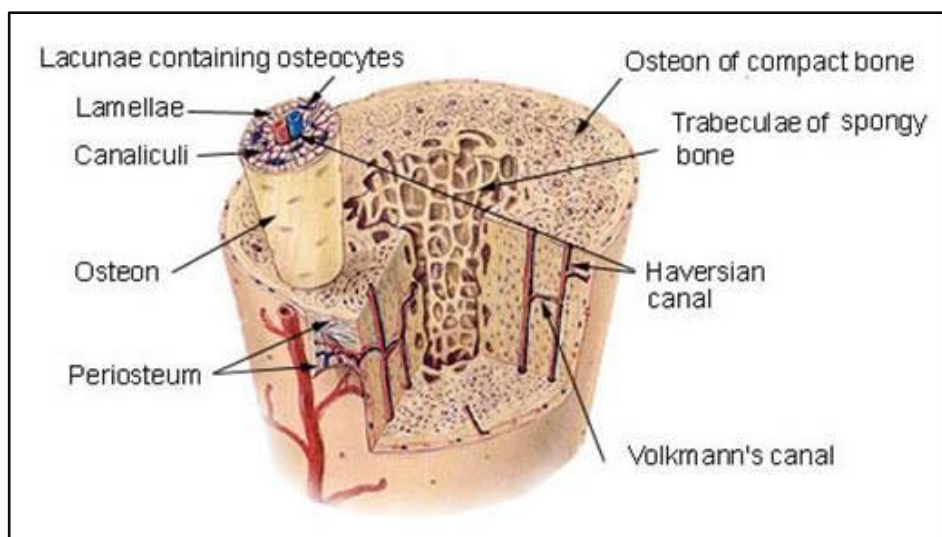


**Figure 1.4.** Schematic representation of bone structure (Spence, 1990).

Human cortical bone exhibits 5-30% porosity and has an apparent density of  $1.85 \text{ g.cm}^{-3}$  in average whereas porosity of cancellous bone varies between 30-80% and its apparent density has a broad range due to differing composition and architecture changing in accordance with the anatomic location. These fundamental differences between cortical and cancellous bones result in particular mechanical properties for both bone segments. Cortical bone exhibits a compressive strength of 130-190 MPa whereas this value is 0.1-10 MPa for cancellous bone due to its low matrix to volume ratio. Bone has a mechanically anisotropic structure meaning that its mechanical properties depend on the direction of loading. Mechanical properties of cortical bone can easily be calculated in relationship with mineral content and porosity. On the other hand, cancellous bone exhibits highly variable values proportional to its apparent density as given in Figure 1.5. (Cowin, 2001). Additionally, mechanical characteristics of different types of bones show variation. For example, Young's modulus of cortical bone has a value of 17.4 GPa in longitudinal direction and 9.6 GPa in transverse direction for long bone whereas the values are 22.5 GPa and 13.4 GPa respectively for human femur.

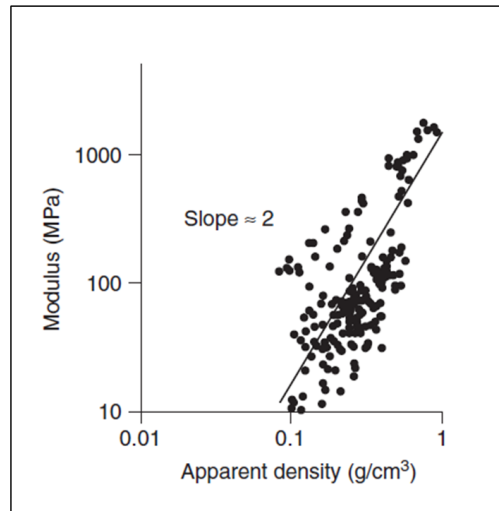


**Figure 1.5.** Compressive modulus of cancellous bone as a function of apparent density (Morgan and Keaveny, 2001).

### 1.1.2. Bone Repair

Bone goes under continuous remodeling throughout life, therefore it is these continuous changes that give the bone tissue the ability to repair and regenerate itself in response to injuries.

Fracture healing is a progressive process involving cells, growth and differentiation factors, hormones and extracellular matrix that all together regulate the contiguous cellular events ultimately resulting in bone healing. Fracture healing occurs in three continuously following stages as early inflammatory stage, reparative stage and remodeling stage (Flick *et. al.*, 2003; Al-Aql *et. al.*, 2008). From the start to the end, healing process is controlled and progressed by release of growth factors and hormones in a time and concentration dependent manner. During inflammation, hematoma formation occurs between bond ends where relevant cells and bioactive agents migrate to. Angiogenesis and formation of granulation tissue is observed. In

reparative phase, through proliferation and differentiation of cells, callus formation which corresponds to bridging between the fractured sites of bone, occurs followed by mineralization and transition to new bone tissue. Resultant new tissue then undergoes remodeling phase where bone resorption and formation proceed cooperatively to gain bone back its original shape, function and mechanical strength (Schindeler *et. al.*, 2008).

## **1.2. Approaches in Bone Repair and Regeneration**

In the cases of large defects caused by trauma, degenerative diseases or tumor resection, or as a result of infection, intrinsic repair mechanism of bone may fail. Therefore, several clinical approaches have been developed for treatment.

Bone grafting, transplantation of bone from a donor site to fracture site with the aim of inducing new bone formation, is the most commonly used procedure (Khan *et. al.*, 2005; Bormann *et. al.*, 2012). Supplying the transplanted bone from patient's own body is called autografting and serves as the golden standard in clinical applications. Autografts have the advantages of containing bone cells and proteins within, being osteoconductive and osteoinductive and possess no risk of viral transmission. However, availability limitations and harvest associated morbidity at the donor site are the major drawbacks of this procedure together with possible nonunion in large bone loss.

Allograft usage, bone transplantation from another human, stands as an alternative treatment that overcomes the availability issues but possess the risk of evoking immune response and viral transmission as significant concerns. In order to overcome these problems, allografts are decellularized and devascularized prior to usage. Yet, processing may cause alterations in biomechanical and biochemical properties of the tissue and deplete its osteoinductive properties (Eppley *et. al.*, 2005; Mroz *et. al.*, 2006). Cadavers are used as source of allografts through bone banks. As

an example, they correspond to 3.64% of total grafting procedures took place in Japan between the years 1985-2004 (Urabe *et. al.*, 2007).

Bone substitutes can also be obtained from other species which are called xenografts. In order to fill bone defects and provide bone union, deproteinized bovine and porcine xenografts have been offered. Prior to usage, these materials should be cleaned in order to reduce their antigenicity. It was demonstrated that untreated bovine xenografts initiated a transient antibody response but the inflammatory response was significantly lowered when they were cleaned by hydrogen peroxide and isopropanol. Additionally, after 24 weeks of implantation it was shown that bone integration with xenografts was same as allograft controls (Katz *et. al.*, 2009). Bovine origin xenografts investigated in vivo also shown to be osteoconductive besides being biocompatible (Ramirez-Fernandez *et. al.*, 2011). Investigation of porcine xenografts revealed the main antigens that should be removed to prevent xenogeneic immune reactions for using them as bone substitutes safely (Feng *et. al.*, 2012). Incorporation of magnesium on the surface of porcine origin xenografts was appeared to behave osteoconductive and increase new bone formation upon 4 weeks of implantation when compared to untreated bovine and porcine xenografts (Park *et. al.*, 2012). Another study demonstrated the advantageous effects of using porcine graft as a paste with collagen to fabricate biocompatible, bioresorbable and osteoconductive scaffolds (Calvo-Guirado *et. al.*, 2012).

Natural coral obtained from the exoskeleton of marine madreporic corals have also been used as bone xenografts in humans since 1979 due to being biocompatible, osteoconductive, biodegradable and having resembling structure to that of cancellous bone (Demers *et. al.*, 2002). In animal models, simultaneous bone formation was demonstrated as the coral grafts were resorbed over time (Guillemin *et. al.*, 1987). Incorporation of cellular components into natural coral has also led to successful results. Implants of coral loaded with mesenchymal stem cells (MSCs) were studied for the repair of large bone defects and it was reported that engineered bone tissue formation followed by formation of mature lamellar cortical bone was

achieved (Petite *et. al.*, 2000). Seeding marrow derived osteoblasts into coral resulted in vascularized, predetermined shaped bone grafts for human mandibular ramus that can be used in clinical applications (Chen *et. al.*, 2004).

Another procedure employed is direct injection of bone marrow to the nonunion defect sites. Since bone marrow is a source of osteoprogenitor cells, autogeneic grafting accelerates fracture healing and new bone formation (Healey *et. al.*, 1990). However, this method also has shortcomings similar to autografting such as limited availability.

Injectable bone cements are used as bone fillers at defect sites as an alternative to bone grafts. Mostly used bone cements are made up of acrylics or ceramics which are mainly composed of calcium phosphate compounds existing in natural bone structure. Injectable cements have the superiority of filling customized gaps within damaged bone ends. Acrylic bone cements produced from poly methylmethacrylate (PMMA) show good compressive strength and stability. They have been used in bone fixation as implant materials (Saha and Pal, 1984). Main drawbacks of acrylic bone cements are highly exothermic setting reactions, necrosis of bone due to unreacted monomer release and stiffness mismatch (Lewis, 1997). Bone cements prepared from calcium phosphate compounds stand as an alternative to acrylic cements with the additional advantages of biocompatibility and osteoconductivity. Hydroxyapatite bone cements were evaluated in a clinical study lasting for 29 years with the attempt of fixation of prostheses to the bone and results showed that no loosening or osteolysis occurred (Oonishi *et. al.*, 2012). Resorbable forms of calcium phosphate cements have also been used for bone repair and regeneration process with the advantage of being replaced by newly forming bone tissue. Fully resorbable calcium phosphate cement was evaluated in a clinical study with 107 patients in terms of its safety and performance as a substitute material. Clinical, histological and radiologic examinations revealed that no immunological response occurred and during bone remodeling resorption and osseous integration were observed (Bloemers *et. al.*, 2004). In order to improve the resorption rate of

calcium phosphate cements to accelerate the replacement with newly formed bone, doping of magnesium, carbonate and calcium sulphate into hydroxyapatite cements was proposed as an implant material exhibiting high potential for bone regeneration (Zima *et. al.*, 2012). As another approach to enhance bone repair abilities of bone cements, they have been used with incorporation of chondroitin sulphate that increased the rate of new bone formation (Schneiders *et. al.*, 2012). The major drawback associated with calcium phosphate based bone cements is the mismatching stiffness with bone tissue that causes failure in transferring of load.

### **1.3. Bone Tissue Engineering**

In the design and production of bone supporting materials there is a progressive success but still strategies to improve the current state of treatment are being investigated. The need for better bone substitutes especially for large bone defects, and the necessity of regulation of treatment according to each patient's needs make tissue engineering an advantageous alternative in the field of bone repair and regeneration.

Tissue engineering is defined as 'an interdisciplinary field that applies the principles of engineering and life sciences toward the development of biological substitutes that restore, maintain or improve tissue function' by Langer and Vacanti (Langer and Vacanti, 1993). In tissue engineering approach, constructs to be used for that purpose mainly contains a carrier or template structure called as scaffold, cells and bioactive agents. When specialized to bone tissue engineering, any attempt would be directed towards stimulating bone formation and the components to be used should be chosen to address that purpose specifically.

As scaffolding material, a biocompatible, biodegradable and preferably an osteoconductive material should be employed to construct three dimensional (3D) templates for bone ingrowth and vascularization. Cells and bioactive agents to be used should enable the proliferation and differentiation of specific bone cells. In this

ideal environment for bone repair and regeneration, cells directed by bioactive agents start to proliferate and differentiate together with extracellular matrix (ECM) deposition and vascularization on the scaffold. In time, scaffold integrates with the surrounding tissue and replace with new tissue formed as it undergoes complete remodeling (Van Blitterswijk *et. al.*, 2007). A schematic presentation of the tissue engineered bone formation through an activated scaffold is given in Figure 1.6.

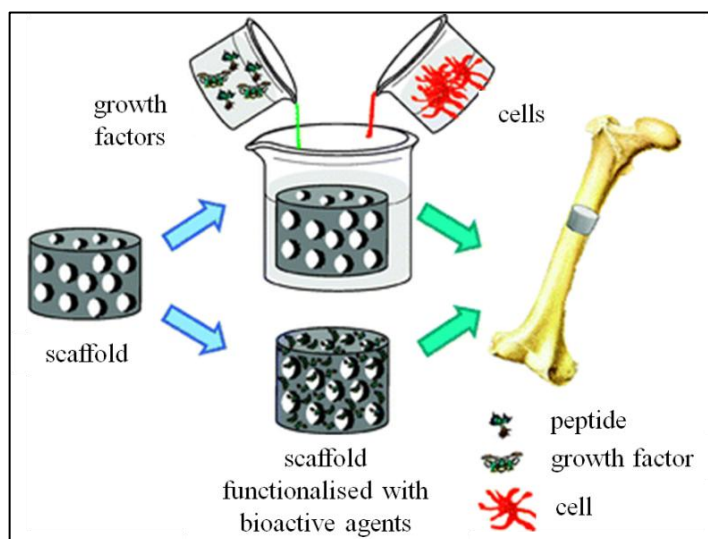


**Figure 1.6.** Scaffold based tissue engineering approach (Vallet-Regi *et. al.*, 2011).

### 1.3.1. Scaffolds in Bone Tissue Engineering

Scaffolds are basically the support and guidance systems for cells to undergo necessary cellular events leading tissue regeneration and remodeling. In bone tissue engineering applications main function of scaffolds is to act as a template that permit migration, proliferation and differentiation of bone cells with maintaining their

phenotypes. Scaffolds support 3D tissue formation both mechanically and biologically that would eventually result in new bone formation and restoring of function. Scaffold systems may be cellular or acellular with the feature of bioactive agent delivery. Therefore, while mechanically supporting the defect site during regeneration they also act as reservoirs of osteogenesis regulating agents such as bone growth factors (Salgado *et. al.*, 2004).

Having such important functions requires detailed design in scaffold production. There exists certain criteria a scaffold must meet. The most important requirement that a scaffold should have is being biocompatible. The scaffold should have no or minimal inflammatory response and immunogenicity throughout the period of use (Burg *et. al.*, 2000).

For scaffolds to be used in bone tissue engineering applications, the bone-bonding ability of the material used is crucially important. If the scaffold does not exhibit bonding ability to natural bone tissue, encapsulation by a fibrous tissue occurs upon implantation which in turn leads to isolation of the material from surrounding bone and prevents biomaterial-tissue integration. Bone-bonding ability of materials is shown to be correlated with bone like apatite formation on the surface upon implantation (Kokubo, 1991). In vivo apatite formation on scaffolds can be reproduced in simulated body fluid (SBF), therefore, in vivo bioactivity of a scaffold can be examined by incubation in SBF and evaluating the apatite formation on its surface (Kokubo and Takadama, 2006). Assessment of bioactivity both qualitatively and quantitatively through biomineralization in SBF is proven to be a validated method and have been used extensively (Lee *et. al.*, 2007; Peter *et. al.*, 2010; Vitale-Brovarone *et. al.*, 2011; Padmanabhan *et. al.*, 2012; Irineu *et. al.*, 2012; Beherei *et. al.*, 2012).

Osteoconductivity is the ability of a material to support bone formation and a crucial property to be possessed by a scaffold to be successful in bone tissue engineering. Incorporation of osteoconductive materials into the scaffold structure such as hydroxyapatite,  $\beta$ -tricalcium phosphate or similar compounds results in

significant increase in cell proliferation and alkaline phosphatase activity which indicates bone formation (John *et. al.*, 2012; Valenzuela *et. al.*, 2012; Rungsiyanont *et. al.*, 2012; Chen *et. al.*, 2012; Wang *et. al.*, 2012). Osteoinductivity, on the other hand, is the ability of a scaffold to induce bone formation by directing cell differentiation into mature bone cells and has been very advantageous especially in the cases of large defects to ensure bone union. Functionalization of scaffolds by the use of osteoinductive materials shows promising outcomes as directing cellular events towards osteoblastic activity that results in dramatic enhancement in bone tissue formation. Functionalization of starch-polycaprolactone (PCL) wet spun scaffolds with silanol groups resulted in higher matrix formation and increased alkaline phosphatase (ALP) activity indicating the osteoinductive characteristic of silanol (Leonor *et. al.*, 2011). As another osteoinductive material  $\beta$ -calcium silicate incorporation to ceramic scaffolds was reported to led a significant increase in new bone formation (Wang *et. al.*, 2012).

In bone tissue engineering applications, used scaffolds should have interconnective porous structure to facilitate tissue growth and vascularization inside the material that would result in integration with surrounding tissue. Moreover, porous structure enables mass transfer and diffusion of nutrients and oxygen together with removal of metabolic wastes that are essential for new tissue formation. Optimum pore size for bone tissue engineering scaffolds is stated as 200-900  $\mu\text{m}$  range because that size is reported as the suitable size for penetration of both osteoprogenitor cells and endothelial cells into the matrix (Salgado *et. al.*, 2004; Cahill *et. al.*, 2009).

Surface characteristics of scaffolds effect the course of cellular events during healing and regeneration processes. Chemical composition of the surface has great influence on cell adhesion and retention due to changing functionality, hydrophobicity and surface energy. Studies show that hydrophilic surfaces and existance of calcium based materials or certain proteins on the surface promote cell attachment and contribute to bone tissue healing (Hu *et. al.*, 2003; Kim *et. al.*, 2007;

Suarez-Gonzalez *et. al.*, 2010). Biomimetic coating of scaffolds with materials known to favor osteogenic activity also supports and extents new bone tissue formation. Topographical properties of surface effect adhesion, proliferation and maintenance of cell phenotype which is utmost importance to achieve desired biological pathway. Studies reveal that scaffolds with patterned surfaces enhance cell orientation, osteoblast alignment and bone formation (Heath *et. al.*, 2010; Kumar *et. al.*, 2012; Tong *et. al.*, 2012).

Ideally, scaffolds should be designed to match the mechanical characteristics of the tissue it will replace. Firstly, it should provide sufficient support at the defect site until new tissue forms. Secondly, bone is responsive to mechanical stimuli meaning that tissue regeneration and remodeling rely on mechanical signaling. When mechanical compatibility is not ensured, stress shielding occurs. Stress shielding is the failure in adequate transfer of load between the scaffold and neighboring tissues which results in bone resorption near the scaffold (Lin *et. al.*, 2011). The difficulties in designing scaffolds with matching mechanical properties with bone result from;

- i. genuine mechanical characteristics of bone due to its highly hierarchical collagen structure and apatite component varying between different bone types
- ii. dramatic decrease in mechanical strength of scaffolds when porous structures are used.

Mechanical properties of scaffolds must be adjusted according to the site and aim of use. For load bearing and non-load bearing bones, cortical and cancellous parts, mechanical requirements vary significantly. Compressive strength of cancellous bone varies between 0.1-10 MPa, therefore scaffolds to be used should have compatible characteristics. Scaffolds either in fibrous or hydrogel forms with adequate mechanical strength in cancellous bone range were fabricated for that purpose (Ramay and Zang, 2004; Zhao *et. al.*, 2010; Lei *et. al.*, 2012). Likewise, bioactive glass scaffolds with compressive strength values in the range of cortical bone as of 136 MPa and  $140 \pm 70$  MPa were fabricated for load bearing bone defects

repair and regeneration (Fu *et. al.*, 2011; Rahaman *et. al.*, 2011). Additionally, hydrogels that exhibit quite low mechanical strength have also been used in bone tissue engineering applications where scaffolds do not participate in structural remodeling but are aimed to support cell attachment and proliferation via delivery of bioactive agents.

In addition, scaffolds should be biodegradable through enzymatic or hydrolytic degradation in vivo with biocompatible degradation by products. In order to maintain mechanical support provided by the scaffold, its degradation rate should be compatible with the rate of new tissue formation.

Scaffolds used in bone tissue engineering can be employed in a variety of forms such as 2D or 3D sponge, hydrogel, porous disk or fibrous mesh forms. Fibrous structures have the advantage of large surface to volume ratio which magnifies the area for cellular interactions. Also, resemblance to bone tissue structure composed of collagen fibers permit fabrication of biomimetic scaffolds.

#### **1.3.1.1. Materials Used in Scaffold Production**

When designing a scaffold to be used in tissue engineering and drug delivery applications, the choice of material is a critical step since the properties of the scaffold will be influenced by material properties in a great extent. Therefore, for each specific case of usage, the most appropriate material should be considered.

For bone tissue engineering applications; metals, ceramics and polymers have been reported. However, not being biodegradable limits the use of metals and most of the ceramics to be used for scaffolding since gradual replacement of scaffold with newly forming tissue is preferable.

Metals are widely used as implant materials for orthopedics where they act as filler and support in place of use. By altering the surface functionality, bulk characteristics or structure, metal integration with bone tissue and utility in new bone

formation can be enhanced. Therefore inert materials are transformed into potentially bioactive substrates especially for high load bearing bones. Protein adsorption procedures and silane coupling have been used to functionalize metals with bioactive chemical agents for this purpose (Dee and Bizios, 1996). Titanium is the mostly used metal either in pure or alloy forms in bone tissue engineering applications. Covalent attachment of Arginine-Glycine-Aspartic acid (RGD) sequences on titanium surface was shown to improve its biocompatibility since surface chemistry is the utmost important factor effecting bone integration (Xiao *et. al.*, 1998). Coating of hydroxyapatite on titanium substrates with the same purpose was also shown to increase ALP activity which is associated with new bone formation (Kim *et. al.*, 2004). Metals are employed in porous scaffold production as metallic foams with the advantages of adjusted pore size and mechanical properties, long term stability and open cellular structure to allow tissue ingrowth (Wen *et. al.*, 2001; Wen *et. al.*, 2002; Spoerke *et. al.*, 2005). Hybrid scaffold of titanium alloy foam with peptide amphiphile nanofibers were produced and exhibited promising results in vivo (Sargeant *et. al.*, 2008). Tantalum is another metal that has potential use in bone tissue engineering that shows good biocompatibility, fast apatite nucleation and direct bone formation when coated with calcium phosphate (Miyazaki *et. al.*, 2002; Hacking *et. al.*, 2003; Barrere *et. al.*, 2003; Levine *et. al.*, 2006). Another application of metals is preparation of metallic fibers with magnetic properties such as ferritic stainless steel to use magnetic signaling to stimulate bone growth (Clyne *et. al.*, 2005).

Biodegradable bioceramics are a class of materials used in bone tissue engineering applications mainly due to being composed of inorganic materials which are very similar to the apatite composition of natural bone and also being both osteoconductive and osteoinductive. That chemical resemblance results in good biocompatibility together with enhanced healing and regeneration processes. Synthetic or natural origin hydroxyapatite, calcium phosphate and tricalcium phosphate are the mostly employed ceramic materials in scaffold production. Hydroxyapatite scaffolds with defined architecture produced by rapid prototyping

showed bone tissue formation and full vascularization in vivo after 4 weeks of implantation (Wilson *et. al.*, 2004). Additionally, under dynamic cultivation, hydroxyapatite scaffolds produced by 3D printing showed enhanced cell growth on all over and within the cavities of scaffolds (Leukers *et. al.*, 2005). Fully interconnected porous hydroxyapatite scaffolds produced by foam-gel technique revealed mature bone ingrowth in all pores of the scaffolds after 6 weeks of implantation in vivo which was accompanied by a 3 fold increase in compressive strength (Yoshikawa *et. al.*, 2009). 3D printed biphasic calcium phosphate scaffolds treated with bone morphogenetic protein-2 (BMP-2) displayed significant messenger ribonucleic acid (mRNA) expression of bone specific genes after 6 weeks of implantation (Strobel *et. al.*, 2012). In another study, porous tricalcium phosphate scaffolds were prepared and interior surfaces of pores were coated with apatite mineral to increase the bioactivity of the scaffold. Results revealed enhanced proliferation rate and differentiation level for bone cells (Zan *et. al.*, 2012). However, being very hard and brittle are the major drawbacks in the case of bioceramics. The hardness of ceramics which is incompatible with the stiffness of bone tissue causes stress shielding on surrounding tissues that results in bone resorption and cell death. Additionally, brittle nature of ceramics limits their usage since scaffolding material should fulfill the mechanical requirements of bone tissue during healing and regeneration. As a result, ceramics are generally used in composite scaffolds with polymers in order to overcome their mechanical incompatibilities.

Composite scaffolds of ceramics with polylactic acid and polyglycolic acid based polymers are commonly employed in bone tissue engineering applications. Composite scaffolds of hydroxyapatite prepared with both poly-L-lactic acid (PLLA) and polylactic-co-glycolic acid (PLGA) were reported to be successful candidates for bone tissue engineering applications due to enhanced mechanical properties, cell adhesion, stimulation of cell proliferation and osteogenic differentiation (Wei and Ma, 2004; Kim *et. al.*, 2006; Mathieu *et. al.*, 2006). Collagen and gelatin are two of the most frequently used protein based polymers for production of composite scaffolds with ceramics. In a recent study, tricalcium phosphate fibers were prepared

and coated with collagen to mimic the woven bone structure and scaffolds prepared were stated to promote bone cell attachment and proliferation (Zhang *et. al.*, 2010). In another study, collagen fibers and mineral particles were embedded in polycaprolactone (PCL) templates so that in addition to bioactivity features resulting from these components, scaffolds were improved mechanically by PCL presence (Yeo *et. al.*, 2011). In order to improve the mechanical properties of tricalcium phosphate porous scaffolds gelatin with  $K_2HPO_4$  content was also used and increase in compressive strength was reported (Ji *et. al.*, 2010).

Polymers of either natural or synthetic origin are the most commonly used scaffold materials in tissue engineering applications. Wide range of structural varieties corresponds to polymeric materials of differing mechanical, chemical and biological properties, therefore, offer millions of possibilities in materials science.

Synthetic polymers have the advantage of being tailorable in terms of their mechanical properties, degradation kinetics and functionality resulting in specifically modified materials for different applications. They are readily available and easy to process. In addition they can be fabricated in various shapes with differing morphological and topographical features. Most commonly used biodegradable synthetic polymers for bone tissue engineering are polyesters, polycarbonates, polyanhydrides and polyurethanes. Among polyesters, aliphatic ones are frequently employed such as polycaprolactone (PCL), poly-L-lactic acid (PLLA) and polylactic-co-glycolic acid (PLGA). It was revealed by an in vitro study that nanofibrous electrospun PCL scaffolds undergo mineralization and type I collagen deposition and therefore were potential candidates for bone tissue engineering applications (Yoshimoto *et. al.*, 2003). Incorporation of bone morphogenetic protein-7 (BMP-7) into PCL scaffolds fabricated by selective laser sintering showed enhanced tissue formation in vivo along with the advantages of computational analysis of mechanical properties and the ability to be manufactured to fit complex anatomic locations (Williams *et. al.*, 2005). PCL was also used as composites with ceramics. 3D printing of PCL scaffolds with the incorporation of calcium phosphate

was shown to result in high cell proliferation and type I collagen formation in vitro (Sharaf *et al.*, 2012). Composite scaffolds of PLLA and bioceramics have been used extensively in bone tissue engineering applications since the bioactivity and mechanical properties of the polymer can be enhanced that way. Hybrid scaffolds of hydroxyapatite and PLLA fabricated by electrospinning showed enhanced cell adhesion and proliferation and mechanical stability compared to pure PLLA scaffolds (Deng *et al.*, 2007). Coating of electrospun PLLA scaffolds with bioactive glass and hydroxyapatite resulted in bone substitutes with the capacity to induce osteoconduction and osseointegration (Dinarvand *et al.*, 2011). PLLA blends with either natural or synthetic polymers have also been reported. PLLA/gelatin blends were used in scaffold production in order to increase the yield stress and elastic modulus of pure PLLA scaffolds that showed no significant difference in supporting cell attachment and differentiation (Andric *et al.*, 2011). Composite scaffolds of poly-L-lactic acid (PLLA) and poly-3-hydroxybutyrate-co-3-hydroxyvalerate (PHBV) prepared by emulsion freezing/freeze drying technique were evaluated. It was shown that coating with collagen improved cell attachment whereas incorporation of hydroxyapatite significantly increased cell proliferation and alkaline phosphatase (ALP) activity and resulted in a potential scaffold to be used in bone tissue engineering applications (Sultana and Wang, 2012). In vivo studies revealed that scaffolds prepared from the blends of PLGA with hydroxyapatite and tricalcium phosphate are also good candidates for bone tissue as they show integration with host bone tissue (Kim *et al.*, 2012). Since PLGA is a hydrophilic polymer, using it pure results in poor cell attachment. Apart from blending, RGD modification of surface of the PLGA scaffolds can also overcome this problem (Tao *et al.*, 2012).

Among polycarbonates, tyrosine derived ones have been applied as biomaterials because they are regarded as pseudo polyamino acids and exhibit the biocompatible nature of amino acids. Therefore they provoke less immunogenic response while maintaining the mechanical strength (Agrawal and Ray, 2001). Poly-desaminotyrosyl-tyrosine-ethyl ester (PDTE) carbonate membrane was used to cover bone defects in vivo and reported to support new bone formation (Asikainen *et al.*,

2005). Biomimetic scaffolds produced from tyrosine derived polycarbonates with ethyl ester side chains were used in recombinant BMP-2 delivery and shown to promote osteogenic lineage, ALP activity and mineralization (Kim *et. al.*, 2012).

Polyanhydrides are polymers prone to hydrolysis showing surface degradation characteristics. Therefore they have primarily attracted attention in the field of drug delivery applications. Biocompatibility of polyanhydrides in vitro was examined through their cytotoxicity on osteoblast-like cells and shown to be suitable for use in orthopaedic applications (Attawia *et. al.*, 1996). Additionally evaluation of photopolymerizable degradable polyanhydrides in vivo presented osteocompatibility of these materials (Anseth *et. al.*, 1999). Biodegradable polyurethanes (PU) are another class of polymers used in scaffold production. In the use of aliphatic PUs, it was shown that the percentage of hard and soft segments directly effects the cell-material interaction, mechanical strength and architecture of resultant scaffolds (Bil *et. al.*, 2010; Wang *et. al.*, 2011). PU foams have been widely investigated for bone tissue engineering applications. Their ability to support cell proliferation and differentiation was investigated and observed to stimulate cell adhesion and differentiation into osteoblasts together with mineral deposition starting at 7<sup>th</sup> day of incubation in vitro (Zanetta *et. al.*, 2009). In order to enhance the biological activity of PU scaffolds towards bone formation and tailor mechanical and structural properties, composite scaffolds with hydroxyapatite and bioactive glass were produced successfully (Ryszkowska *et. al.*, 2010; Laschke *et. al.*, 2010; Wang *et. al.*, 2011; Vasile *et. al.*, 2012; De Oliveira *et. al.*, 2012). Injectable biodegradable PU scaffolds were also suggested as potential therapies for bone failures where properties of scaffolds were tailored by altering the monomers used for synthesis (Hafeman *et. al.*, 2008).

Despite the advantages of synthetic polymers, they are lack of biological functions and the degradation by products of synthetic polymers may be hazardous to body when accumulated. On the other hand natural polymers consist of components of living systems, therefore, possess biological and chemical resemblance to natural

tissues. This characteristic gives natural polymers the advantage of bioactivity due to enhanced cell-material interaction and the disadvantage of recognizable sites that may cause immune response. Degradation of natural polymers occurs through hydrolytic or enzymatic degradation resulting in nonhazardous degradation products.

Natural polymers frequently used in bone tissue engineering scaffolds can mainly be classified as protein origin polymers and polysaccharides. Protein based polymers exhibit the advantage of being highly abundant in extracellular matrix and intracellular medium which gives them the potential to create a favorable environment for healing and regeneration. Among protein origin polymers, collagen has always been popular due to being a natural component of bone tissue and osteoinductive. Collagen scaffolds in the forms of sponge, gel and fiber are studied and commercialized for bone tissue engineering applications (Chen *et. al.*, 2008). Collagen/hydroxyapatite composite scaffolds prepared and examined in vitro showed promising results by combining the osteoinductive properties of collagen with stronger bioactivity of hydroxyapatite and resulting in mechanically superior constructs compared to pure collagen ones (Rodrigues *et. al.*, 2003; Wahl *et. al.*, 2007). Composite scaffolds of collagen-glycosaminoglycan prepared by lyophilisation were also shown to have osteogenic potential by in vitro studies (Farrell *et. al.*, 2006; Murphy *et. al.*, 2010). Collagen-PCL composites were studied for bone tissue engineering either in fibrous or hydrogel forms.

Fibrous scaffolds obtained by electrospinning of collagen-PCL blend were shown to modulate attachment and proliferation of pig bone marrow cells. Additionally, culturing of these scaffolds under dynamic conditions was shown to enhance bone-like tissue formation and mechanical strength (Ekaputra *et. al.*, 2009). In another study, collagen hydrogel containing marrow derived human mesenchymal stem cells was prepared and pipetted on PCL scaffolds fabricated by fused deposition modeling. Evaluation of this composite construct revealed the convenience of collagen hydrogels to facilitate cell seeding of scaffolds for bone tissue engineering applications (Reicherdt *et. al.*, 2009). A recent study showed the potential

of collagen sponges for immobilized delivery of bioactive agents. Collagen microsponges were prepared and placed within the openings of PLGA mesh. Composite scaffolds were then treated with BMP-4 with a collagen binding domain. In vivo evaluation showed that resultant scaffolds exhibited strong osteoinductivity (Lu *et. al.*, 2012).

Gelatin, derived from collagen, is also used frequently either in hydrogel or rigid scaffold forms and exhibit successful results in bone healing. Hydrogels of gelatin employed in bone defects are mostly used as composites in order to improve weak mechanical characteristics of the biopolymer. Incorporation of calcium and phosphate as separate solutions into the gelatin hydrogel resulted in transforming of the inorganic contents to hydroxyapatite mineral after incubation in simulated body fluid (SBF) and an increase in mechanical strength. This biomimetic transform of precursors into bone mineral pointed the prepared scaffolds as potential constructs to be used in bone healing process (Azami *et. al.*, 2012). As another method to increase the stiffness of gelatin hydrogels which is necessary for both mechanical support and cell proliferation, PCL nanofibers produced by electrospinning were incorporated into gel matrix. As a result, increase in Young's modulus values and enhancement in cell proliferation was observed (Kai *et. al.*, 2012). Gelatin sponges are candidate materials for bioactive agent delivery in bone tissue engineering. However, their mechanical weakness should be overcome to support bone regeneration and loaded bioactive agents should be protected from loss due to fast degradation. For that purpose, rapid mineralization of gelatin sponges with electrodeposition method was employed. It resulted in a homogenous apatite formation on the surface of scaffolds which enhanced both proliferation and osteoblastic differentiation of cells (He *et. al.*, 2012). With the aim of fabricating scaffolds that are structurally similar to bone tissue, possessing good biological activity and adequate mechanical strength, electrospun fibrous scaffolds of gelatin blended with PCL and PLLA were also reported (Guo *et. al.*, 2012; Andric *et. al.*, 2012).

Silk fibroin is a fibrous protein produced by silk worms with the additional advantage of high mechanical strength compared to natural polymers. It has been processed by various techniques into different forms to be used as bone tissue engineering scaffolds. Mechanical properties of silk can be tailored regarding to the aim of use. Silk was even proposed as a temporary implant material for bone due to its high mechanical strength, low degradation and low immunogenicity (Meinel *et. al.*, 2005). For degradable scaffolding purposes in load bearing bone tissue engineering, high strength silk was studied in microfiber form and shown to meet the mechanical and biological requirements in vivo (Mandal *et. al.*, 2012). Scaffolds with resembling structure to bone lamellae was fabricated by aligned silk fibroins and resultant morphology was reported to constitute a useful pattern onto which human mesenchymal stem cells (hMSC) attach and proliferate for guided formation of a highly oriented extracellular matrix (Oliveira *et. al.*, 2012). Apart from highly stable forms, low molecular weight silk fibroin with fast degradation was also investigated and the effect of degraded silk fibroin on osteoblastogenic gene expression was confirmed by observing up-regulation of ALP activity. Therefore, it was suggested that silk fragments emerged by controlled degradation of the polymer may have an accelerating effect on new bone formation (Kim *et. al.*, 2010). Silk scaffolds have been extensively used in bioactive agent delivery for bone tissue engineering applications. Silk hydrogels combined with electrospun PCL meshes were used for local delivery of BMP-2 and the results demonstrated the effectiveness of silk hydrogel as BMP-2 carrier (Diab *et. al.*, 2012). Fibrous silk fibroin fabricated by electrospinning also showed the efficiency of silk scaffolds for BMP-2 delivery (Li *et. al.*, 2006). Investigation of silk fibroin scaffolds on BMP-7 delivery for critical size bone defects in vivo supported the bioactive agent carrier potential of silk scaffolds by maintained activation of the growth factor (Zhang *et. al.*, 2011).

Polysaccharides are biopolymers consist of monosaccharides linked via O-glycosidic bonds. They perform a variety of functions in living organisms, thus, conveniently used in tissue engineering where mimicking the nature is the fundamental inspiration. Due to being a major component of extracellular matrix,

hyaluronan is used in bone tissue engineering along with its applications in drug delivery and wound healing (Prosdocimi and Bevilacqua, 2012; Bhakta *et. al.*, 2012). Injectable gels of hyaluronan prepared via acrylation or crosslinking with poly vinyl alcohol (PVA) were employed in BMP-2 delivery and demonstrated significant bone formation with no sign of inflammation in vivo (Kim *et. al.*, 2007; Bergman *et. al.*, 2009). Delivery of BMP-2 through hyaluronan hydrogel was also achieved by introduction of the bioactive agent containing hydrogel into polymeric composite scaffolds. Results showed hyaluronan hydrogel supported growth of osteoblasts over 8 weeks and allowed sustained release of BMP-2 over 35 days with expression of bone related genes (Rath *et. al.*, 2011). Incorporation of hydroxyapatite into hyaluronan hydrogel was also shown to reveal osteoinductive effect and increased bone density where applied in vivo (Nageeb *et. al.*, 2012).

Starch is another member of polysaccharide family that attracts attention by its success in bone tissue engineering applications when used as blends with polycaprolactone. Investigation of fibrous mesh scaffolds of starch-PCL blend in vivo, revealed the suitability of these scaffolds to be used in bone tissue engineering due to exhibited abilities of proliferation and differentiation of bone marrow cells and vascularization (Santos *et. al.*, 2007). Supporting these findings, in another study, the fiber mesh scaffolds of starch-PCL blend were shown to promote osteogenic lineage and new bone formation in vivo (Rada *et. al.*, 2012). In order to increase the efficiency of starch-PCL scaffolds hierarchical structures were prepared by combination of rapid prototyping and electrospinning. A significant increment in cell proliferation and osteoblastic activity was observed on the hierarchical fibrous scaffolds which indicated the improved biological performance (Martins *et. al.*, 2009). As another method, modifying starch-PCL scaffolds with introducing Si-OH groups and cultivating the scaffolds under dynamic conditions showed improvement in cell proliferation, penetration into the scaffold and ALP activity (Rodrigues *et. al.*, 2011).

In this study, chitosan and alginate are used in the fabrication of fibrous scaffolds and will be explained in detail.

#### 1.3.1.1.1. Chitosan

Chitosan is a linear polysaccharide that is obtained by deacetylation of chitin which is the second most abundant natural polymer found in nature especially in the exoskeletons of arthropods and cell walls of fungi. Chitosan is composed of 1-4 linked D-glucosamine and N-acetylated D-glucosamine units either in random or block distribution depending on the processing method.

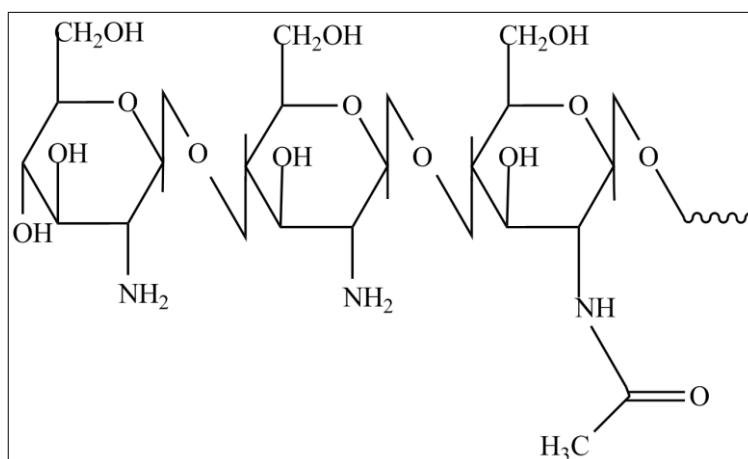


**Figure 1.7.** Chemical structure of chitosan.

Molecular weight of chitosan ranges from 300 to over 1000 kDa, depending on the source and processing conditions, with a degree of deacetylation ranging in between 30-95%. Deacetylation degree of chitosan is an influential factor on both

chemical and biological properties of the polymer because as deacetylation degree increases, so does the presence of free amino groups which effects the overall chemical properties and biological functions related. Chitosan is a semi-crystalline polymer whose crystallinity highly depends on the degree of deacetylation. Maximum crystallinity is observed for 0% and 100% deacetylated forms and minimum values are obtained in the intermediate range of deacetylation degree. Additionally, crystallinity increases with increasing degree of deacetylation in intermediate range (Yuan *et. al.*, 2011). Crystallinity of the polymer affects its degradation rate inversely whereby enhancing the polymer stiffness and stability.

Chitosan gains its high potential as a biomaterial most essentially from its cationic nature and high charge density. Owing to embody amino groups with pKa around 6.5, chitosan is soluble under mild acidic conditions. At low pH, amino groups become protonated and positively charged resulting in a cationic polyelectrolyte nature. These properties enable chitosan to interact electrostaticly with anionic species such as proteoglycans and glycosamineglycans that modulate cytokine and growth factor activities (Costa-Pinto *et. al.*, 2011). As a result, chitosan becomes a good substrate for cell propagation in addition of being a good vehicle for anionic drug or bioactive agent delivery. Polyelectrolyte complex (PEC) formation between chitosan and negatively charged polyions of either natural or synthetic origin has also been used in biological applications. Among PECs of chitosan, the ones prepared by alginate are specifically employed in controlled drug delivery systems. Delivery of vascular endothelial growth factor (VEGF) and human mesenchymal stem cells (hMSCs) from chitosan-alginate PEC scaffolds were reported to be successful indicating the potential of these structures to be used in controlled delivery of proteins and cells (De La Riva *et. al.*, 2009; Tai *et. al.*, 2010).

Chitosan possesses intrinsic antibacterial activity which stands as an advantage for the use of it as a biomaterial. Composite scaffolds incorporating chitosan were employed in orthopaedic applications to gain the scaffold antibacterial characteristics (Madhumathi *et. al.*, 2009; Wu *et. al.*, 2012).

Due to proven to be biodegradable, biocompatible, non-antigenic, non-toxic, antibacterial and biofunctional, chitosan has gain much of an interest as a useful material in the field of tissue engineering. Additionally, chitosan has been shown to promote mineral rich matrix deposition by osteoblast cells and enhance bone formation; therefore, it is an excellent material for bone tissue engineering applications in particular (Mathews *et. al.*, 2011; Zhong and Chu, 2012).

Chitosan is an easily processable polymer so that scaffolds can be fabricated by a variety of techniques such as spinning, freeze drying, robocasting and rapid prototyping. Chitosan scaffolds modified with addition of protein binding peptides, dexamethasone, carbon nanotubes, silicon dioxide and zirconia to the structure have shown enhanced biomineralization, bioadhesion and alkaline phosphatase (ALP) activity (Pattnaik *et. al.*, 2011; Tsai *et. al.*, 2012; Chiang *et. al.*, 2012; Venkatesan *et. al.*, 2012). In order to improve already existing favorable properties of chitosan in the field of bone tissue engineering, it is also used as composites with natural polymers, synthetic polymers and ceramics. Collagen, silk, gelatin and alginate are some of the mostly used polymers for that purpose together with hydroxyapatite as the most frequently used bioceramic.

Blending chitosan with a novel human like collagen and fabricating electrospun scaffolds resulted in structures with the potential to mimic native ECM and grow bone marrow stromal cells (Chen *et. al.*, 2011). Silk fibroin/chitosan scaffolds were reported to support chondrogenic differentiation of MSCs with enhanced mechanical properties compared to pure chitosan (Bharwaj and Kundu, 2012). Chitosan-gelatin scaffolds including hydroxyapatite were shown to be appropriate cell carriers for bone tissue engineering (Isikli *et. al.*, 2012). Incorporation of  $\beta$ -tricalcium phosphate into chitosan-gelatin scaffolds produced by radiation synthesis were examined in vivo and revealed accelerated bone regeneration (Zhou *et. al.*, 2012). Scaffolds composed of chitosan and ceramics such as hydroxyapatite, calcium phosphates and bioactive glass, were studied yielding applicable scaffolds for bone defects exhibiting highly bioactive and mechanically

strengthened scaffolds (Dorj *et. al.*, 2012; Karakecili and Arikan, 2012). Chitosan has also been employed in the form of injectable scaffolds that hydrogelation occurs after injection into the body (Huang *et. al.*, 2011). Biomimetic scaffold production by using chitosan fibrous structures is another emerging approach for successful bone tissue engineering scaffolds (Tanase *et. al.*, 2011, Li *et. al.*, 2012).

### 1.3.1.1.2. Alginate

Alginate is a linear polysaccharide copolymer, derived from brown sea algae and composed of 1-4 linked  $\beta$ -D-mannuronic acid (M) and  $\alpha$ -L-guluronic acid (G) residues. Repeating units of alginate, differing only in orientation, can either be sequenced in a repeating or alternating manner. Composition and sequential structure are highly effective on the properties and functionality of this natural polymer mainly through G units as the binding sites.

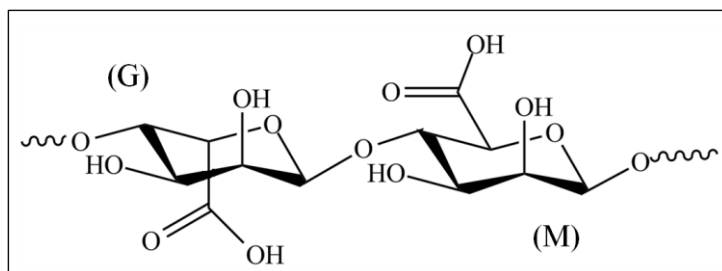


**Figure 1.8.** Chemical structure of alginate composed of G and M units.

Sodium salt of alginate is soluble in water but when ionically crosslinked, alginate can stay stable in distilled water even at moderately high temperatures.

Ionic crosslinking of alginate is achieved through cooperative binding of functional negatively charged carboxyl groups of G units to divalent cations. The structure formed as a result is defined as egg-box model. Among many candidates, calcium ( $\text{Ca}^{2+}$ ) is the most frequently used cation for alginate crosslinking since it is also a natural component of our biological system and considered biocompatible. However, ionic crosslink of alginate tends to break down easily when subjected to solutions containing salt ions like phosphate buffer saline (PBS) or simulated body fluid (SBF) due to cation exchange. Covalent crosslinking can be used to enhance the stability of alginate however the methods and chemicals required often shows toxicity towards cells. Covalent crosslinking of alginate by photopolymerization is a commonly used method where photoinitiators that are incorporated in the structure start radical polymerization upon exposure to UV light. However, the photoinitiators used and formation of free radicals during polymerization lead to cell toxicity (Kerim and Cherie, 2009; Hall *et. al.*, 2011). Carbodiimide chemistry is an alternative for covalent crosslinking of alginate. Adipic hydrazide and poly ethylene glycol (PEG) are often employed in crosslinking of alginate for that purpose resulting in increased stability and enhanced mechanical properties (Eiselt *et. al.*, 1999; Lee *et. al.*, 2000; Augst *et. al.*, 2006).

Being nontoxic, biodegradable and biocompatible makes alginate a useful biomaterial in tissue engineering and drug delivery applications. However, depending on the conditions of use, mechanical weakness, poor stability and lack of cellular interactions resulting from the hydrophilic nature of alginate may need to be handled through modifications.

In order to overcome the cellular interaction deficiency of alginate, modification by cell adhesion ligands of either peptide or protein origin are proposed. The tripeptide Arginine-Glycine-Aspartic acid (RGD) sequence is a binding motif for integrins which are the receptors mediating cell-tissue attachment. RGD modification of alginate for tissue engineering applications has been reported to be effective in promoting cellular interactions of the material. When modified via RGD

containing peptide, alginate hydrogel scaffold was shown to develop significantly higher bone formation in vivo (Alsberg *et. al.*, 2001; Alsberg *et. al.*, 2003). Investigations of the effects of RGD modification on MSC behavior on alginate revealed high viability, proliferation and differentiation of cells (Duggal *et. al.*, 2009; Re'em *et. al.*, 2010). Strontium crosslinked alginate hydrogels with RGD modification resulted in well designed scaffolds for bone tissue engineering applications combining cell adhesion properties of peptide sequence and osteoconductivity of strontium ion (Place *et. al.*, 2011). Besides RGD sequence, polyproline-rich synthetic peptides were also shown to enhance cell adhesion and gene expression when incorporated in alginate scaffolds due to their compositional resemblance to natural bone ECM components (Rubert *et. al.*, 2012). Modification of alginate by proteins that are natural components of bone ECM structure improve cellular interactions as well. Including collagen type I, fibronectin and laminin to alginate structure displayed efficiency in regulating cell-matrix communications (Kreeger *et. al.*, 2006).

Alginate has low mechanical strength and stability, therefore, in bone tissue engineering applications it is generally used within composite scaffolds with natural polymers, synthetic polymers or ceramics to overcome such drawback. Due to being a polyanion, alginate can form polyelectrolyte complex (PEC) with cationic polymers such as chitosan. Blending alginate with chitosan results in mechanically improved, promising scaffolds (Tai *et. al.*, 2010; Florczyk *et. al.*, 2011). Composite sponge scaffolds of alginate and collagen have been proposed for bone repair procedures with adequate mechanical strength and bioactive delivery features (Wu *et. al.*, 2011; Lee *et. al.*, 2012). Alginate-gelatin injectable scaffolds were studied where bone healing and formation was observed in vivo (Xia *et. al.*, 2012). Among synthetic polymers, PLGA and PLA were often used in composite scaffolds of alginate. Infiltrating the macropores of alginate scaffold with PLGA or using PLGA scaffold as a template to incorporate alginate hydrogel increased the mechanical properties of scaffolds in a great extent and made them suitable to be used in bone defects (Qi *et. al.*, 2009; Hsu *et. al.*, 2011). PLA-alginate composites were also

evaluated and shown to be good candidates for vascular endothelial growth factor release (VEGF) to enhance neovascularization in bone healing in vivo (De La Riva *et. al.*, 2009). Blends of alginate with ceramics resulted in successful scaffolds for bone tissue engineering as well. Alginate-hydroxyapatite composite scaffolds were reported to be designed in a similar structure to trabecular bone (Turco *et. al.*, 2009). Calcium phosphate compounds were blended with alginate to enhance both the mechanical properties and the osteoconductivity of scaffolds (Shiraishi *et. al.*, 2010; Beherei *et. al.*, 2011). Incorporation of bioactive glass into alginate matrix was another attempt eventuated successful for bone repair and regeneration applications with improved bioactivity, stability and mechanical strength (Valenzuela *et. al.*, 2012).

Alginate has been employed in bone tissue engineering applications in solid scaffold, hydrogel or injectable forms. Another application of alginate, also used in this work, is using alginate as a coating material for the scaffolds to enhance the control over the release of bioactive agents and prevent burst release to some extent (Lee *et. al.*, 2012; Erol *et. al.*, 2012).

### **1.3.1.2. Methods Used in Scaffold Production**

In the case of scaffold production, the fabrication process to be used plays a significant role on the properties of the resultant scaffold. Therefore, choosing an appropriate production technique gains much importance in order to have a scaffold that fulfills the desired properties for a specific tissue engineering application (Sachlos and Czernuszka, 2003).

When deciding on the method of use one should consider certain criteria. Most importantly, the process should not unfavorably alter the material properties which would also result alterations in the chemical properties and biological performance of the material. Method to be used should enable the production of scaffolds bearing desired properties accurately and consistently such as porosity,

interconnectivity etc. Moreover, scaffolds prepared from different batches should possess minimal variations in their properties. Being economically favorable, easily manufacturable and reproducible are also desired characteristics for a scaffold production method.

In scaffold fabrication for bone tissue engineering applications, some of the techniques frequently used are solvent casting, gas foaming, phase separation, melt moulding, spinning and rapid prototyping.

In solvent casting method, polymer is first dissolved in a volatile organic solvent or water, then, removal of the solvent takes place that results in a porous structure. Solvent removal can be achieved by freeze drying process, also named as lyophilization. In freeze drying, samples are cooled down to very low temperatures at about  $-80^{\circ}\text{C}$  under vacuum that eventually results in removal of the solvent by sublimation. In order to create tailored pore size and highly porous structure, salt particles may be added into the dissolved polymer solution as porogens. After molding and removal of the solvent, salt particles are washed out and removed in a bath which is referred as salt leaching process (Karageorgiou and Kaplan, 2005). Solvent casting method has been used extensively in 2D membrane fabrication. Chitosan membranes containing bioactive glass or calcium phosphate were prepared by solvent casting method to be used in bone tissue engineering applications (Caridade *et. al.*, 2010; Lee *et. al.*, 2011). 3D scaffolds of synthetic or natural polymers and ceramics for bone repair have also been manufactured by a combined solvent casting/ salt leaching process. Gelatin/bioactive glass nanocomposite structures were fabricated by solvent casting with tailored pore size and porosity (Mozafari *et. al.*, 2010). By a combined solvent casting/salt leaching process hydroxyapatite/nylon 6,6 scaffolds were prepared and characterized to be used in bone defects (Mehrabanian and Nasr-Esfahani, 2011). Similarly, PCL scaffolds were fabricated with using sodium chloride particles as porogens and resultant scaffolds were proposed to be used in bone defects (Wu *et. al.*, 2012).

In gas foaming process, polymer solution is saturated with carbon dioxide or another inert gas at high pressure followed by stepwise lowering to atmospheric level, thus, decreasing the solubility of gas within the polymer solution and forming pores (Mooney *et. al.*, 1996). Gas foaming process is used for fabricating scaffolds with tailorable pore size and pore density which are critical variables for bone tissue engineering scaffolds. Polylactic acid (PLA) scaffolds containing  $\beta$ -tricalcium phosphate was prepared by gas foaming process and shown to be successful in bone tissue repair in vivo (Van Der Pol *et. al.*, 2010). Gas foaming was used for fabricating poly-d-lactic acid (PDLA) foams with tunable structure and mechanical anisotropy which holds an important aspect for bone tissue engineering applications (Floren *et. al.*, 2011). In another study, calcium phosphate cements were prepared by gas foaming with adequate pore size to encapsulate human umbilical cord stem cells and scaffolds were prepared with adequate pore size, scaffold density and mechanical strength for cancellous bone tissue engineering (Chen *et. al.*, 2012). Combination of gas foaming with salt leaching was also used for production of designed scaffolds with tuning the scaffold properties by varying processing parameters (Leung and Naguib, 2012).

Phase separation technique can be employed with two different processes to obtain porous structures. First method includes dissolution of polymer in an organic solvent and adding water into the system to form an emulsion. After the solution is quenched, removal of dispersed water and solvent by lyophilization results in porous scaffolds. Second method of liquid-liquid phase separation employs polymer rich and polymer poor phase formation in a single polymer solution prepared by dissolving polymer in an easily subliming solvent. Cooling down the solution below the melting point of the solvent and applying vacuum gives porous scaffolds as solvent of polymer poor portions sublimes (Lo *et. al.*, 1995). Phase separation is widely used to prepare bone tissue engineering scaffolds. Composite scaffolds of titanium/gelatin/hydroxyapatite and gelatin/silica, differing in compositions, were prepared by using phase separation technique which enabled production of hybrid scaffolds with homogenous phase distribution (Kailasanathan *et. al.*, 2012; Lei *et. al.*,

2012). Phase separation method was used for fabrication of scaffolds from synthetic polymers with designed architecture. Using room temperature ionic liquids (RTIL) as porogens, PLA scaffolds with open-channeled network and tuned pore size were fabricated (Lee *et. al.*, 2012). By combining phase separation with salt leaching method, tyrosine derived polycarbonate scaffolds mimicking bone architecture were produced and shown to promote bone regeneration in vivo (Kim *et. al.*, 2012). Phase separation is a convenient method to fabricate chitosan composite scaffolds as well. Scaffolds of chitosan composited with either PLA or hydroxyapatite/gelatin blend were fabricated with phase separation method having biomimetic structure (Zhao *et. al.*, 2012; Selgren and Ma, 2012).

In the case of melt molding, polymers are melt, therefore, it is a nonsolvent technique. In order to obtain porous scaffolds by this method it is combined with particulate leaching process. After addition of porogens into the melt polymer, the solution is molded and cooled down. As the last step, porogens are removed by dissolution and porous scaffolds are obtained by this process. Melt molding can be used to produce scaffolds from polymer blends without the use of organic solvents. PLGA/PVA scaffolds were prepared by melt molding method with the aim of using in bone defects and in vivo studies supported their compatibility via observed bone ingrowth (Oh *et. al.*, 2003). PLGA/hydroxyapatite composites were also prepared by melt molding and particulate leaching methods. Resultant scaffolds were reported as highly porous with evenly distributed interconnected pore structure (Cui *et. al.*, 2009). Melt molding method can be applied to chitosan as well. Chitosan composite scaffolds with polybutylene succinate were prepared by compression molding followed by particulate leaching and shown to be suitable for trabecular bone repair with adequate mechanical properties and confirmed high ALP activity levels (Costa-Pinto *et. al.*, 2008; Oliveira *et. al.*, 2008).

Rapid prototyping, also named as solid free form manufacturing, represents a number of sophisticated manufacturing techniques based on using computer-aided design (CAD) data to fabricate scaffolds with any specific visual design. Since the

morphology of scaffolds is highly effective on protein adsorption, cell behavior and tissue formation rapid prototyping is an advantageous method for scaffold production. In a recent study, it was reported that 3D structure of scaffolds has important effects on the permeability as well which is a measure of scaffold's ability to allow for the flow of nutrients and waste products. 3D printed scaffolds with defined geometries were stated as potential scaffolds to be produced with adjusted permeability (Lipowiecki *et. al.*, 2012). Rapid prototyping methods has also been used to prepare scaffolds with determined pore size and pore distribution and geometry with the aim of achieving precise control on biological and mechanical properties of produced scaffolds (Alge *et. al.*, 2012; Chen *et. al.*, 2012). Additionally, rapid prototyping is considered as a primal step for organ printing which is a newly developing technology as the future of organ repair and regeneration approach (Federovich *et. al.*, 2011).

Spinning techniques include melt spinning, dry spinning, electrospinning, gel spinning and wet spinning methods by which fibrous structures can be obtained. Melt spun fibers are obtained by rapid cooling and solidification of extruded solution of melt polymer. Starch-PCL and starch-PLA composite scaffolds were reported convenient for bone defects prepared by melt spinning method (Gomes *et. al.*, 2008). In dry-spinning, polymers are dissolved in a solvent first and solidification is achieved by the removal of the solvent by a stream of air or inert gas. Electrospinning is the most commonly used spinning procedure in fabrication of scaffolds and it uses an electrical charge to draw very fine fibers from a liquid solution. By using electrospinning, fibers in nano scale can be produced which has the advantage of very high surface to volume ratio for enhanced cell interactions and resemblance to native bone structure composed of collagen fibers. Hierarchical fibrous structure of bone was mimicked by electrospinning of titanium oxide nanonets in a recent study (Kao *et. al.*, 2012). Additionally, electrospinning was used for fabrication of scaffolds with adjusted fiber roughness that affects the cellular behaviors (Luo *et. al.*, 2012). Fiber orientation is a parameter effective on

mechanical strength and bone regeneration ability of scaffolds and can be modulated by use of electrospinning process as well (Andric *et. al.*, 2012).

#### **1.3.1.2.1. A Comprehensive Technique for Scaffold Production: Wet Spinning**

Wet spinning is a comprehensive technique used in order to produce fibers from viscous polymer solutions. The main principle behind this technique is the coagulation of a viscous polymer solution in a nonsolvent liquid bath through diffusional interchange of components present in both phases (Paul, 1968). As polymer solution is injected into the coagulation medium, the solidification may occur as a result of either a chemical reaction between the polymer solution and coagulant, or a physical exchange of solvent and nonsolvent resulting in precipitation of the polymer. The progress of solidification proceeds from outer shell to inner core of the filaments as the diffusion process continues which is called as boundary motion (Knaul and Creber, 1997). Therefore, the rate of diffusion defines the rate of fiber formation in a wet spinning process. The properties of produced fibers are affected by spinning conditions such as components and concentration of coagulation bath and incubation period.

In the case of wet spinning of chitosan with amine groups (Ch-NH<sub>2</sub>), the precipitation occurs through an acid-base reaction. In a system involving chitosan solution dissolved in acetic acid and wet spun into NaOH solution, the reaction mechanism proceeds by the proton exchange between acid and base that results in precipitation of chitosan in the form of fibers as given in Figure 1.9.

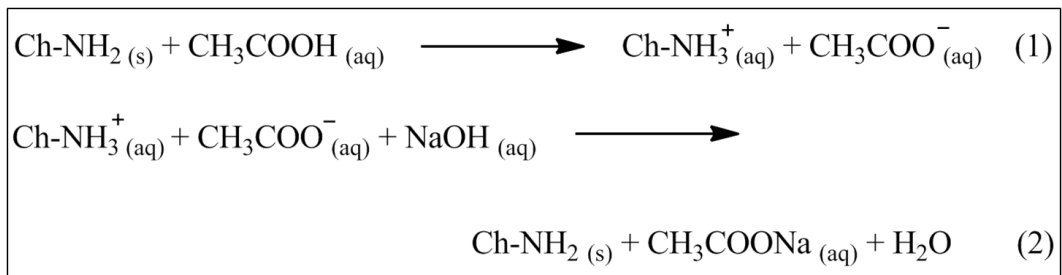


**Figure 1.9.** Reaction mechanism for dissolution of chitosan in acetic acid (1) and coagulation in sodium hydroxide bath as a result of proton exchange (2).

The rate of chitosan fiber formation in basic coagulation bath and effects of variables were investigated by following the boundary motion in filaments. It was shown that the boundary position is linearly proportional to the square root of time spent in coagulation bath and proceeds forward with increasing concentration of coagulant agents. Additionally, it was demonstrated that as the diffusivity of ions increase by increasing temperature so does the rate of chitosan fiber formation (Knaul and Creber, 1997; El-Tahlawy and Hudson, 2005).

In bone tissue engineering applications, wet spinning technique has been employed successfully with both synthetic and natural polymers to fabricate scaffolds with defined and controlled fibrous structure. Wet spun PLGA fibrous scaffolds with human bone marrow stromal cell (hBMSC) incorporation were proposed to initiate bone repair and regeneration and shown type I collagen deposition, mineralization and high ALP activity in vivo (Morgan *et. al.*, 2007). Among synthetic polymers, PCL has also been used widely for wet spun scaffold preparation to be used in bone tissue engineering applications. PCL scaffolds carrying antimicrobial agents were produced by wet spinning and cultured with pre-osteoblast cells. Results demonstrated good cell adhesion and viability on scaffolds (Puppi *et. al.*, 2011). Wet spinning of PCL blends with natural polymers were employed in scaffold production for bone tissue. PCL-chitosan blend resulted in

adjustable fiber characteristics such as roughness, porosity and fiber diameter via wet spinning (Malheiro *et. al.*, 2010). Wet spinning was also applied as a new method to produce fibrous starch-PCL scaffolds and their modification via argon plasma treatment or incorporation of silanol groups resulted in successful scaffolds for stimulating bone ingrowth (Tuzlakoglu *et. al.*, 2010; Leonor *et. al.*, 2011).

Successful applications of fibrous chitosan scaffolds prepared by wet spinning technique in bone repair have been mentioned in literature. Wet spun chitosan meshes were characterized and proposed as suitable scaffolds for tissue engineering applications (Tuzlakoglu *et. al.*, 2004). Chitosan fiber meshes fabricated by this method were simply coated with bioglass via spraying to form an apatite layer and specialized for bone tissue engineering purposes. They were shown to promote adhesion and spreading of human osteoblast-like cells accordingly (Tuzlakoglu and Reis, 2007). Using chitosan fibrous mesh scaffolds as delivery systems for BMP-2 and BMP-7 eventuated in promising results for the production of tissue engineered bone (Yilgor *et. al.*, 2009).

Also, recent studies show that incorporation of wet spinning and electrospinning may be promising for fabrication of scaffolds possessing similar properties to natural extracellular matrix by the combination of nano and micro fibers (Tuzlakoglu *et. al.*, 2011).

### **1.3.2. Controlled Delivery of Bioactive Agents in Bone Tissue Engineering**

Administration of bioactive agents into the body can be achieved through either systematic or local delivery. In the case of systematic delivery, bioactive agent is supplied to the blood stream and distributed over by the circulatory system. Shortcomings associated with that type of administration can be stated as systematic toxicity due to use of high doses, liver complications, disperse of supplied agent to non targeted sites and inadequate penetration at target site (Su *et. al.*, 2012). In local

delivery, on the other hand, these problems can be overcome and concentration of delivered agent can be enhanced at target site with avoiding use of overdose in body.

Along with local delivery, introduction of bioactive agents to the defect site with respect to time should also be regulated for the most effective treatment in healing and regeneration of tissues. The main objective of controlled release is maintaining the optimal concentration of bioactive agent at the target site for a desired time frame (Blitterswijk, 2008). Regulating the time period of delivery and the release rate of agents to maintain effective concentration instead of burst release is highly beneficial since tissue regeneration is a progressive long term process.

Bone tissue engineering scaffolds are used for local delivery of bioactive agents in a controlled manner in order to achieve the most beneficial treatment at the target site. Due to the patient-specific requirements in delivery mode of bioactive agents, tunable release kinetics is essential.

Bioactive agents may either be interspersed or immobilized into the scaffolds. In the interspersed loading, primary consideration should be the safe encapsulation and protection of bioactive factors. In that case, release kinetics depends on both the diffusional characteristics of the encapsulated agent and the degradation rate of the carrier. Bioactive agents can be loaded into the scaffolds directly or through the use of micro and nano capsules, spheres, micelles and liposomes as carriers. Scaffolds either in hydrogel or solid forms have been mentioned for delivery of bioactive molecules without incorporation of an additional carrier system. Drug release from poly vinyl alcohol (PVA) and poly ethylene glycol (PEG) hydrogels revealed that the typical release behavior for hydrogels is an initial burst release occurring during the swelling of hydrogel (Jeong *et. al.*, 2000; Huang and Brazel, 2003; Leach and Schmidt, 2005). Scaffolds of chitosan prepared by lyophilization was studied in delivery of dexamethasone loaded via impregnation by vacuum but results showed poor release profile (Duarte *et. al.*, 2009). PLGA-calcium phosphate hybrid scaffolds prepared by 3D printing were examined for growth factor delivery by incorporation of BMP-2 either within the matrix or onto the scaffolds. Sustained release of BMP-2

was observed when loaded onto the scaffolds whereas no release was observed for incorporation of the growth factor within the matrix due to strong interactions in between (Chen *et. al.*, 2012). In order to have a better control on the release behavior of scaffolds, delivery of bioactive molecules are carried out by incorporating the molecules to the scaffolds via loading to additional carriers. Growth factor delivery from porous hydroxyapatite scaffolds were carried out by the use of PLGA microspheres and a sustained release profile up to 4 weeks was achieved (Son *et. al.*, 2011). Similarly, delivery of fibroblast growth factor (FGF) loaded in heparin based nanoparticles from chitosan electrospun scaffolds was shown to be successful (Zomer *et. al.*, 2012). By controlled release of BMP-2 from chitosan microspheres incorporated in collagen sponge, enhanced bone repair and regeneration was observed in vivo (Hou *et. al.*, 2012).

In order to regulate the delivery characteristics and release rate, bioactive factors can be immobilized within the scaffold matrix so that scaffold itself interacts with the surrounding. The release kinetics of immobilized agents become dependent on binding sites, affinity of the active molecules to these binding sites and degradation rate of the scaffold (Biondi *et. al.*, 2008). Comparison of the efficacy of BMP-2 delivery either by immobilization or adsorption on chitosan nanofibrous template revealed promoted cell adhesion, increased ALP activity and enhanced mineralization on scaffolds with immobilized growth factor on the surface (Park *et. al.*, 2006). Immobilization of growth factor carrying nanospheres on fibrous PLLA scaffolds was considered as another approach yielding prolonged release profile from the scaffold with the growth factor maintaining its activity (Wei *et. al.*, 2007). Chemically crosslinking platelet derived growth factor (PDGF) to the demineralized bone matrix resulted in efficient delivery of the growth factor maintaining its activity and functionalized scaffold material (Chen *et. al.*, 2009). Binding bone specific enzymes on scaffolds has been proposed for superior bone repair and regeneration. Immobilization of alkaline phosphatase and soybean peroxidase on fibrin or bioactive glass scaffolds were shown to amplify mineral deposition (Osathanon *et. al.*, 2009; Aina *et. al.*, 2011).

Different release modes can be induced in a delivery system as continuous or pulsatile delivery as represented in Figure 1.10.

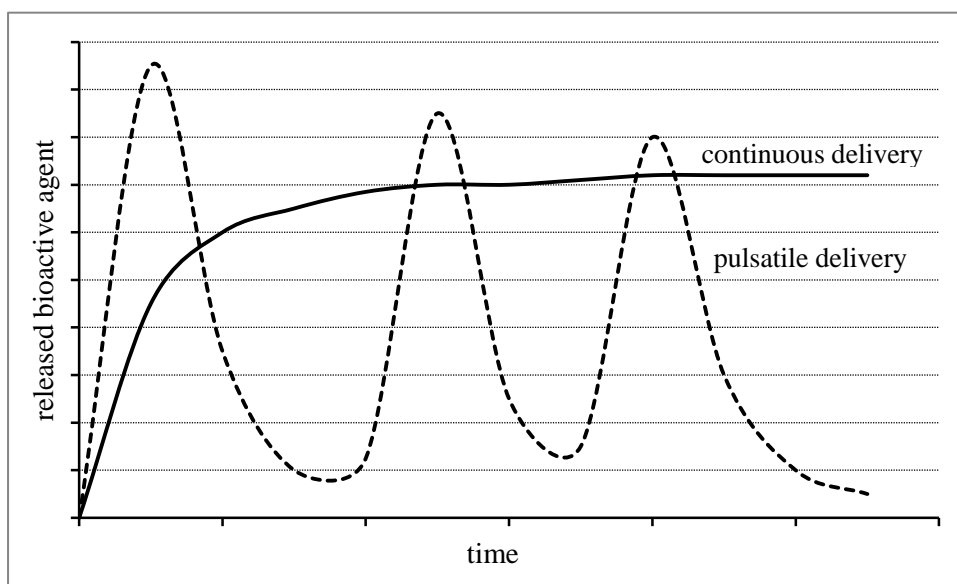


**Figure 1.10.** Representative release curves for continuous and pulsatile delivery.

Continuous delivery of bioactive molecules can be induced from biodegradable or non biodegradable scaffolds, and by regulating the release rate sustained release of molecules can be achieved. The impacts of growth hormone (GH) delivery on bone metabolism were examined in a human study by comparing the effects of continuous versus pulsatile release. It was shown that continuous delivery of GH attained by sustained release was more efficient on bone metabolism (Laursen, 2004). Layered films of hydroxide clay and PLGA were used for antibiotic administration to orthopedic surgical sites and delivery of the drug with a continuous release profile was stated as favorable (Chakraborti *et. al.*, 2012). Sustained release

of growth factors achieved by immobilization on the scaffolds was featured long term delivery systems for bone repair and regeneration (Schliephake *et. al.*, 2012; Zumstein *et. al.*, 2012). Pulsatile release profiles are used when periodic release of bioactive factors is aimed and can be achieved by either programmed or triggered release modes. In programmed release, release kinetics is regulated by inner mechanism of the scaffold whereas in triggered mode release kinetics is governed by the physiological changes in the environment such as pH or temperature.

Polymeric micelles and vesicles with tailorable release mechanisms have been employed in pulsatile delivery of bioactive agents. (Rijcken *et. al.*, 2007). In order to attain pulsatile release, microspheres that were sequentially layered as loaded and empty were used and demonstrated to be successful in on-off release of simvastatin acid which is reported to stimulate bone formation upon daily injection (Jeon *et. al.*, 2007). Parathyroid hormone (PTH) is known to improve mineral density and strength of bone, therefore, has been used in treatment of osteoporosis by daily injection. For the purpose of subcutaneous pulsatile delivery of PTH, three layered polymeric device was fabricated and pulsatile release profile was demonstrated (Liu *et. al.*, 2007). Dexamethasone containing N-(2-hydroxypropyl) methacrylamide (HPMA) copolymer was synthesized and used in pH triggered release of dexamethasone which inhibits bone resorption (Liu *et. al.*, 2008).

By the use of controlled delivery approach, antibiotics and proteins to prevent infections and regulate the progress of repair and regeneration can be administered locally with optimized concentrations in a time dependent manner.

### **1.3.2.1. Antibiotic Delivery in Bone Tissue Engineering**

In bone tissue engineering applications, antibiotic delivery is aimed for both prophylaxis and treatment purposes against micro organisms causing infections.

Upon implantation of a biomaterial, there may occur bacterial infection as a result of bacteria adhesion to the surface of the implant. Sources of contamination include air, resident bacteria on patient's skin and body (Mourino and Boccaccini, 2010). When accumulated, bacteria inhibit the wound healing process and form a biofilm on the implant surface that prevents the integration of the implant with surrounding tissue. In order to avoid associated problems, use of antibiotics as prophylactic agents is necessary. Since systematic administration of drugs shows lack of efficiency, controlled delivery systems are used for antibiotic delivery to the defect site. Local release profiles of antibiotics should display a burst release first as a response to elevated risk of infection upon implantation and a following sustained release to keep the antibiotic level at an efficient concentration to suppress latent bacteria activities (Zilberman and Elsner, 2008). Incorporation of antibiotics to the bone tissue engineering scaffolds was shown to be effective in reducing bacterial activity and enhancing healing and regeneration through inhibition of bacterium proliferation and biofilm formation (Zhu *et. al.*, 2010; Zhang *et. al.*, 2012).

Antibiotics are also used as therapeutic agents in the treatment of bone diseases. Osteomyelitis is infection of bone which is conventionally treated by administration of high doses of antibiotics intravenously for 4-6 weeks. Use of local controlled delivery systems for treatment of osteomyelitis has been proposed lately. Administration of antibiotics through scaffolds made up of PLA, glass ceramics and calcium phosphate were reported as potential therapeutic approaches against osteomyelitis (Cao *et. al.*, 2012; Thanyaphoo and Kaewsrichan, 2012; Kundu *et. al.*, 2012).

Among antibiotics vancomycin, tobramycin, and gentamicin sulphate have been commonly employed in orthopedic applications. In vivo studies show that sustained release of vancomycin from polyurethane scaffolds inhibits infection of bone wounds and improve healing (Li *et. al.*, 2010; Guelcher *et. al.*, 2011). Delivery of tobramycin together with demineralized bone matrix proteins demonstrated total healing of bone defects in vivo (Galjour *et. al.*, 2005). Tobramycin loaded ceramic

capsules were also proposed as potential delivery systems to bone defect sites in order to prevent infection (Benghuzzi *et. al.*, 2006). Gentamicin, also used in this study, is a commonly employed broad range antibiotic in orthopedic applications. Scaffolds possessing sustained release of gentamicin were demonstrated to show excellent antibacterial properties and potential to treat bone infections (Lee *et. al.*, 2012; Balmayor *et. al.*, 2012).

### **1.3.2.2. Protein Delivery in Bone Tissue Engineering**

Repair and regeneration processes proceed through the cellular activities; therefore, regulating cellular activities is the key to have a control on the progress of fracture healing. Cellular behaviors such as proliferation, adhesion and function are known to be modulated by signaling protein molecules (Baldwin and Saltzman, 1998). Therefore, administration of proteins is a commonly used approach to enhance bone healing. Due to the short half-life and potential toxicity of proteins upon systematic administration, local delivery to the defect site has been employed as a successful tissue engineering approach.

In the case of bone healing, tissue repair and regeneration is mainly controlled by growth factors. Growth factors are signaling molecules that initiate and regulate cellular activities through specific binding to receptor sites on cell membranes. Dependent on their role, growth factors can stimulate or inhibit cell adhesion, proliferation, directed differentiation and so on. Growth factors which are secreted by cells, act in a time and concentration dependent manner in order to regulate cellular activities in body, therefore, release profiles from scaffolds should be adjusted as well when delivered locally. In bone tissue engineering applications, fibroblast growth factors (FGFs), transforming growth factor beta (TGF- $\beta$ ) with the subgroup of bone morphogenetic proteins (BMPs), vascular endothelial growth factor (VEGF), insulin like growth factor (IGF) and platelet driven growth factor (PDGF) are the most commonly employed ones due to being the most effective factors acting on bone (Schilephake, 2002).

FGFs are polypeptides responsible of proliferation of bone marrow cells, osteoblasts, chondrocytes, fibroblasts and endothelial cells. FGF-1 and FGF-2 are the most abundant members of this family secreted in early phases of one healing process. Controlled in vivo release of FGF-2 from ceramic scaffolds and adipose stem cell containing biomimetic scaffolds was shown to induce and significantly increase bone formation (Tsurushima *et. al.*, 2010; Kwan *et. al.*, 2011). Use of FGF delivery as an alternative to bone marrow derived stem cell transfer was investigated and revealed promising results (Takagi *et. al.*, 2011). VEGFs are secreted by endothelial cells and osteoblasts. During healing, they are responsible of angiogenesis and act on the conversion of cartilage into bone tissue. Effects of incorporating VEGF to PLGA porous scaffolds were examined and neovascularization of scaffold, which is critical for successful tissue engineering, was observed (Lindhorst *et. al.*, 2010). In vivo release of VEGF from calcium phosphate ceramic scaffolds were shown to promote vascularization and bone formation in critical size bone defects (Wernike *et. al.*, 2010). Delivery of VEGF as an angiogenesis agent together with BMP-2 as an osteogenic factor from alginate-PLLA scaffolds resulted in new bone formation and proposed for critical size defect treatment (Kanczler *et. al.*, 2010). There exist two IGFs identified as IGF-1 and IGF-2. IGF-1 stimulates osteoblast proliferation and bone matrix formation whereas IGF-2 acts in the later phases of healing by acting on bone resorption. Release of IGF-1 from PLLA coatings on implants was shown to stimulate cell proliferation continuously (Strobel *et. al.*, 2011). Multiple delivery of IGF-1 and BMP-2 was demonstrated to result in higher ALP activity associated with bone formation (Kim *et. al.*, 2012). PDGF acts in the early phase of bone repair by stimulating osteoprogenitor proliferation and also shows activity during remodeling stage. It is secreted by  $\alpha$ -granules at the beginning of fracture healing and then, by bone cells at bone repair site. Incorporation of PDGF into chitosan delivery system containing VEGF was stated to enhance bone formation (De La Riva *et. al.*, 2010). Dual delivery of PDGF with FGF from hydrogels established a sustained release profile and improved osteoblast total protein synthesis (Dyondi *et. al.*, 2011). For treatment

of critical size osteoporosis defects, bioglass-silk composite scaffolds loaded with PDGF and BMP-7 was evaluated *in vivo* and confirmed new bone formation (Zhang *et. al.*, 2012). TGF- $\beta$  superfamily consists of growth and differentiation factors (GDF), activins, inhibins and BMPs participating at all stages of healing and regeneration process. BMPs are critical components of bone formation process, therefore also crucial in fracture healing and regeneration. Among BMPs, BMP-2 and BMP-7 delivery are studied most commonly since both of these proteins are approved by food and drug administration (FDA). It is shown by numerous studies that, delivery of BMPs to the defect site dramatically enhances repair process of bone tissue (Bhakta *et. al.*, 2012; Zhang *et. al.*, 2012; Wehrhan *et. al.*, 2012; Hunziker *et. al.*, 2012; Bae *et. al.*, 2012; Shi *et. al.*, 2012). Delivery of BMPs in combination with other growth factors and multiple BMP delivery in a single system are also proven to be efficient especially when their release is sequenced in such a manner that mimics the natural healing process. Effects of sequential release of VEGF and BMP-2 on bone formation were investigated and efficiency of combining angiogenic and osteogenic growth factors were verified (Kempen *et. al.*, 2009). Sequential release of BMP-2 and BMP-7 from 3D scaffolds was associated with an increase in ALP activity (Yilgor *et. al.*, 2010). Sequestering the delivery of BMP-2 and IGF-1 by using layered scaffolds demonstrated enhanced early osteoblastic differentiation since both growth factors are secreted in early phases of fracture healing in body (Kim *et. al.*, 2012).

In this study, bovine serum albumin (BSA) was used as a model in order to investigate the release kinetics of proteins from the scaffolds.

#### **1.4. Aim, Novelty and Approach of the Thesis**

The aim of this study was designing a polymeric scaffold with adequate physical, chemical and biological properties to be used in bone tissue engineering with the feature of enabling delivery of bioactive agents.

For that purpose, two types of fibrous scaffolds either chitosan or alginate coated chitosan scaffolds, were prepared. Chitosan core was prepared by wet spinning in order to have fibrous structure with the advantages of large surface area for cell-scaffold interactions, porous structure and resemblance to native bone tissue. Alginate coating was introduced to enhance mechanical characteristics and controlled delivery of bioactive agents from the scaffolds. Resultant structures were characterized in terms of their morphology, chemical composition, mechanical properties, stability, bioactivity and water uptake and retention capacities with the aim of investigating their acceptability to be used in bone tissue engineering applications. Release kinetics of bioactive agents from the scaffolds were examined by use of gentamicin as a model antibiotic and bovine serum albumin (BSA) as a model protein.

As a result, it was concluded that produced scaffolds possesses favorable physical, chemical and biological characteristics to be used in bone repair and regeneration applications with the features of adjustable size, shape and mechanical strength. Additionally, they can be used for local delivery and controlled release of antibiotics and proteins either separately or simultaneously in accordance with the needs of treatment procedure.

## CHAPTER 2

### MATERIALS AND METHODS

#### 2.1. Materials

Chitosan low viscous (75-85% deacetylated) was obtained from Fluka (Osaka, Japan) and alginic acid sodium salt from brown algae was obtained from Sigma-Aldrich (St. Louis, USA). Salts of sodium sulphate (anhydrous extra pure), sodium hydrogen carbonate (extra pure, food grade), magnesium chloride hexahydrate (extra pure, food grade) and potassium hydrogen phosphate (anhydrous, extra pure) were purchased from Merck (Darmstadt, Germany). Potassium chloride ( $\geq 99\%$  purity) and sodium hydroxide ( $\geq 98\%$  purity) were obtained from J.T. Baker (Deventer, Holland). Methanol (free from acetone, pure) and glacial acetic acid were bought from Sigma-Aldrich (St. Louis, USA). Calcium chloride (pure, granular) used as crosslinker was from Riedel De Haen (Seelze, Germany). Bovine serum albumin was obtained from Boehringer-Mannheim (Mannheim, Germany) and coomassie plus the better Bradford assay kit was purchased from Thermo Scientific (Rockford, USA). Lysozyme from chicken egg white (activity of 96831 U/mg) was bought from Fluka (Bornem, Belgium). Dulbecco's Modified Eagle Medium (DMEM, high glucose) was supplied from Hyclone (Utah, USA). Gentamicin was purchased from Ulagay (Istanbul, Turkey).

## **2.2. Methods**

### **2.2.1. Preparation of Scaffolds**

Two types of scaffolds were prepared as fibrous chitosan and alginate coated chitosan scaffolds as described below.

#### **2.2.1.1. Production of Fibrous Chitosan Scaffolds by Wet Spinning**

Chitosan was dissolved in 2% (v/v) aqueous acetic acid to yield 4% (w/v) chitosan solution. Then, 0.6 mL portions of the prepared solution were injected into a coagulation bath of Na<sub>2</sub>SO<sub>4</sub> (0.5 M): NaOH (1 M): distilled water solution prepared in 3:1:6 (v/v) ratio using a syringe pump at a speed of 5 mL/h (New Era NE-1000, New York, USA). Fibers formed were kept in the coagulation bath overnight. They were then washed with distilled water few times and incubated in distilled water for 30 min. In order to dehydrate, fibers were incubated in 50% (v/v) methanol / water solution for 1 h and then 100% methanol for 3 h. After completion of the dehydration process, the fibers were placed into plastic cylindrical molds, with diameter of 1.2 cm and height of 1.0 cm, and dried at 54 °C for 2 h in oven. The process was schematically shown in Figure 2.1.

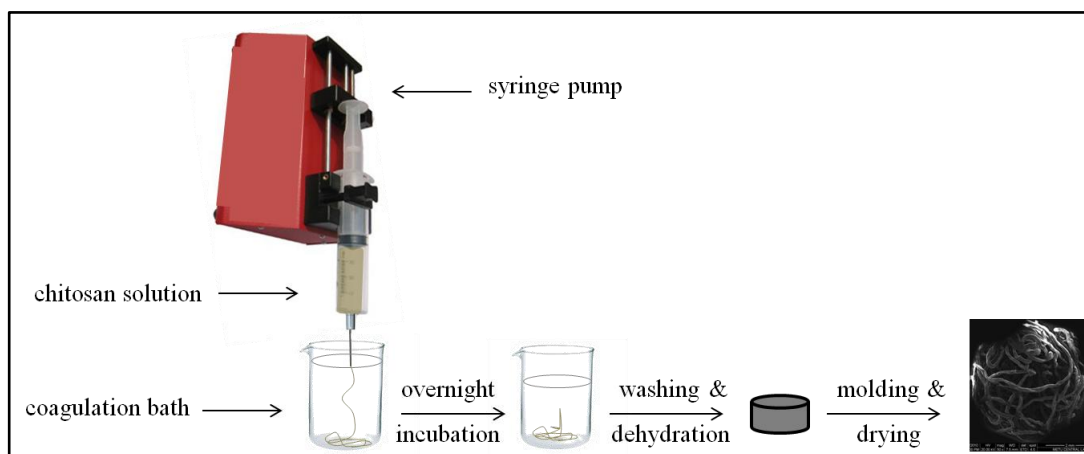


**Figure 2.1.** Schematic representation for the preparation of fibrous chitosan scaffolds by wet spinning technique.

### 2.2.1.2. Alginate Coated Fibrous Chitosan Scaffolds

The prepared chitosan scaffolds were put into 24 well-plates and 0.3 mL of 2% (v/v) aqueous alginate solution was introduced onto each structure by vacuum-pressure cycling. For this purpose, 0.1 mL portions of alginate were added and after each addition vacuum-cycling were performed. It is aimed to introduce alginate to all the fiber surfaces by vacuum pressure cycling process. Then the scaffolds were placed in clean well-plates for drainage overnight. Alginate layer was stabilized by using  $\text{CaCl}_2$  as crosslinker. Crosslinking was carried out through two different procedures as incubation crosslink and vacuum crosslink. In incubation crosslink, scaffolds were immersed in ethanol (2 mL) for 5 min and then incubated in 10% (w/v)  $\text{CaCl}_2$  solution (2 mL) prepared in 75% (v/v) aqueous ethanol solution for 10 min. Then, the samples were kept in 5% (w/v) aqueous  $\text{CaCl}_2$  solution (2 mL) for 1 h and in distilled water (2 mL) for an additional 1 h. Finally, scaffolds were rinsed with excess distilled water to remove any  $\text{CaCl}_2$  remaining on the surface and washed with ethanol before let to dry under vacuum. In vacuum crosslink, the same solutions

given above were used in the same order but instead of incubating scaffolds, the solutions were introduced in small portions (200  $\mu$ L) and after each addition vacuum-cycling was applied.

## **2.2.2. Structural Characterization of Scaffolds**

Scaffolds prepared were characterized in terms of presence of core-shell model structure and fiber thickness.

### **2.2.2.1. Determination of Fiber Thickness**

Fiber thickness determination of scaffolds was carried out by using light microscopy (Leica TCS SPE, Wetzlar, Germany). For that purpose, individual filaments of both uncoated and alginate coated chitosan fibers were prepared. Single filaments of chitosan were wet spun and for production of alginate coated filaments, they were immersed in 2% (w/v) alginate solution for 5 min, followed by incubation crosslinking process as described in section 2.2.1.2. Obtained filaments were imaged and thickness of fibers was measured from ten different points along each fiber using Adobe Photoshop program. Fiber thickness measurements were carried out on scaffolds as well, by the use of scanning electron microscopy (SEM) micrographs (Jeol JSM-6400 Electron Microscope, Tokyo, Japan).

### **2.2.2.2. Structure Analysis of Coated Scaffolds**

In order to investigate coating formation, scaffolds were frozen by immersing in liquid nitrogen and cut into half with a sharp razor. Cross sectional micrographs of the scaffolds were taken by SEM. In addition, SEM images of single filaments prepared as described above were obtained from an upper view to distinguish the formed alginate coat on chitosan core. Surface composition of both coated and

uncoated single filaments were examined by attenuated total reflectance Fourier transform infrared spectroscopy (ATR-FTIR) (Perkin Elmer Spectrum 65, Massachusetts, USA).

### 2.2.3. Water Uptake and Retention Capacities of Scaffolds

Water uptake and retention capacities of scaffolds were investigated for both uncoated and alginate coated chitosan scaffolds and calculated according to Equation (2.1) and Equation (2.2), respectively. Initial dry weights of scaffolds ( $W_d$ ) were recorded prior to incubation in distilled water for 24 h. In order to determine percent water uptake values ( $E_u$ ), scaffolds were weighed at the end of incubation period ( $W_u$ ). Then, each scaffold was placed in a centrifuge tube within a piece of filter paper at the bottom of the tube, and centrifuged at 1000 rpm for 3 min. Weight measurements after centrifugation ( $W_r$ ) were used to calculate the percent water retention values ( $E_r$ ) of scaffolds. Five replicate samples were used for each group. Same procedure was also repeated with high glucose culture medium instead of distilled water.

$$E_u(\%) = \frac{W_u - W_d}{W_d} \times 100 \quad \text{Equation (2.1)}$$

$$E_r(\%) = \frac{W_r - W_d}{W_d} \times 100 \quad \text{Equation (2.2)}$$

### 2.2.4. Degradation of Scaffolds

Degradation behavior of scaffolds was investigated in three different mediums namely as enzyme solution, phosphate buffer saline (PBS) and distilled water ( $dH_2O$ ).

Enzymatic degradation behavior of scaffolds was investigated by incubating both uncoated and alginate coated chitosan scaffolds in 5 mL of 1 mg/mL lysozyme solution, prepared in PBS (10 mM, pH=7), at 37°C in a shaking water bath. Enzyme solutions were refreshed in every two days to maintain enzyme activity. At predetermined time intervals (3, 7, 14, 21, 28, 45 and 70 d), samples were taken out, rinsed thoroughly with distilled water and then lyophilized. Weight changes were recorded. Five replicate samples were used for each group.

In order to observe degradation behavior in PBS and dH<sub>2</sub>O, scaffolds were incubated in 5 mL of relevant medium at 37°C in a shaking water bath. In every two days, medium was drawn out and replaced with fresh medium. At determined time intervals (3, 7, 14, 21 and 28 d), samples were taken out, rinsed thoroughly with distilled water and then lyophilized. Weight measurements were recorded. Three replicate samples were used for each group.

#### **2.2.5. Determination of Bioactivity**

Bioactivity of scaffolds was examined through biomineralization studies conducted in 5 times concentrated simulated body fluid (SBF-5). SBF-5 solution was prepared by dissolving corresponding amounts of salts in 1 L of distilled water followed by adjustment of pH to 7.4 with 1.0 M HCl (Table 2.1). Both uncoated and alginate coated chitosan scaffolds were incubated in 10 mL of SBF-5 solution at 37°C in a shaking water bath for 3 different time periods as 48 h, 7 d and 14 d. In one set of 7 d and 14 d incubated scaffolds, SBF-5 solution was refreshed in every 3 days whereas in a second set it remained unchanged to see the effect on alginate dissolution and biomineralization. At the end of the incubation period all samples were taken out and lyophilized after washing with excess distilled water. SEM analysis and elemental analysis by energy dispersive X-ray analyzer (EDX), which is a configuration of SEM, were conducted in order to investigate mineral deposition on

scaffolds and characterization of deposited minerals. Two replicate samples were used for each group.

**Table 2.1.** Composition of 1 L SBF-5 solution prepared in distilled water.

salt	amount (g)	concentration (mM)
NaHCO <sub>3</sub>	1.7642	21.0
NaCl	39.9456	684
KCl	1.1184	15
K <sub>2</sub> HPO <sub>4</sub>	0.8709	5
MgCl <sub>2</sub> .6H <sub>2</sub> O	1.4231	7.7
Na <sub>2</sub> SO <sub>4</sub>	0.3551	2.5
CaCl <sub>2</sub>	1.4096	12.7

### 2.2.6. Mechanical Analysis of Scaffolds

The compressive mechanical properties of scaffolds were studied by using mechanical tester (Lloyd LRX 5K, West Sussex, UK). Scaffolds were incubated in 1 mL of DMEM, high glucose medium for 24 h at 37°C in a shaker prior to testing. For compression tests, scaffolds were placed between compression presses and compressive speed was arranged to 1 mm/min. The maximum load applied on scaffolds was 20 N and maximum compression allowed was 5 mm. Five replicate samples were used for both uncoated and alginate coated chitosan scaffolds. Mechanical tests were conducted on scaffolds after biomineralization process also. Scaffolds incubated in SBF-5 solution for 48 h and 7 d were tested under 40 N of

maximum load applied with a speed of 1 mm/min. Three replicate samples were used for both uncoated and alginate coated chitosan scaffolds.

The compressive moduli of scaffolds were calculated from the linear elastic region of the resultant load versus deformation curve according to Equation (2.3). Hooke's law states that compressive modulus (E) is equal to the slope of the stress versus strain curve in the elastic region. Stress ( $\sigma$ ) corresponds to the force or load (L) applied per unit area (A) and strain ( $\epsilon$ ) is the relative deformation ( $\Delta l$ ) from initial state ( $l_0$ ). E has the unit of MPa since stress has the unit of N/mm<sup>2</sup> (MPa) and strain is a unitless quantity.

$$E \text{ MPa} = \frac{\sigma}{\epsilon} = \frac{L}{A} \frac{1}{\frac{\Delta l}{l_0}} \quad \text{Equation (2.3)}$$

### **2.2.7. Release Studies**

In release studies, release kinetics of both gentamicin and bovine serum albumin (BSA) from the scaffolds were examined. Gentamicin was used as a model antibiotic and BSA was used as a model protein to investigate the release behaviors of bioactive agents from the scaffolds.

#### **2.2.7.1. BSA Release from Scaffolds**

BSA was loaded to different layers of scaffolds as 'in' and 'on' models. Release kinetics was studied from four different loading models presented as; Ch-ON, Ch-ON/Alg, Ch-IN/Alg, Ch/Alg-IN that are shown schematically in Figure 2.2. In each loading model, total of 50  $\mu$ g of BSA was incorporated per scaffold.

Preparation of each model of scaffolds is explained in detail. For all models incubation crosslink was carried out after the loading process.

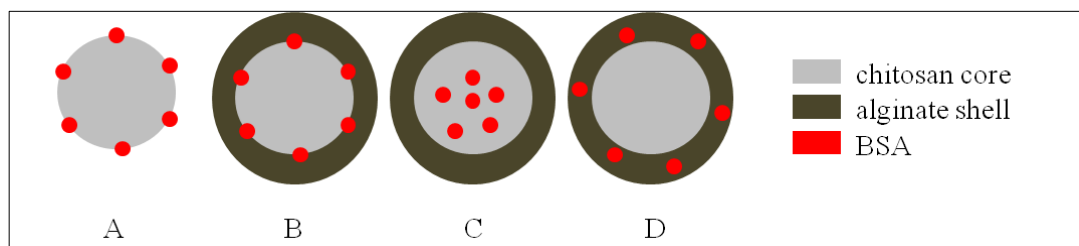


**Figure 2.2.** Schematic representation of four different BSA loading models as (A) Ch-ON; (B) Ch-ON/Alg; (C) Ch-IN/Alg and (D) Ch/Alg-IN.

A. Ch-ON model: After preparation of chitosan scaffolds, 100  $\mu\text{L}$  of 0.5 mg/mL BSA solution prepared in  $\text{dH}_2\text{O}$  was added on the scaffolds in 25  $\mu\text{L}$  portions. Through vacuum-cycling after each addition, absorption of BSA was achieved on the scaffolds. BSA addition was performed on both sides of the scaffolds to have a uniform distribution by turning the scaffold upside down after adding half of the total protein solution. Then, scaffolds were let to dry under vacuum.

B. Ch-ON/Alg model: After loading BSA on chitosan layer as described in part A, scaffolds were coated with 0.3 mL of alginate via vacuum addition as described in section 2.2.1.2 and incubated in  $\text{CaCl}_2$  solution for crosslinking.

C. Ch-IN/Alg model: Chitosan solution containing BSA was prepared and then wet-spun. For this purpose, first, 1.2 g chitosan was dissolved in 2.4% (v/v)

aqueous acetic acidic solution (25 mL) by mixing overnight. Then, 5 mL of 0.5 mg/mL BSA solution was added and mixed that overall yields 4% (w/v) of chitosan concentration in aqueous solution of 2% (v/v) acetic acid and containing 50  $\mu$ g of BSA per scaffold. Scaffold preparation proceeded in the same manner, except while molding, scaffolds were not dried at 54°C to prevent protein denaturation but let dry under vacuum instead. Scaffolds were then coated with 0.3 mL alginate via vacuum addition and incubation to obtain crosslinking with CaCl<sub>2</sub>.

D. Ch/Alg-IN: Alginate solution of 2% (w/v) concentration containing 50  $\mu$ g of BSA per scaffold was prepared by dissolving 0.3 g alginate in a solution of 10 mL dH<sub>2</sub>O and 5 mL aqueous BSA solution with the concentration of 0.5 mg/mL. Previously wet-spun chitosan scaffolds were coated by using 0.3 mL of this solution per scaffold via vacuum addition. After CaCl<sub>2</sub> crosslinking by incubation, scaffolds were let to dry under vacuum.

Additionally, B and D models were studied by preparing the scaffolds through the same procedure but crosslinking the alginate layer by introduction of CaCl<sub>2</sub> solution via vacuum cycling in small portions instead of incubating the scaffolds. These two models are presented as B\* and D\* and schematically represented in Figure 2.3.



**Figure 2.3.** Schematic representation of loading models with vacuum crosslinked alginate layer.

After preparation of 3 replicates of scaffolds for each model, together with their control groups not containing BSA, release studies were carried out by incubating them in 1 mL PBS solution in 24 well plates. At determined time points (1<sup>st</sup>, 3<sup>rd</sup> and 6<sup>th</sup> hours; 1, 3, 7, 15, 25 days) PBS solution on each scaffold was collected and 1 mL fresh solution was added. Released amount of BSA into the solutions from scaffolds were determined by Bradford Assay, microplate protocol. In Bradford Assay, 150  $\mu$ L from each sample in 3 replicates were taken into 96 well plates and 150  $\mu$ L of coomassie blue reagent was added. Coomassie dye binds to proteins and a shift in absorbance maximum occurs to 595 nm with the change of dye color from red to blue. Microplate reader was used to measure the absorbance at 595 nm according to the protocol. Calibration curve for Bradford Assay is given in Appendix A.

#### **2.2.7.2. Gentamicin Release from Scaffolds**

Gentamicin was loaded either onto or into the chitosan part of the scaffolds. Release kinetics was studied from three different loading models represented as; Ch-ON (A), Ch-ON/Alg (B) and Ch-IN/Alg (C) models which are schematically described in Figure 2.4 as A,B and C, respectively. In each loading model, 2 mg of gentamicin was incorporated per scaffold. Preparation of each model of scaffolds is explained in detail below.

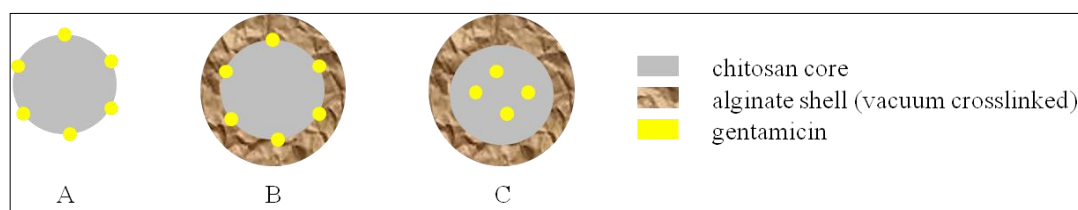


**Figure 2.4.** Schematic representation of three different gentamicin loading models as (A) Ch-ON; (B) Ch-ON/Alg and (C) Ch-IN/Alg.

A. Ch-ON model: After preparation of chitosan scaffolds as described in section 2.2.1.1., 100  $\mu\text{L}$  of 20 mg/mL aqueous gentamicin solution was added onto the scaffolds in 25  $\mu\text{L}$  proportions. Each addition was followed by vacuum-cycling. Gentamicin addition was performed on both sides of the scaffolds to have a uniform distribution by turning the scaffold upside down after adding half of the total antibiotic solution. Then, scaffolds were let to dry under vacuum.

B. Ch-ON/Alg model: After loading gentamicin on chitosan layer as described in part A, scaffolds were coated with 0.3 mL of alginate via vacuum addition as described in section 2.2.1.2 and crosslinked with  $\text{CaCl}_2$  under vacuum cycling.

C. Ch-IN/Alg model: Gentamicin was added into the chitosan solution prior to wet spinning. Chitosan solution containing gentamicin was prepared by dissolving 240 mg of chitosan in 5 mL of 2.4% (v/v) aqueous acetic acid solution overnight and adding 1 mL of 20 mg/mL aqueous gentamicin solution with further mixing. Overall, an aqueous solution with 4% (w/v) chitosan concentration in 2% (v/v) acetic acid that contains 2 mg of gentamicin per scaffold was obtained. Prepared solution was wet spun and scaffold production proceeded as described in section 2.2.1.1. Scaffolds were coated by 0.3 mL of alginate by vacuum-cycling and alginate layer was crosslinked with  $\text{CaCl}_2$  under vacuum cycling.

After preparation of 3 replicate sample scaffolds for each model, together with their control groups not containing gentamicin, release studies were carried out by incubating them in 5 mL PBS solution at 37°C in a shaker. At determined time points PBS solution on each scaffold was collected and 5 mL fresh solution was added. Sample collection was carried out in every 2 h for the first 12 h of incubation and continued daily afterwards. Released gentamicin amount was determined by reading the absorbance values of collected PBS solutions at 256 nm in UV-vis spectrophotometer.

### **2.2.7.3. Antibacterial Tests**

Antibacterial activity of released gentamicin from scaffolds was examined by disk diffusion method. For this purpose, Escheria Coli (E.coli) was spread on agar plates with cotton swabs from bacterial suspensions. Then, Ch-ON, Ch-ON/Alg and Ch-ON/BM scaffolds were loaded with 100 µg of gentamicin each, and placed on top of the inoculated agar together with unloaded chitosan scaffold as control and 10 µg gentamicin tablet as the standard. The plate was then incubated at 37°C for 24 h. The zones of inhibition indicating the absence of bacteria colonies demonstrated the maintenance of gentamicin activity.

## CHAPTER 3

### RESULTS AND DISCUSSION

#### 3.1. Preparation of Scaffolds

Two different types of scaffolds were prepared by wet spinning technique. The general principle behind the technique is injection of a viscous polymer solution into a coagulation bath through a needle, therefore, obtaining precipitates in the form of fibers. In the case of chitosan, viscous polymer solution was prepared by dissolving chitosan in mild acidic medium and using a basic coagulation bath to have precipitation.

In order to optimize the concentration of chitosan and acidity of medium, polymer solutions of 3% (w/v) and 4% (w/v) concentrations in 1% (v/v) and 2% (v/v) acetic acid media were prepared and tested for wet spinning. When chitosan solution was prepared in 1% (v/v) acetic acid with pH of 2.75, stable fiber formation was not observed in coagulation bath. Increasing the acidity of solution to the pH of 2.6 by using chitosan solution prepared in 2% (v/v) acetic acid yielded proper fiber formation. Therefore this acidity was chosen for the chitosan solutions.

In chitosan solutions, another critical parameter is the concentration which controls the viscosity of resultant solution. Therefore, various concentrations of chitosan were prepared. Chitosan concentrations of 3% (w/v) and lower resulted in solutions with low viscosities that were inadequate for wet spinning. On the other hand when the concentrations were higher than 6% (w/v), chitosan became too

viscous to wet spin. Best results were obtained for 4% (w/v), and therefore it was chosen as the optimal polymer concentration.

Coagulation bath used was highly basic with a pH of 13 and composed of sodium hydroxide (NaOH) as the strong base, and sodium sulphate ( $\text{Na}_2\text{SO}_4$ ) as salt. As the polymer solution was injected into the coagulation bath, coagulants diffused into the polymer and acid-base reaction resulted in precipitation of chitosan. Diffusion of coagulants and precipitation reaction occurs initially at the surface and proceeds inner through diffusion which is called as boundary motion. Therefore, wet spun fibers were kept in coagulation bath overnight for completion of the ongoing acid-base reaction. As the ionic strength of coagulation solution increases so does the diffusivity of chitosan which in turn improves the precipitation by addition of salt (Tsaih and Chen, 1999). Thus,  $\text{Na}_2\text{SO}_4$  salt was used in coagulant solution.

Alginate solution used for coating of fibrous scaffolds was prepared in 2% (w/v) concentration in aqueous medium. When prepared in 3% (w/v) concentration, alginate solution became too viscous that did not enable homogenous addition by vacuum cycling. Alginate is easily soluble in distilled water ( $\text{dH}_2\text{O}$ ) but when crosslinked it is stable even at high temperatures. Crosslinking of alginate was achieved through linkage of carboxyl groups of G units with divalent  $\text{Ca}^{2+}$  ions. Among other cations  $\text{Ca}^{2+}$  was chosen due to its presence in natural bone mineral. When alginate is directly incubated in aqueous  $\text{CaCl}_2$  solution for crosslinking, two processes compete with each other that are dissolution of alginate in water and crosslinking of carboxyl ends via  $\text{Ca}^{2+}$  ion (Rhim, 2004). Therefore, in order to prevent any loss during crosslinking, scaffolds were first immersed in 100% EtOH which is a nonsolvent for alginate. Subsequently, they were immersed in  $\text{CaCl}_2$  solution of EtOH- $\text{dH}_2\text{O}$  mixture and aqueous  $\text{CaCl}_2$  solution afterwards. Resultant scaffolds had a thickness of 0.5 cm and diameter of 0.8 cm.

## **3.2. Characterization of Scaffold Properties**

Scaffolds were characterized in terms of their structural formation, chemical and biological properties to evaluate if they were suitable to be used in bone tissue engineering applications.

### **3.2.1. Structural Characterization**

The aim in this study was to fabricate chitosan based fibrous scaffolds to deliver bioactive agents for bone treatment purposes. For this purpose, fibrous scaffolds were prepared by wet spinning technique and some of them were coated with alginate to control the delivery of the agents. Resultant scaffolds were characterized in terms of their structure to investigate if the aim was achieved.

Fibrous structure gives the scaffold the advantages of high surface to volume ratio, porous, interconnected structure and resemblance to natural bone tissue. In order to examine the structure of scaffolds SEM images of both uncoated and alginate coated scaffolds were obtained and given in Figure 3.1. Formation of fibrous structure with interconnected porosity and its maintenance with alginate coating were observed clearly.

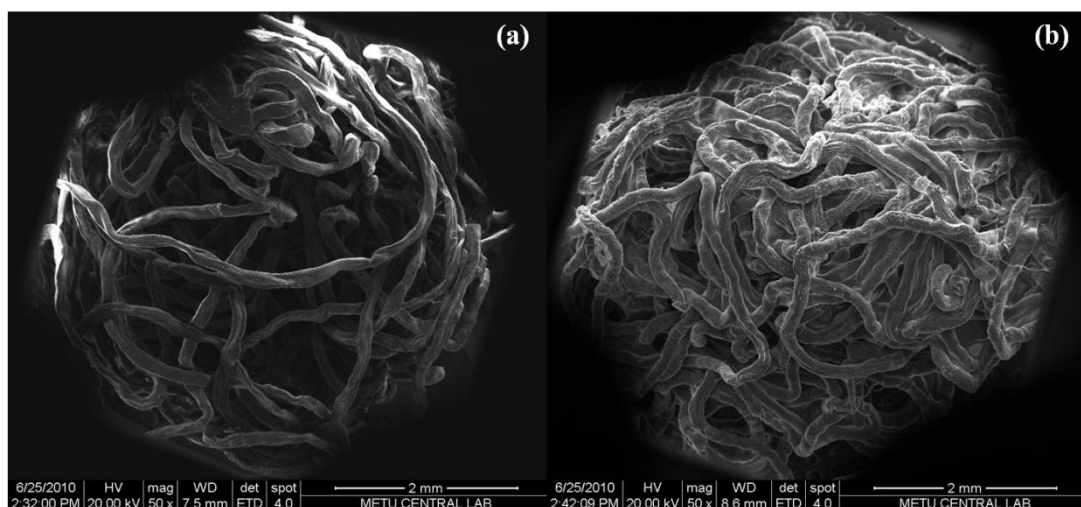


**Figure 3.1.** SEM images of (a) chitosan scaffold and (b) alginate coated chitosan scaffold (x50 magnification).

Alginate coating formation was investigated by FTIR-ATR and SEM analyses. For this purpose single chitosan filaments were wet spun and treated with alginate to allow specific investigation of coating formation. FTIR-ATR analyses of uncoated and coated filaments support the formation of alginate layer on chitosan through the surface layer composition. The spectra for both chitosan filament and alginate coated chitosan filament are given in Figure 3.2.

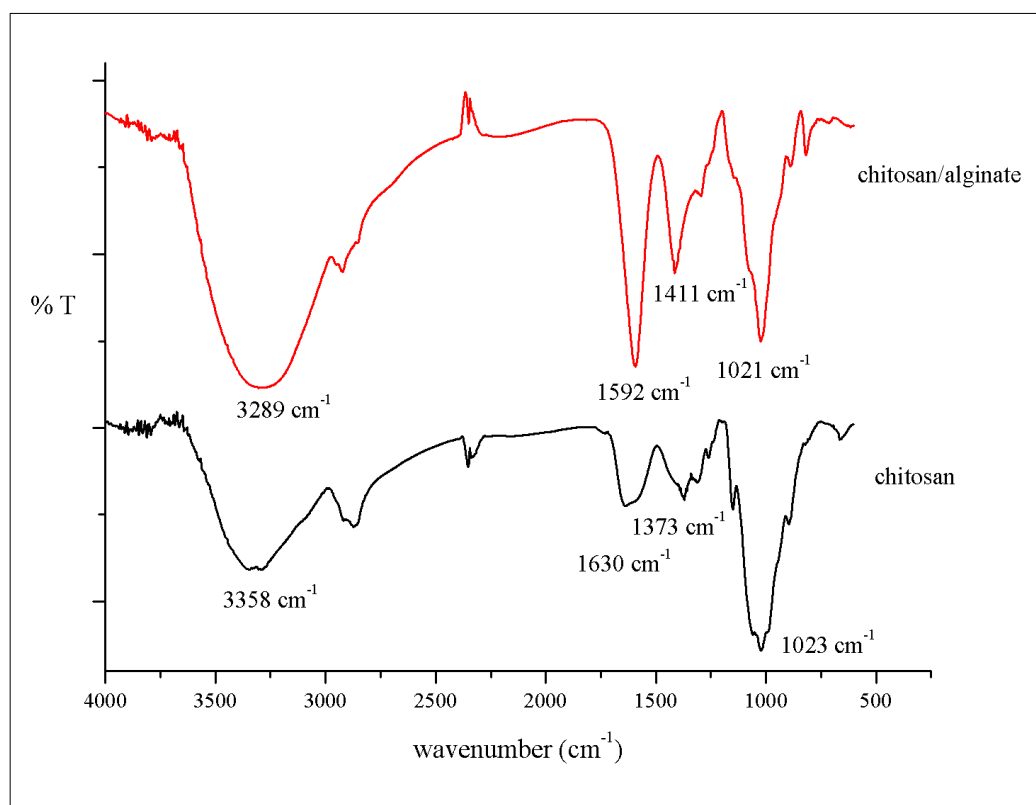


**Figure 3.2.** FTIR-ATR spectra of alginate coated and uncoated chitosan filaments.

In the FTIR-ATR spectrum of chitosan filament, there observed two characteristic peaks at  $1630\text{ cm}^{-1}$  and  $1373\text{ cm}^{-1}$  which were attributed to amine vibration and symmetric vibration of  $\text{CH}_3$ , respectively (Wang *et. al.*, 2007). When the filaments were treated with alginate, those peaks were observed to be replaced by typical absorption bands of alginate detected at  $1592\text{ cm}^{-1}$  and  $1411\text{ cm}^{-1}$  resultant from antisymmetric and symmetric stretching of  $\text{CO}_2^-$  groups. Both spectra exhibited peaks around  $1020\text{ cm}^{-1}$  that were assigned to skeletal vibrations of C-O-C which exists in the ring structure of both chitosan and alginate (Tam *et. al.*, 2005; Lawrie *et. al.*, 2007). Similarly, OH stretching was observed in both spectra in  $3200\text{-}3500\text{ cm}^{-1}$  range due to hydroxyl groups of both polymers. Additionally, in the case of chitosan OH stretching overlapped with NH stretching and resulted in a broad peak. Since

FTIR-ATR has a penetration depth in micrometer scale and after alginate addition characteristic peaks of chitosan were replaced by absorption bands corresponding to alginate functional groups, it was concluded that upon addition, alginate formed a coating layer on chitosan filaments.

Additionally, cross sectional images of scaffolds were taken by SEM and it was clearly observed from the fiber ends that chitosan fibers were layered by an alginate coat as shown in Figure 3.3.

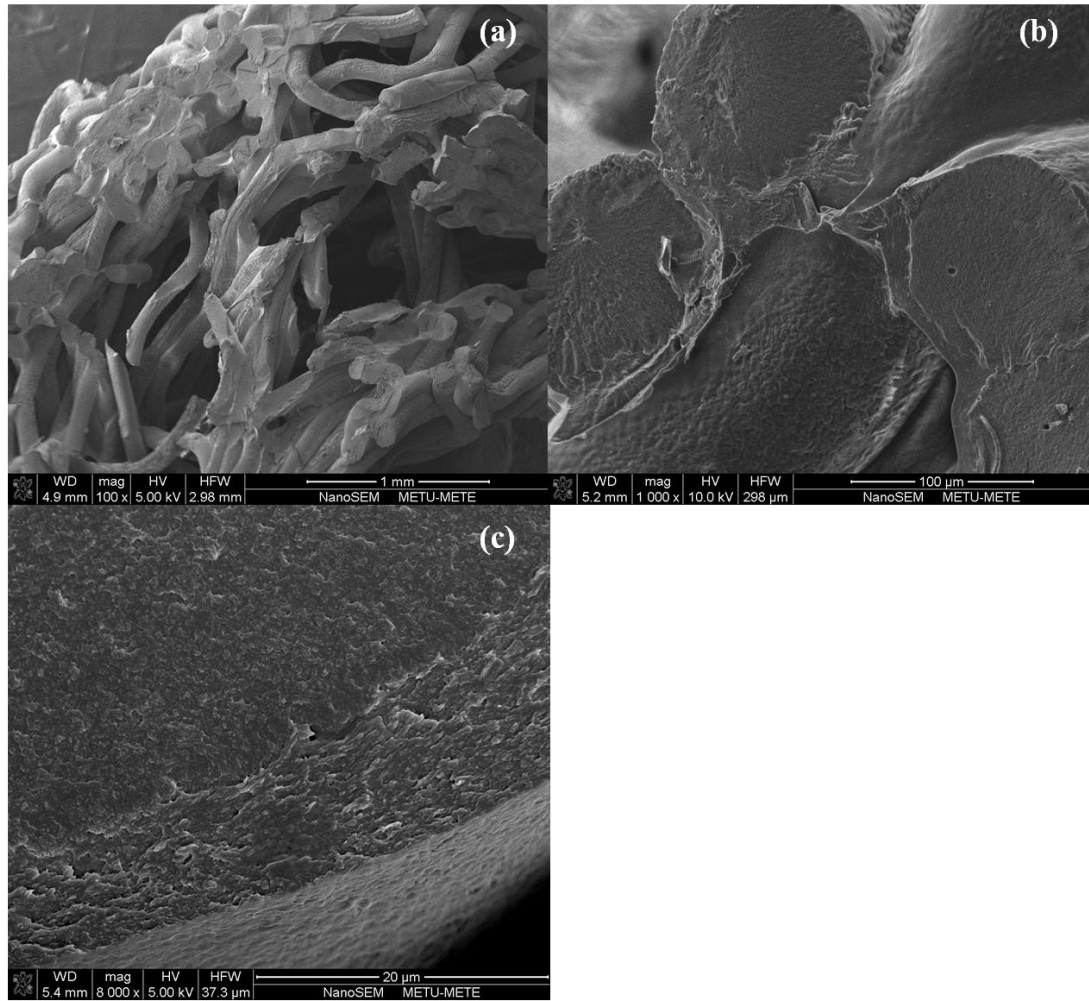


**Figure 3.3.** Cross section SEM images of alginate coated scaffold (a) x100, (b) x1000 and (c) x8000.

In order to measure the fiber and coating thickness single filaments were used again. According to the measurements done by using light microscopy images of filaments, average diameter of uncoated and coated chitosan filaments were  $87.09 \pm 1.58\mu\text{m}$  and  $95.09 \pm 1.43\mu\text{m}$  respectively (Figure 3.4). The difference in diameters corresponded to formation of a  $4 \mu\text{m}$  thick alginate layer on the outer surface of chitosan filaments.

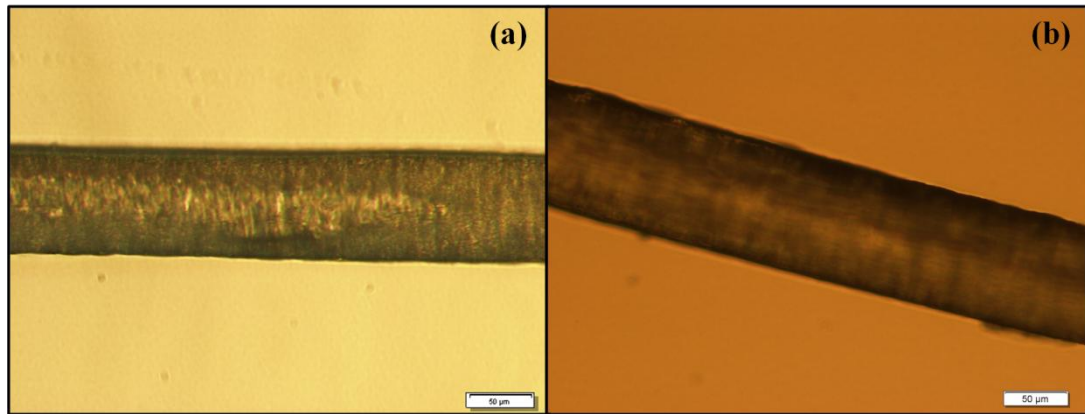


**Figure 3.4.** Light microscopy images of (a) uncoated and (b) coated filaments.

When coating thickness was measured by using cross sectional SEM image of alginate coated scaffold, corresponding value was found to be  $8.51 \pm 0.88 \mu\text{m}$ . On single filaments, alginate introduction was carried out by incubating the chitosan filaments in alginate solution for 5 min and then crosslinking the alginate layer, however, during the preparation of scaffolds alginate was added onto chitosan cores by vacuum cycling. Therefore, it was observed that vacuum addition of alginate resulted in the formation of a thicker coating layer on chitosan fibers.

### **3.2.2. Water Uptake and Retention Capacities of Scaffolds**

Water is a major component of bone tissue and water uptake ability is critical for a scaffold to be used in bone tissue engineering applications. Absorption of body fluid to all parts of the structure, transfer of nutrients and metabolic wastes are influenced by water uptake capacity as does the cell attachment and migration all over the scaffold that eventually affects the morphology of newly grown tissue (Yeo and Kim, 2012).

After incubation in distilled water for 24 h, percent water uptake values for chitosan and alginate coated chitosan scaffolds were obtained by weight measurement. Corresponding values were  $427.32 \pm 30.26\%$  and  $279.43 \pm 19.70\%$ , respectively as given in Figure 3.5. Upon incubation, fibrous chitosan scaffolds demonstrated excellent water uptake capacity which was attributed to water absorbed into the dehydrated fibers and adsorbed within the voids of structures. Absorption of water into the chitosan fibers were observable through the swelling of filaments and it was also supported by literature that chitosan has high water absorption ability (Mao *et. al.*, 2003; Oliveira *et. al.*, 2009). In addition, studies showed that increasing porosity enhances water uptake values through adsorption of water within the void volume of scaffolds (Arpornmaeklong *et. al.*, 2008; Karakeçili and Arıkan, 2012). Therefore, highly porous structure of chitosan scaffolds was stated as a contributor to water uptake capacity. In the case of alginate coated chitosan scaffolds there observed a remarkable decrease in water uptake capacity. Once crosslinked with  $\text{CaCl}_2$ , alginate becomes insoluble in distilled water and exhibits low water uptake ability that varies with crosslinker concentration and crosslinking time. Remunan-Lopez and Bodmeier demonstrated that when alginate was crosslinked in 5% (w/v)  $\text{CaCl}_2$  solution for 1 h, its water uptake value was 70% (Remunan-Lopez and Bodmeier, 1997). Therefore, when crosslinked alginate was coated on chitosan fibers, access of water to the fibers was blocked to some extent. Additionally, introduction of alginate decreased the volume of void space within the scaffolds. As a result, observed percent water uptake values were decreased. However, the values were still efficacious for both kinds of scaffolds.

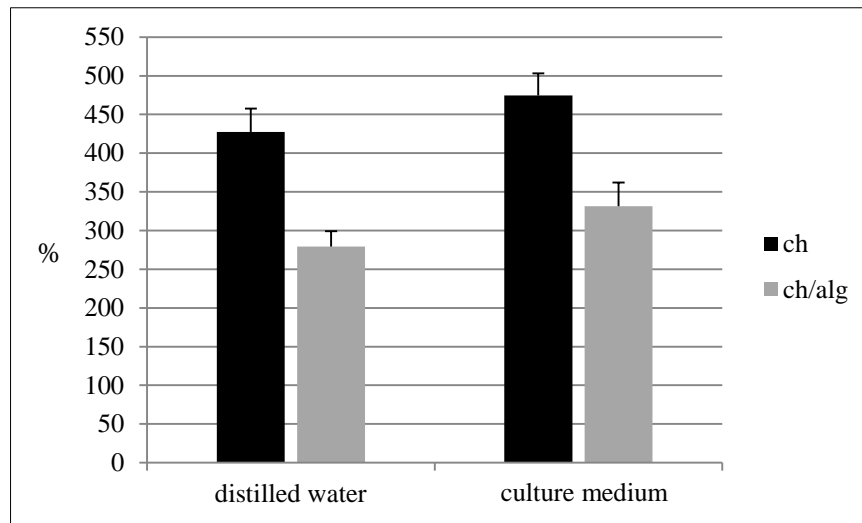


**Figure 3.5.** Percent uptake values for uncoated (ch) and alginate coated (ch/alg) scaffolds examined in distilled water and culture medium.

Uptake studies were also repeated in high glucose DMEM, culture medium in order to hold a better view of scaffold behavior in vitro conditions. Results showed the same trends as in distilled water but with higher values as  $474.39 \pm 28.65\%$  and  $331.25 \pm 30.98\%$  for uncoated and alginate coated scaffolds, respectively. The small increments in the values were resultant from the higher density of culture medium compared to distilled water.

Water retention ability was investigated by centrifuging the scaffolds after incubation in distilled water in order to remove free water from the structures. By means of this process, the amount of bound water which was retained in the structures was obtained as given in Figure 3.6. Chitosan and alginate coated chitosan scaffolds were shown to have the capability to retain as much water as their weight with the values of  $121.87 \pm 4.44\%$  and  $113.41 \pm 4.44\%$ , respectively. Water retention was demonstrated to be a crucially important ability for natural tissues especially to maintain their viscoelastic properties (Badylak *et. al.*, 2009). Additionally, it was

stated that glycosaminoglycans (GAGs) are dominantly effective on water retention capacity of tissues through their high charge density and inherent hydrophilicity (Lovekamp *et. al.*, 2006). Therefore, high water retention capacities of both chitosan and alginate were attributed to their chemical structures similar to GAGs.

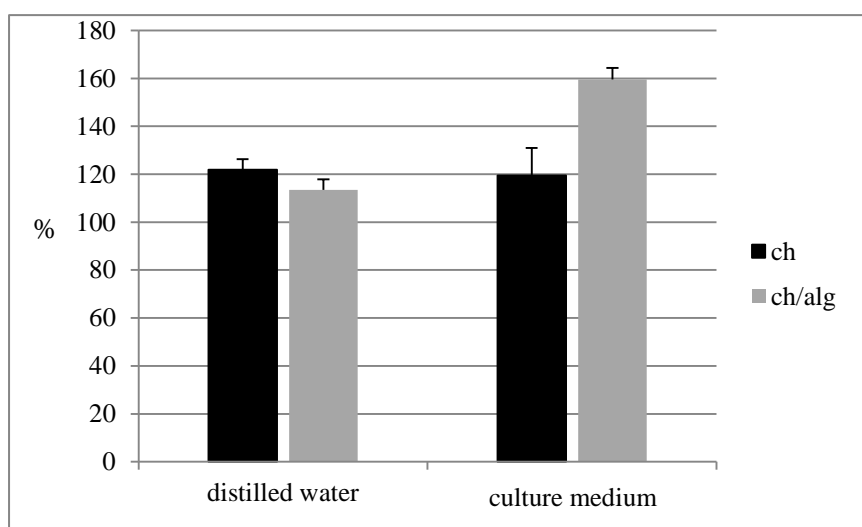


**Figure 3.6.** Percent retention values for uncoated (ch) and alginate coated (ch/alg) scaffolds examined in distilled water and culture medium.

Retention studies were also repeated in high glucose DMEM, culture medium. Chitosan scaffolds exhibited a medium retention capacity of  $119.43 \pm 11.53\%$  which was quite comparable to their water retention capacity. In the case of alginate coated scaffolds, medium retention capacity was observed to be higher and the value obtained by weight was  $159.55 \pm 4.76\%$ .

### 3.2.3. Degradation Behavior of Scaffolds

Degradation behavior of scaffolds was investigated in three different mediums as enzyme solution, phosphate buffer saline (PBS) and distilled water (dH<sub>2</sub>O) by incubation at 37°C in a shaker and following the mass loss at predetermined time points.

Both chitosan and Ca<sup>2+</sup> crosslinked alginate are insoluble in water, as a result, neither chitosan nor alginate coated chitosan scaffolds showed any mass loss upon incubation in distilled water. The degradation behaviors of scaffolds in PBS and enzyme solution are given below in Figure 3.7. When the scaffolds were incubated in PBS solution which refers to inorganic content of body fluid, chitosan scaffolds again showed no loss in weight. However, alginate coated scaffolds lost 7.20% of their total weight upon 24 h of incubation in PBS and total weight loss increased to 11.1% at 14 d. After that point no further mass loss was observed. Since no mass loss was observed in chitosan scaffolds during PBS incubation, it was concluded that the decrease in total mass observed in alginate coated scaffold results from the dissolution of alginate layer. Ionic crosslinking of alginate by Ca<sup>2+</sup> was subjected to cation exchange with monovalent K<sup>+</sup> ions and subsequent dissolution which was also documented in literature (Bajpai and Sharma, 2004; Gao *et. al.*, 2009).

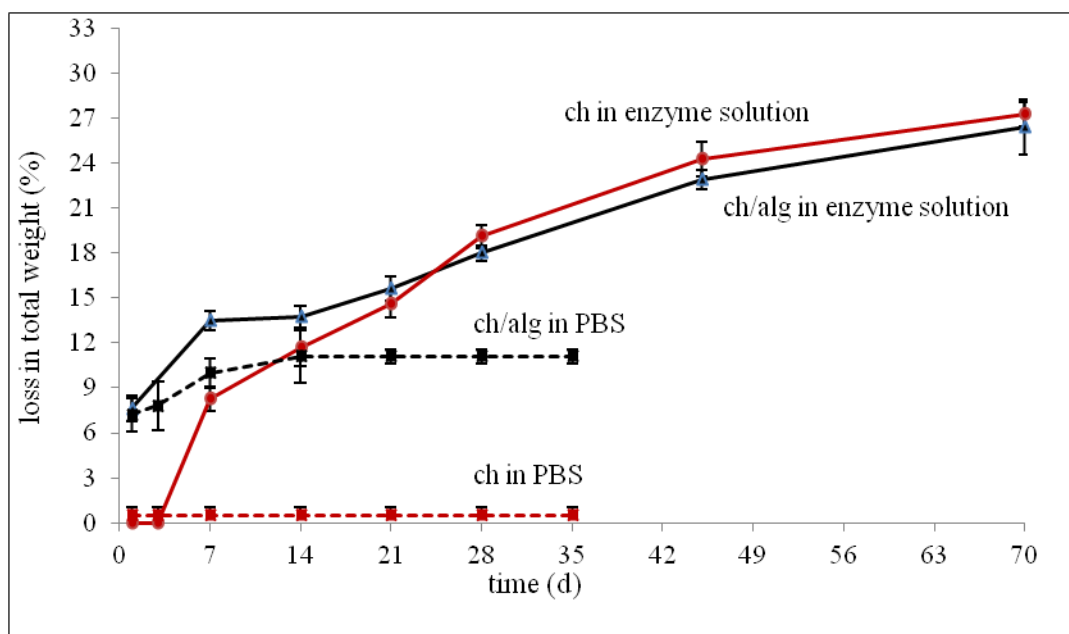


**Figure 3.7.** Degradation graphs of both chitosan (red lines) and alginate coated chitosan (black lines) scaffolds in PBS (dashed lines) or 1mg/mL lysozyme solution (solid lines).

Lysozyme is an enzyme abundant in body fluids which cleaves the glycosidic bonds of polysaccharides and result in their degradation. Additionally, it was stated that chitosan degradation mainly occurs enzymatically by lysozyme *in vivo* (Peluso *et. al.*, 1994; Silva *et. al.*, 2004). Therefore, lysozyme was used to investigate enzymatic degradation behavior of scaffolds *in vitro*. Incubation of scaffolds in 1mg/mL lysozyme solution prepared in PBS caused degradation in both kinds of scaffolds that reached to loss of 27% of total weight at 70 d. It was observed that chitosan scaffolds showed no degradation during the first 3 d of incubation followed by a fast degradation rate afterwards. On the other hand, alginate coated chitosan scaffolds showed a fast mass loss upon initial incubation resultant from removal of alginate layer due to coactions of PBS dissolution and enzymatic degradation. SEM images of scaffolds taken upon 3 d of incubation in enzyme solution clearly showed

the erosion of chitosan surface in uncoated scaffolds and removal of alginate layer from coated ones which are given in Figure 3.8.

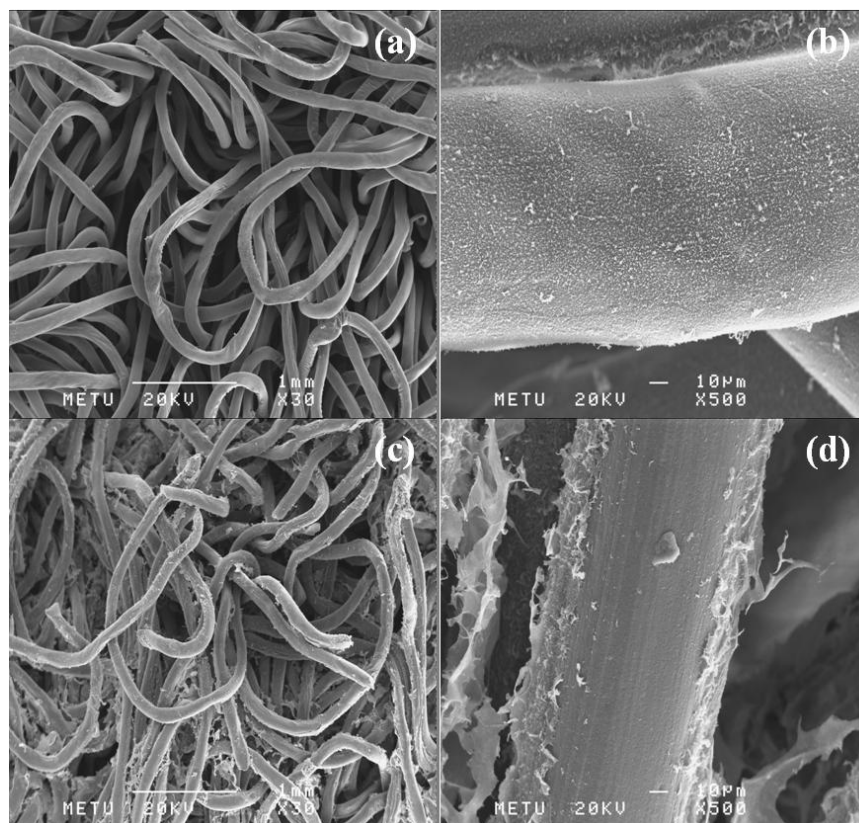


**Figure 3.8.** SEM images of (a,b) chitosan and (c,d) alginate coated chitosan scaffolds on 3<sup>rd</sup> d of incubation in enzyme solution at (a,c) x30 and (b,d) x500 magnifications.

The course of degradation, either surface degradation or bulk degradation, affects the mechanical stability and release behavior of scaffolds. Therefore, SEM

images of enzymatically degraded scaffolds were taken from an upper view and cross section at the end of incubation period and given in Figure 3.9. The degradation mode observed on scaffolds by using SEM images was surface degradation since surface erosion could be observed clearly and integrity of fibers was maintained.

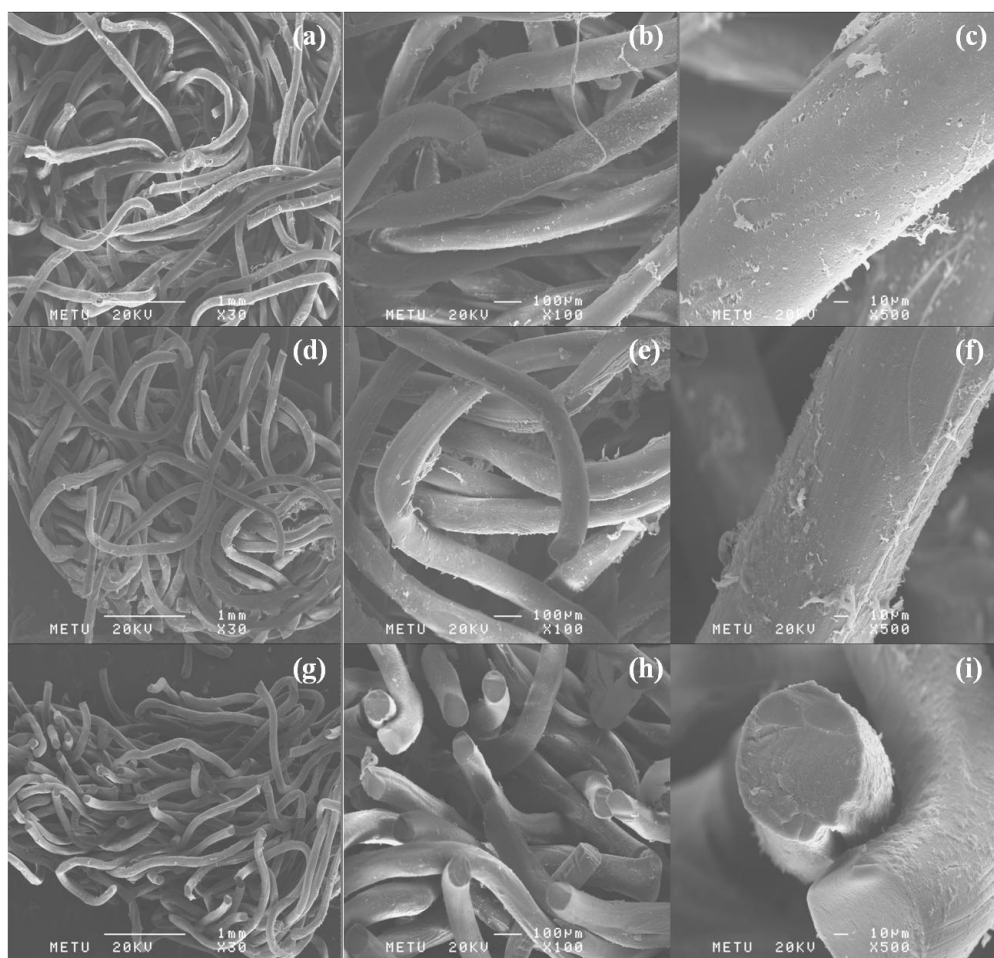


**Figure 3.9.** SEM images of (a,b,c) chitosan and (d,e,f) alginate coated chitosan scaffolds from upper view and (g,h,i) chitosan scaffolds from cross section on 70<sup>th</sup> d of incubation at (a,d,g) x30, (b,e,h) x100 and (c,f,i) x500 magnifications.

As a result, it can be concluded that produced scaffolds would undergo surface degradation in vivo so that they would enable controlled release of bioactive agents with a rate closely related to the rate of degradation and scaffolds could maintain their structural integrity and stability up to 70 d in order to support the defect site until complete replacement with newly forming tissue occurs.

#### **3.2.4. Determination of Bioactivity**

Bioactivity of scaffolds was correlated with the calcium phosphate mineral deposition when incubated in SBF solution. Deposition of calcium phosphate minerals onto the surface of scaffolds indicates bone-bonding ability, thus, a favoring environment for bone tissue formation (Kokubo, 1991). In order to accelerate the process of crystal formation five times concentrated simulated body fluid (SBF-5) solution was used.

Scaffolds of both uncoated and alginate coated ones were incubated in SBF-5 solution for 48 h, 7 d and 14 d. SEM analyses of the samples incubated for 48 h are given in Figure 3.10. SEM micrographs clearly showed the occurrence of mineral deposition on uncoated chitosan scaffolds after 48 h of incubation. Elemental analysis of deposited mineral revealed that the composition of salt was 68.67% Ca and 29.47% P in weight. On the scaffolds coated with alginate no mineral deposition was observed after 48 h of incubation. Since SBF solution is a highly ionic environment it caused dissolution of alginate layer. As a result, the presence of an unstable surface prevented the agglomeration of minerals on coated scaffolds.

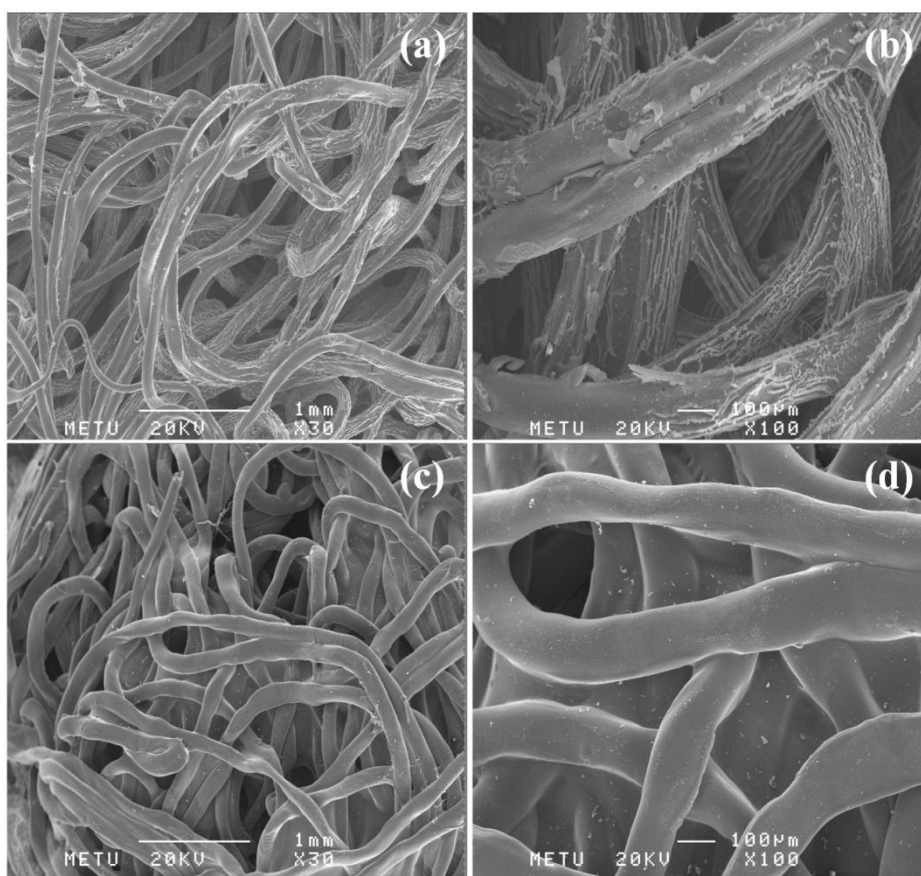


**Figure 3.10.** SEM images of uncoated scaffolds at (a) x30, (b) x100 and alginate coated scaffolds at (c) x30, (d) x100 magnifications incubated in SBF-5 solution for 48 h.

During incubation of scaffolds for 7 and 14 days, in one set for each time period, SBF-5 solution was refreshed in every two days. For the other set, the samples were kept in the same solution. The effects of alginate presence in the medium and introduction of fresh solution on the mineral deposition were estimated.

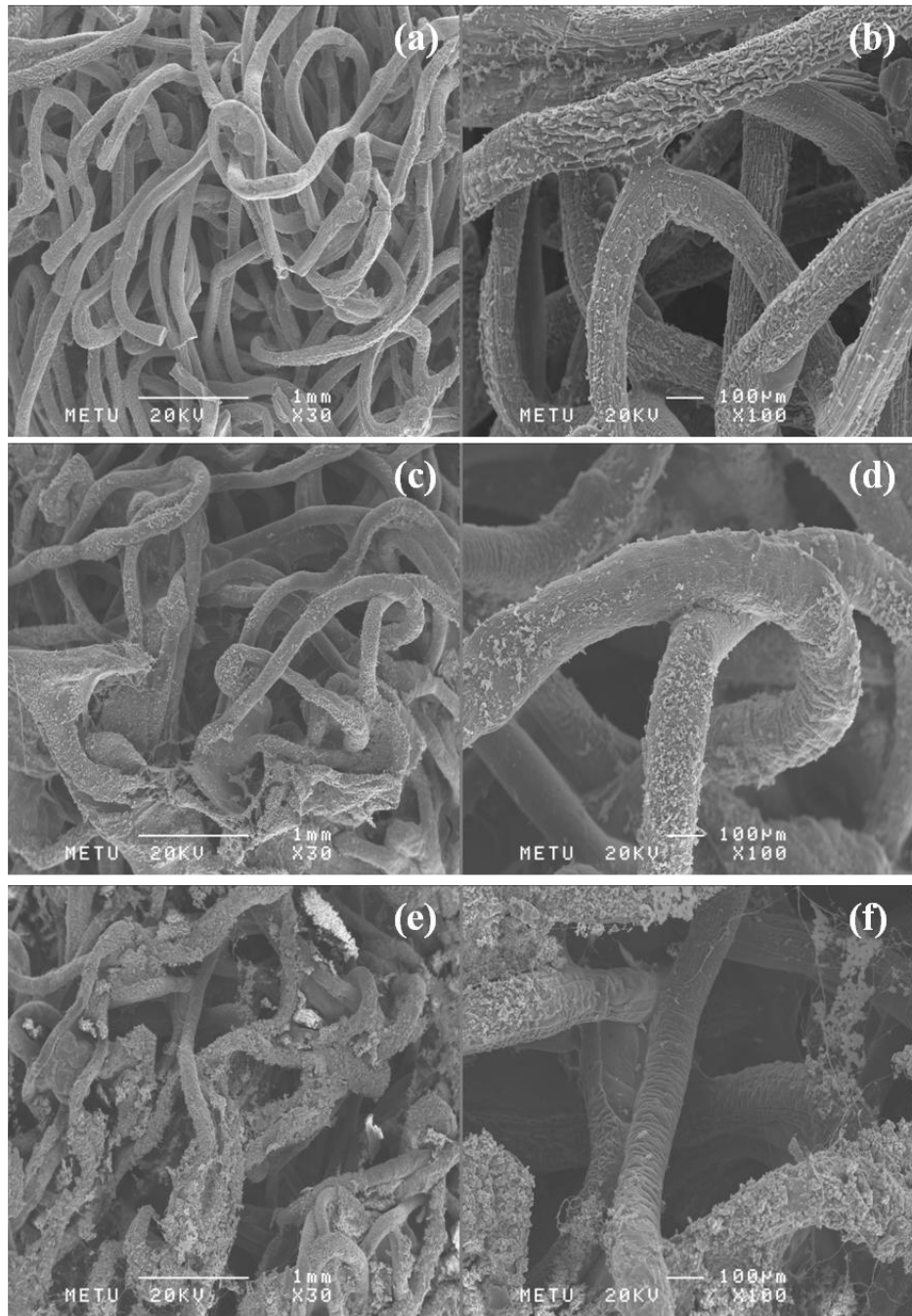


**Figure 3.11.** SEM images of uncoated scaffolds at (a) x30, (b) x100 and alginate coated scaffolds at (c,e) x30, (d,f) x100 magnifications incubated in SBF-5 solution for 7 d in (c,d) same solution and (e,f) refreshed solution.

After 7 days of incubation (Figure 3.11.) uncoated scaffolds again showed good mineral deposition. In elemental analysis Ca peak was observed with 88.05% weight concentration but P peak could not be detected due to the overlapping with Au peak resulting from the coating of scaffolds prior to analysis. In the case of alginate coated scaffolds mineralization was observed to start on the fibers as alginate layer was removed. In the scaffolds of which SBF-5 solution was refreshed in every two days, there observed significantly higher amount of mineralization due to regular supply of ions to the incubation medium. Elemental analysis of minerals deposited on scaffolds kept in the same solution showed 61.89% Ca and 34.75% P in weight whereas the values were 68.82% Ca and 31.18% P in weight for the scaffolds incubated in refreshed SBF-5 solution.

When incubated for 14 d (Figure 3.12.), uncoated chitosan scaffolds got completely covered by minerals and alginate coated scaffolds also showed enhanced mineral deposition. When looked at the amount of deposited salts, same trend as in 7 d incubation was observed as among coated scaffolds the ones incubated in fresh solution in every two days were more mineralized. Elemental analysis results given in weight percentage revealed 62.46% Ca and 32.76% P for uncoated chitosan scaffolds, 58.83% Ca and 41.17% P for alginate coated scaffolds that were kept in the same solution during incubation period, 67.02% Ca and 32.98% P for alginate coated scaffolds incubated in refreshed solution.

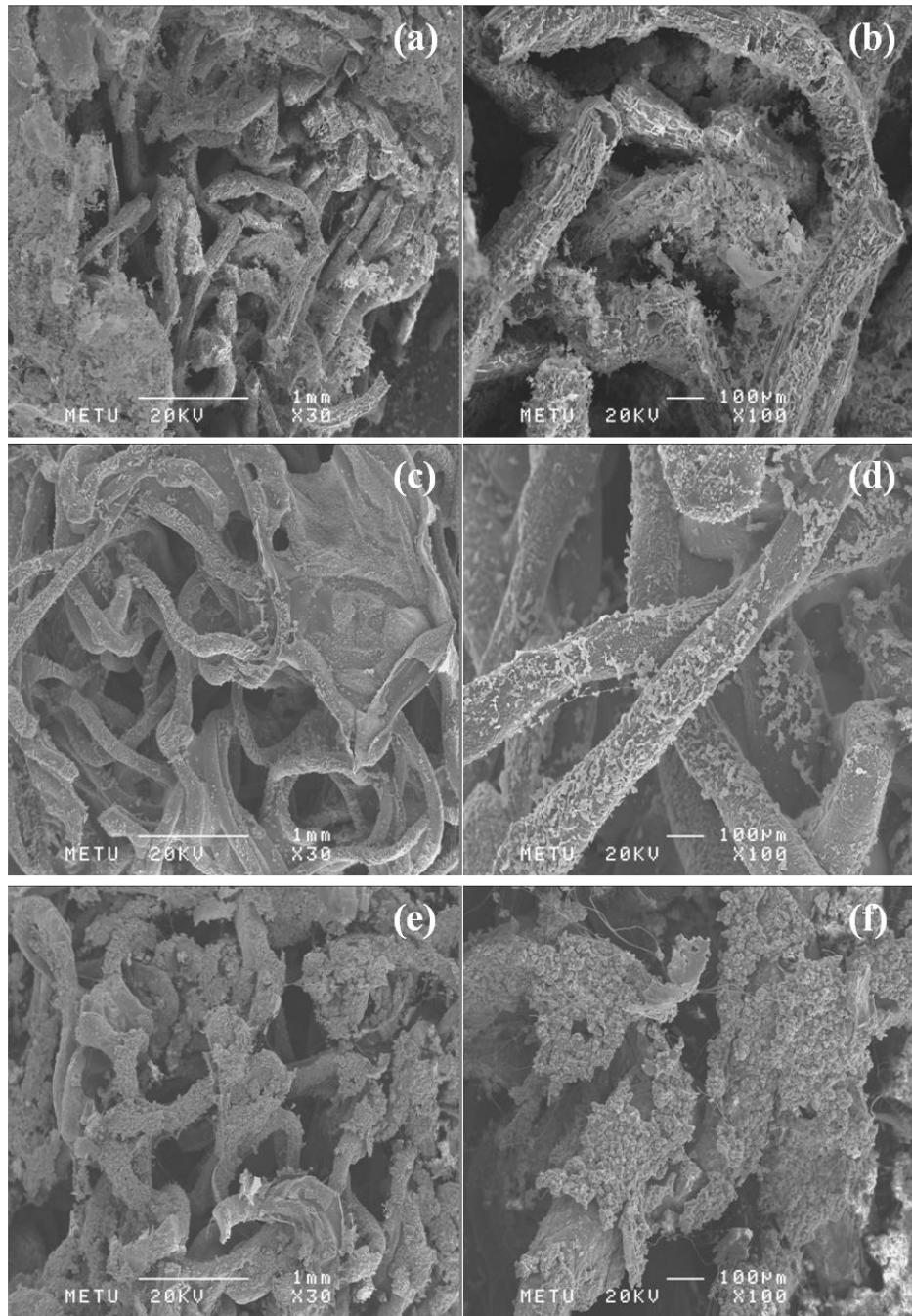


**Figure 3.12.** SEM images of uncoated scaffolds at (a) x30, (b) x100 and alginate coated scaffolds at (c,e) x30, (d,f) x100 magnifications incubated in SBF-5 solution for 14 d in (c,d) same solution and (e,f) refreshed solution.

Calcium phosphate minerals are chemically similar structures to the mineral component of bone, therefore, they exhibit the ability of integration to the bone tissue and support bone mineralization. Recent studies revealed that in bone tissue, the interface interaction and stabilization between mineral phase and the organic matrix is provided predominantly via polysaccharides in the structure, most likely glycosamine glycans (GAGs) (Wise *et. al.*, 2007; Zhong and Chu, 2012). Chitosan and alginate are both polysaccharides with resembling structures to GAGs, therefore, they both have the ability to promote bone mineralization. In literature it was also supported by studies that formation of calcium phosphate minerals on chitosan scaffolds shows their bioactivity towards bone tissue integration and mineralization (Kong *et. al.*, 2006; Xue *et. al.*, 2009; Budiraharjo *et. al.*, 2010).

There exists several types of calcium phosphate minerals that can be distinguished by their atomic Ca:P ratios and crystal structures. Thus, deposited minerals on scaffolds were investigated for their resemblance to bone apatite and the extent of their ability to induce bone formation and mineralization depending on their atomic Ca:P ratios given in Table 3.1.

**Table 3.1.** Atomic Ca:P ratio of deposited minerals on scaffolds.

<b>incubation medium \ incubation time</b>	<b>48 h</b>	<b>7 d</b>	<b>14 d</b>
chitosan	1.80	-	1.47
chitosan/alginate same solution	no mineral deposition	1.38	1.10
chitosan/alginate refreshed solution	no mineral deposition	1.70	1.57

Stoichiometric hydroxyapatite has the formula of  $\text{Ca}_{10}(\text{PO}_4)_6(\text{OH})_2$  where the atomic ratio of Ca:P is 1.67 and bone mineral is a carbonated analogue of hydroxyapatite where Ca:P ratio varies between 1.67-1.50 (Yubao *et. al.*, 1994). For tricalcium phosphate,  $\text{Ca}_3(\text{PO}_4)_2$ ; octacalcium phosphate,  $\text{Ca}_8\text{H}_2(\text{PO}_4)_6 \cdot 5\text{H}_2\text{O}$ ; and dicalcium phosphate  $\text{CaHPO}_4 \cdot 2\text{H}_2\text{O}$ ; which act as precursors in the crystallization of bone-like apatite, Ca:P values are 1.50, 1.33 and 1.00, respectively. Additionally for the values above 1.67, it was stated that CaO would be present in hydroxyapatite phase (Hench, 1993). The Ca:P ratios in between these values can be ascribed to co-existence of the relevant forms of calcium phosphates in the sample. In Table 3.1., it was observed that, Ca:P ratio for chitosan scaffolds decreased as incubation period was prolonged and showed a value close to bone range at 14 d of incubation. In their study, Lu and Leng stated that in SBF solutions with pH 7, formation of octacalcium phosphate and dicalcium phosphate are kinetically favorable whereas hydroxyapatite is the thermodynamically most stable form (Lu and Leng, 2005). Hence, deposition of hydroxyapatite precursors can be stated for chitosan scaffolds according to observed Ca:P ratio and higher nucleation rate of those compounds.

In alginate coated chitosan scaffolds when incubation conditions are compared, it can be concluded that refreshing the SBF solution resulted in nucleation of minerals with similar composition to that of bone apatite with Ca:P ratio ranging between 1.70-1.57. On the other hand, minerals deposited when the scaffolds were kept in the same solution can be attributed to the nucleation of kinetically favorable precursors of apatite according to Ca:P values that indicated the presence of octacalcium phosphate and dicalcium phosphate minerals.

It was clearly observed from the given results that, upon incubation in concentrated SBF solution, produced scaffolds were subjected to calcium phosphate mineral deposition either in a similar form of bone apatite or in the forms of precursors that would promote the formation of biological apatite in body by transformation to the most stable structure (Grynblas and Omelon, 2007). Therefore,

mineralization results can be attributed to the capability of produced scaffolds to support bone mineralization and integration with natural tissue *in vivo*.

### 3.2.5. Mechanical Properties

Mechanical properties of the scaffolds were characterized in terms of their compressive modulus (E) in both uncoated and alginate coated forms. Effects of biomineralization on the mechanical strength of scaffolds were also examined. Compressive modulus refers to the relative deformation in longitudinal dimension of a scaffold as a result of applied compression, therefore, can be used to evaluate the durability behavior of a scaffold under compressive stress. E values were calculated from the slope of the linear elastic region of stress-strain curves obtained for scaffolds. Calculated results are given in Table 3.2.

**Table 3.2.** Compression modulus values for scaffolds.

<b>incubation medium / time</b>	<b>sample</b>	<b>E (avg) / kPa</b>	<b>standard dev.</b>
DMEM medium / 24 h	ch	16.83	2.53
	ch/alg	26.93	6.08
SBF-5 solution / 48 h	ch	69.62	1.34
	ch/alg	76.01	3.20
SBF-5 solution / 7 d	ch	126.72	26.15
	ch/alg	128.95	32.62

Mechanical testing results demonstrated that produced scaffolds, without mineralization, exhibit low compressive moduli. The E values of chitosan and alginate coated chitosan scaffolds were  $16.83 \pm 2.53$  kPa and  $26.93 \pm 6.08$  kPa, respectively. It was concluded that the strength of the scaffolds was mainly contributed by chitosan since it forms the core structure and shown to be mechanically superior to alginate by means of compressive modulus (Lai *et. al.*, 2003). Addition of alginate resulted in a 60% increase in the value of compressive moduli of scaffolds. It was emphasized in literature that mechanical strength of scaffolds is inversely proportional to their porosity and optimization of both properties through tailoring of scaffolds is necessary (Tunc *et. al.*, 2012; Eshraghi and Das, 2012). Therefore, as the porosity of scaffolds decreased with the incorporation of crosslinked alginate, an enhancement in mechanical properties was observed. Similarly, for cancellous bone, which has a highly porous structure, it is known that E is directly proportional to the square of density (Morgan and Keaveny, 2001). Hence, filling of voids that increases the density of scaffold can also be stated as the reason for the increase in E value with the addition of alginate. Both chitosan and alginate coated chitosan scaffolds displayed E values close to hydrogels used as bioactive agent delivery vehicles in bone tissue engineering applications (Bryant and Anseth, 2002; Kim *et. al.*, 2007; Jeon *et. al.*, 2011). In order to gain the scaffolds the mechanical strength to provide required support to bone tissue, produced scaffolds were reinforced by biomineralization.

As the scaffolds were subjected to biomineralization process, a dramatic increase in their mechanical properties was observed. The enhancing effect of mineralization on mechanical properties of polymeric scaffolds is well stated in literature (Katsanevakis *et. al.*, 2010; Samavedi *et. al.*, 2011; Andric *et. al.*, 2011). Additionally, chitosan and alginate are both polysaccharides with resembling structure to GAGs which contribute dominantly to the interaction between the mineral and organic phases of bone (Wise *et. al.*, 2007; Zhong and Chu, 2012). As a result, they both promote bone mineralization and consequent improvement in mechanical properties.

When incubated in SBF-5 solution for 48 h, E values of scaffolds showed a remarkable increase due to mineral deposition on the scaffolds and reinforcing effect of diffused salt particles into the structure. Chitosan scaffolds showed higher increase in E values compared to alginate coated ones which is attributed to higher amount of mineralization observed on them and easier diffusion of SBF-5 solution into the structure. When incubation period was prolonged to 7 d, E values exhibited by uncoated and alginate coated scaffolds reached nearly equal values since differencing effect of alginate was cancelled due to its complete dissolution in highly ionic SBF-5 solution. The increase in compressive moduli was enormous due to excessive mineral deposition on the scaffolds. The compressive moduli of scaffolds lied within the range to that of cancellous bone which varies between 0.1-10 MPa after 7 d of incubation in SBF-5 solution. According to these results, it can be concluded that use of produced scaffolds as supporting materials along with the feature of bioactive agent delivery for tissue engineering of cancellous bone would be adequate.

### **3.3. Release Studies**

Prepared scaffolds were aimed to be used as drug delivery vehicles for administration of both antibiotics and proteins. Among antibiotics gentamicin, which is a wide range antibiotic, was chosen as a model drug and its release kinetics was studied. As an analogue of proteins, bovine serum albumin (BSA) was incorporated into the scaffolds and its release behavior was also examined.

#### **3.3.1. BSA Release from Scaffolds**

As an analogue of protein delivery BSA release was studied from the scaffolds. For that purpose four different loading models were employed as Ch-ON, Ch-ON/Alg, Ch-IN/Alg and Ch/Alg-IN. 'ON' models represented the structures that BSA was loaded by vacuum cycling onto the scaffolds whereas 'IN' models

represented the structures that BSA was incorporated within the polymer matrix. Along with loading models, alginate crosslinking procedure was also shown to be effective in release behavior of BSA from the scaffolds.

For the scaffolds that alginate layer was crosslinked via incubation, release profiles of BSA from four different models are given in Figure 3.13.

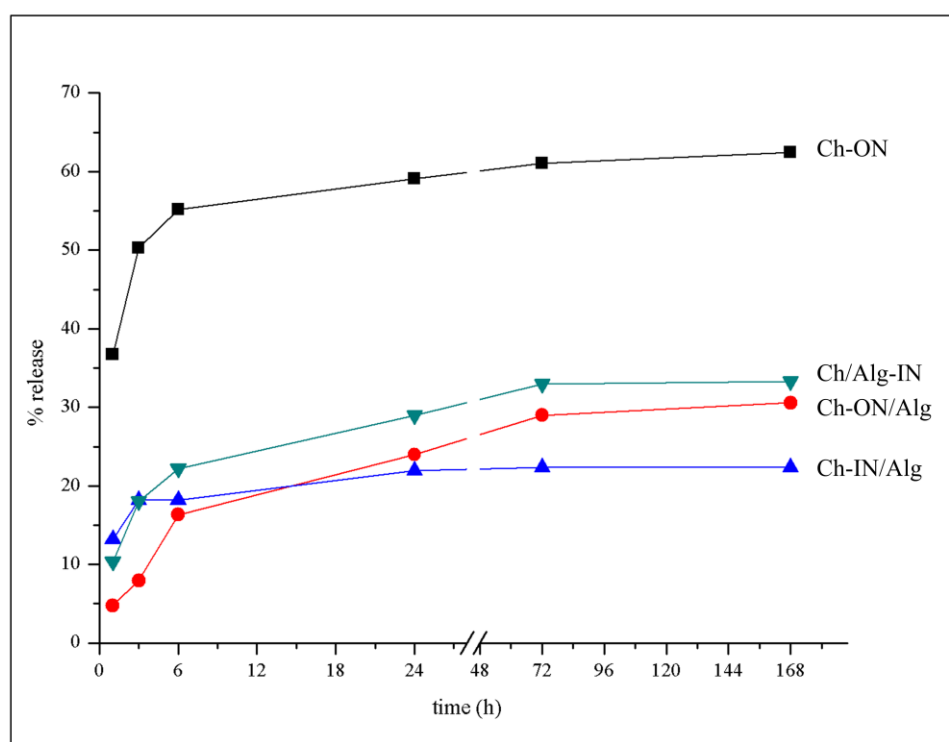


**Figure 3.13.** Release of BSA from scaffolds in 7 d period.

As seen, up to first six hours of incubation a fast release was observed for all models due to initial rapid water uptake of scaffolds that slowed down afterwards.

From day 3 to 7, release of BSA continued with a very slow rate and almost no release was observed after day 7. Fastest release of BSA was observed in uncoated Ch-ON model as expected due to direct release of surface adsorbed BSA into the incubation medium. The maximum amount of release was reached in that model as 62.47% (w/w). When coated with alginate, total amount of released BSA was half decreased to 30.56% (w/w) dramatically as seen in Ch-ON/Alg model. Also in Ch/Alg-IN model, where BSA is loaded within alginate coating, total released amount was 33.31% (w/w) which is quite low. Slowest release profile was observed for Ch-IN/Alg model since BSA was entrapped within the polymeric matrix. In addition, total amount of BSA released was 22.31% (w/w) corresponding to the lowest release amount among all models. It is suggested that, released BSA from this model corresponds to protein molecules which were on the fiber surface so could be released by initial diffusion of the medium into the fibers. Since chitosan does not degrade in PBS, BSA molecules within the fibers were not able to be released due to being entrapped within the polymer matrix and strong interactions between chitosan and BSA. Previous studies of BSA release from chitosan substrates also stated low release results (Xu and Du, 2003; Xu *et. al.*, 2007).

In order to investigate and prevent the possible loss of loaded BSA during incubation crosslink procedure, release kinetics of BSA from Ch-ON/Alg and Ch/Alg-IN models were studied by vacuum crosslinking of alginate layer with  $\text{CaCl}_2$  as described in section 2.2.1.2. Release profiles of BSA from the prepared scaffolds are given together with their incubation crosslinked analogues in Figure 3.14 and 3.16.

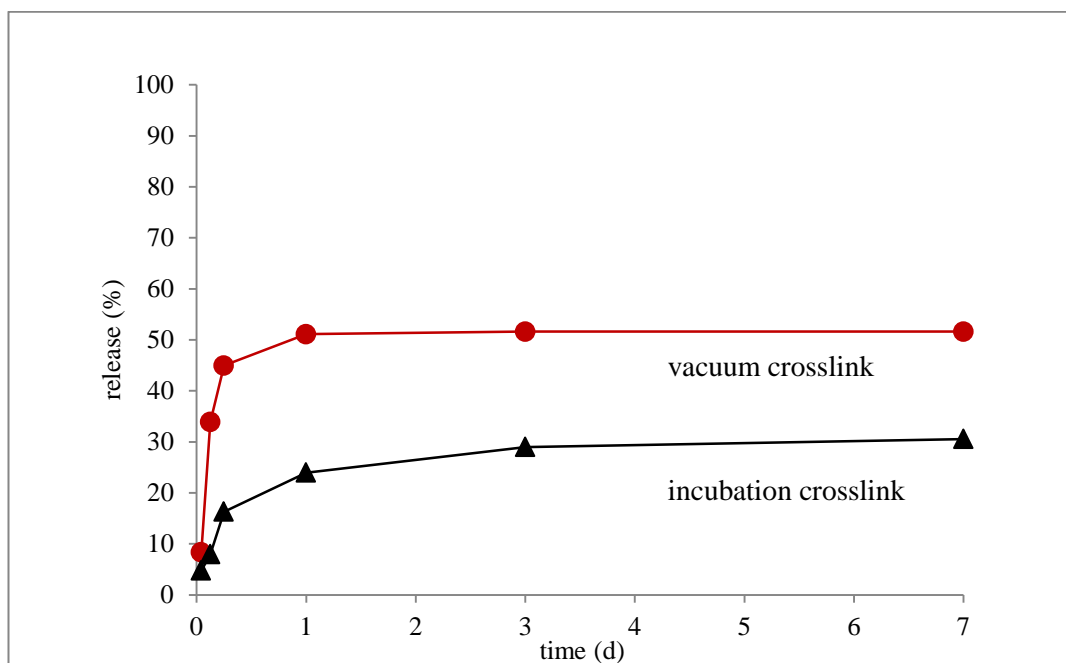


**Figure 3.14.** Release of BSA from Ch-ON/Alg model prepared by crosslinking of alginate layer via either vacuum crosslink or incubation crosslink.

When crosslinking of alginate layer was carried out by vacuum cycling in Ch-ON/Alg model, it was observed that total amount of released BSA increased to 51.63% (w/w) which is close to the observed release amount in Ch-ON model which was 62.47% (w/w). Therefore, it was confirmed that the reason behind the low release profile from Ch-ON/Alg model when incubation crosslink was employed is the loss of BSA during crosslinking process. Vacuum crosslink was demonstrated to be an efficient alternative procedure to prevent the loss of loaded protein. In order to investigate the effect of alginate coating on release profile of BSA, cumulative release graphs for Ch-ON and vacuum crosslinked Ch-ON/Alg models were compared in Figure 3.15.

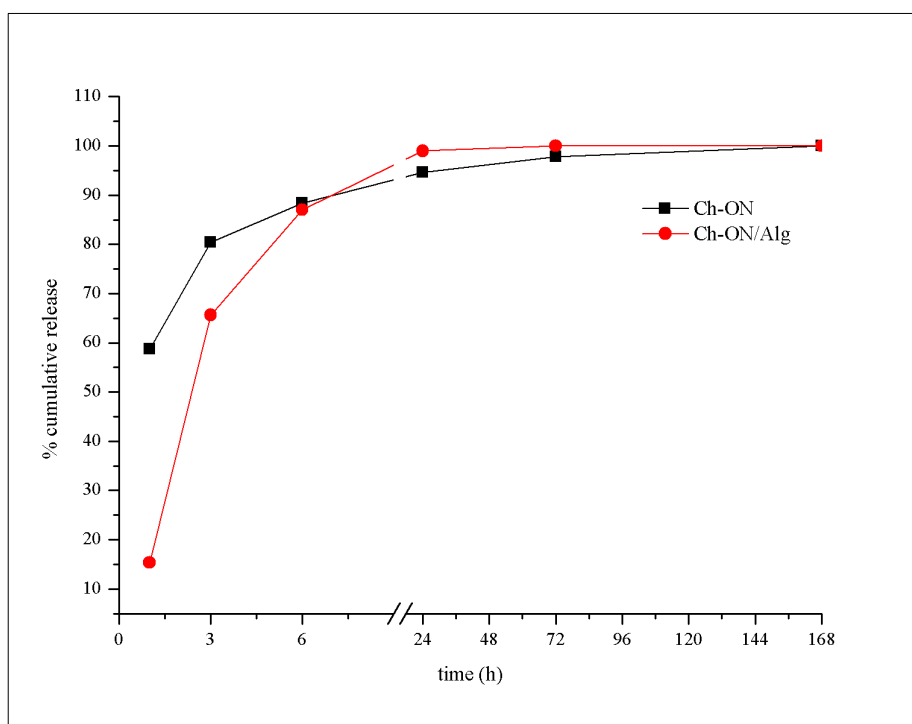


**Figure 3.15.** Cumulative release profiles of BSA from Ch-ON and vacuum crosslinked Ch-ON/Alg models.

Comparison of cumulative release of BSA from Ch-ON model and vacuum crosslinked Ch-ON/Alg model revealed that alginate coating was efficient in decreasing the burst release of BSA during first 6 h of incubation. As incubation period was prolonged, retarding effect of alginate layer on BSA release was lost due to dissolution of ionically crosslinked alginate by cation exchange in PBS solution.

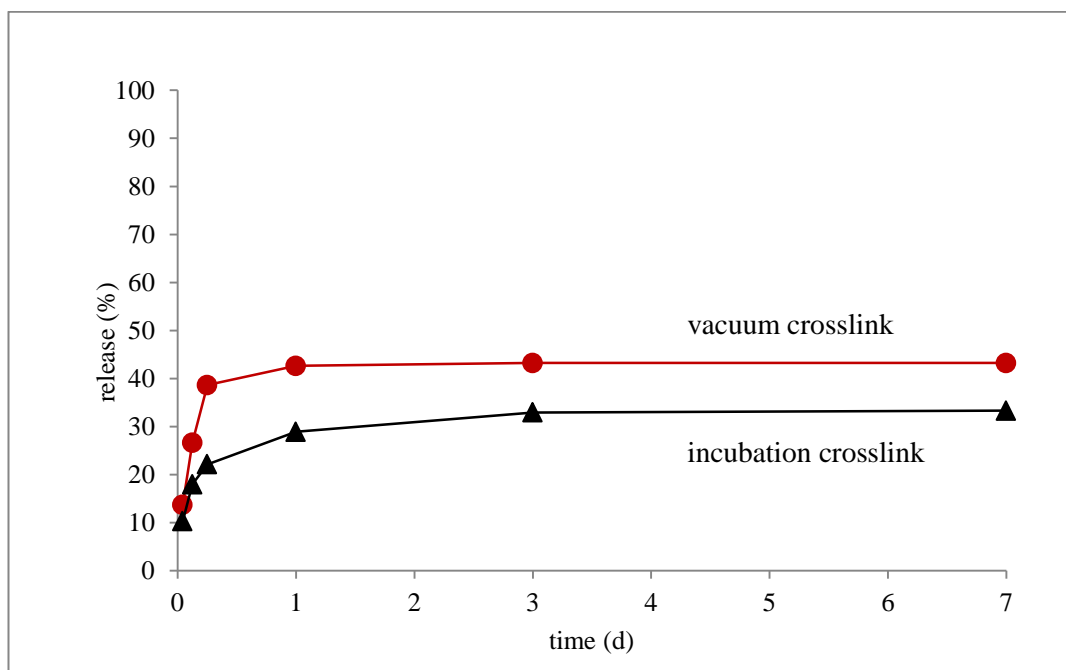


**Figure 3.16.** Release of BSA from Ch/Alg-IN model prepared by crosslinking of alginate layer via either vacuum crosslink or incubation crosslink.

Similarly, released BSA amount from Ch/Alg-IN model was enhanced by the use of vacuum crosslink meaning that when crosslinking was carried out through incubation in  $\text{CaCl}_2$  solution, there occurred a loss of BSA from scaffolds by initial release into the corresponding solution. Although a slight enhancement was observed when vacuum crosslink procedure was employed, release values were still lower than Ch-ON models of either uncoated or alginate coated. In Ch-ON models, BSA was introduced onto the neutral chitosan core and adhered to the surface. When incubated in PBS they were easily desorbed. On the other hand, when introduced into the alginate solution, electrostatic interactions between the oppositely charged amino acids and the anionic polysaccharide macromolecules may have partially restrained the release of BSA.

### 3.3.2. Gentamicin Release from Scaffolds

Gentamicin loading to the scaffolds was carried out by vacuum addition onto the chitosan core of the scaffolds or incorporation within the chitosan solution prior to wet spinning. Release behavior of gentamicin was investigated on three different models as Ch-ON, Ch-ON/Alg and Ch-IN/Alg. Additionally, release kinetics of gentamicin was studied from biomineralized chitosan scaffolds (Ch-ON/BM) that were incubated in SBF-5 solution for 7 d and gentamicin was then loaded via vacuum addition. Release profiles of gentamicin from scaffolds are given in Figure 3.17.

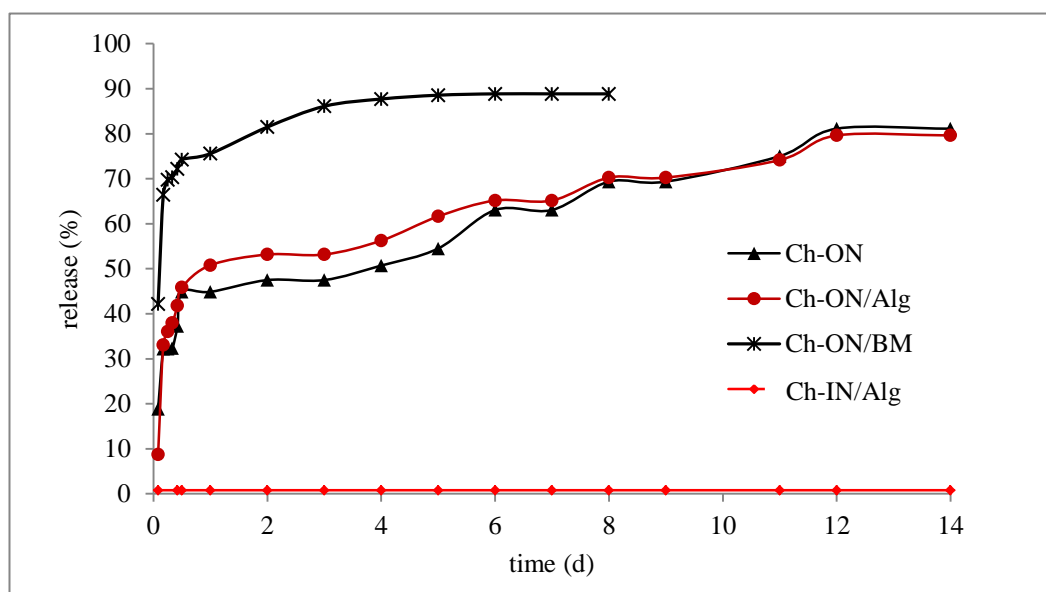


**Figure 3.17.** Release profiles of gentamicin from scaffolds.

In the case of bone tissue engineering applications the most advantageous release profile for antibiotics is a burst release followed by a sustained release period (Zilberman and Elsner, 2008). As seen from the graph, there obtained such kind of a release profile for gentamicin when Ch-ON and Ch-ON/Alg models were used. It was observed that 45% (w/w) of loaded gentamicin was released upon 12 h of incubation and 80% (w/w) recovery of totally loaded drug by release was achieved in 12 d in both models. The fast release of gentamicin seen in first 12 h of incubation was resultant from the rapid water uptake of scaffolds and dissolution of the antibiotic at the surface. Results showed that alginate coating had little effect on slowing the burst release of gentamicin only upon 2 h of incubation. Then, release profiles showed nearly equality for both uncoated and alginate coated scaffolds. Since gentamicin is a small molecule, it was easily diffused into the incubation medium despite of the alginate layer as it swells and dissolves easily in PBS.

No release of gentamicin was observed from Ch-IN/Alg model. Further investigation during scaffold preparation procedure revealed that 51.59% (w/w) of loaded gentamicin was released into the coagulation bath during incubation of fibers after wet spinning and 20.41% (w/w) was released into the distilled water during washing process. An additional 9.12% (w/w) of loaded gentamicin was lost in dehydration procedure. As a result, 81.12% (w/w) of totally loaded drug was observed to be lost throughout the preparation of scaffolds. Therefore, it was concluded that use of Ch-IN/Alg model scaffolds were not efficient for local administration of antibiotics that are small molecules easily diffusing out during incubation periods.

In the case of gentamicin release from Ch-ON/BM scaffolds there again obtained a sustained release curve with an initial burst release. When compared with non biomineralized counterparts, a higher release rate was demonstrated from biomineralized scaffolds. 75.58% (w/w) of loaded gentamicin was released upon 12 h of incubation and total released amount of 88.56% (w/w) was reached at 7 d. For scaffolds that antibiotics are loaded via adsorption, release rate is directly related to

the strength of the chemical interaction between the adsorbent surface and drug (Tamimi *et. al.*, 2012). Gentamicin has amine and hydroxyl functional groups that are also present in chitosan structure so that they can interact through hydrogen bonding. On the other hand, upon mineralization for 7 d, calcium phosphate minerals agglomerate on the surface of scaffolds and previous studies stated uncontrollable fast release of gentamicin when calcium phosphates are used as substrates (Silverman *et. al.*, 2007; Zhu and Kaskel, 2009). Therefore, it can be concluded that the higher release rate of gentamicin observed on biomineralized scaffolds results from weaker chemical interactions between gentamicin and mineral surface compared to that of chitosan surface.

### **3.3.2.1. Antibacterial Effect of Released Gentamicin**

In order to investigate the antibacterial effect of gentamicin upon release from loaded scaffolds disk diffusion method was used. Chitosan scaffold as control and gentamicin tablet as standard were placed on agar plate with gentamicin loaded Ch-ON, Ch-ON/biomineralized and Ch-ON/Alg scaffolds. Upon incubation at 37°C for 24 h inhibition zones indicating the antibiotic activity against E.coli were observed.

As shown in Figure 3.18, chitosan scaffold (a) used as control showed no inhibition against E.coli that was spread over the agar plate. In literature it is given that chitosan has intrinsic antibacterial activity due to its polycationic nature through interaction of positively charged amino groups with anionic components of cell surface proteins of microorganisms. However, during scaffold preparation chitosan was neutralized, therefore, did not cause any inhibition zone on agar plate. On the other hand gentamicin containing scaffolds of Ch-ON (b), Ch-ON/biomineralized (c) and Ch-ON/Alg (d) models resulted in formation of inhibition zones similar to that formed by gentamicin tablet (e) used as standard on the plate. From these results it was concluded that gentamicin was released from prepared scaffolds and exhibited its antibacterial effect.

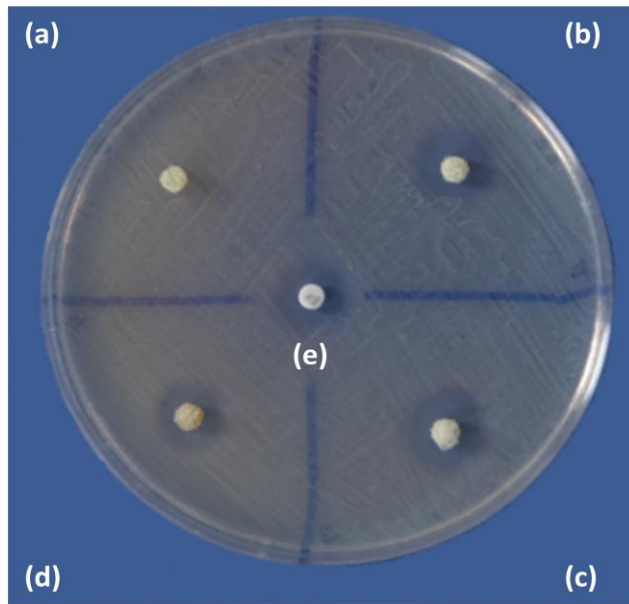


**Figure 3.18.** Photograph of *E.coli* spreaded agar plate after incubation at 37°C for 24 h; (a) chitosan, (b) Ch-ON, (c) Ch-ON biomineralized, (d) Ch-ON/Alg scaffolds and (e) gentamicin tablet.

## **CHAPTER 4**

### **CONCLUSION**

Restoration and reconstruction of bone tissue is a complex procedure that should be managed through patient specific treatment. Conventional clinical approaches lack the functionality that is needed to meet the explicit requirements in each case. Therefore, bone tissue engineering has emerged as a multidisciplinary field enabling the construction of well designed systems that would assist the healing and reconstruction of fractured bone site.

In this study, it was aimed to design a construct that would exhibit optimal physical, chemical and biological properties to be used in the treatment of bone tissue that could be functionalized with the feature of bioactive agent delivery. For that purpose, natural polymers chitosan and alginate was chosen as scaffolding materials possessing the advantages of biocompatibility and osteoconductivity. Scaffolds were produced by wet spinning method that resulted in porous, fibrous structure resembling to natural bone tissue. Then, prepared scaffolds were characterized in terms of their water uptake ability, degradation behavior, bioactivity and mechanical properties. Results showed that produced scaffolds exhibit convenient durability and mechanical strength to be used in engineering of cancellous bone with the characteristic of excellent bioactivity that could promote bone mineralization which is a critical step in healing and regeneration of bone tissue.

In addition, scaffolds were functionalized through incorporation of bioactive agents that are known to enhance biological functioning of the constructs. In the

treatment of bone tissue, it is well documented that both antibiotics and proteins are crucially important that prevent infections and regulate cellular behaviors, respectively. Release studies of gentamicin as a model antibiotic and BSA as a model protein revealed the capability of the scaffolds to be used as delivery agents for these bioactive molecules.

As a conclusion;

- Fibrous scaffolds exhibiting core-shell structure were produced.
- Scaffolds showed high water uptake and retention capacity which are critical for absorption of body fluids; transfer of nutrients, O<sub>2</sub> and metabolic wastes; overall enhance cell attachment and migration.
- Scaffolds were demonstrated to be degradable enzymatically and exhibited surface degradation that would enable prolonged maintenance of structural integrity.
- Upon incubation in SBF-5, CaP mineral deposition was observed on scaffolds which is correlated with the bioactivity of scaffolds towards bone mineralization.
- Compressive moduli of scaffolds showed low values, however, upon biomineralization for 7 d, values reached within the range of cancellous bone.
- Sustained release profiles were observed for BSA which was used as a model protein in all loading models.
- Incubation crosslinking of alginate layer caused BSA loss in Ch-ON/Alg and Ch/Alg-IN models and this problem was overcome via vacuum crosslinking procedure.
- Alginate layer was shown to be effective in decreasing the burst release of BSA up to first 6 h.

- Sustained release profile was achieved for gentamicin which was used as a model antibiotic in Ch-ON, Ch-ON/Alg and Ch-ON/ 7d biom mineralized models.
- For gentamicin, Ch-IN/Alg model was shown to be ineffective due to the loss of small molecule through diffusion during incubation periods of the preparation procedure.
- Alginate layer had no retarding effect on the release rate of gentamicin from the scaffolds.
- Gentamicin release proceeded faster from CaP biom mineralized scaffolds which was associated with weaker interactions between the adsorbent surface and drug.
- It was shown by disc diffusion method that gentamicin preserved its antibacterial activity upon loading on the scaffolds against E.coli.

According to these results it can be concluded that production of polymeric scaffolds possessing advantageous physical, chemical and biological properties together with the feature of bioactive agent delivery to be used in bone tissue engineering applications was successfully achieved.

## REFERENCES

- Agrawal, C. M. and R. B. Ray (2001). "Biodegradable polymeric scaffolds for musculoskeletal tissue engineering." *Journal of Biomedical Materials Research* 55(2): 141-150.
- Aina, V., D. Ghigo, T. Marchis, G. Cerrato, E. Laurenti, C. Morterra, G. Malavasi, G. Lusvardi, L. Menabue and L. Bergandi (2011). "Novel bio-conjugate materials: soybean peroxidase immobilized on bioactive glasses containing Au nanoparticles." *Journal of Materials Chemistry* 21(29): 10970-10981.
- Al-Aql, Z. S., A. S. Alagl, D. T. Graves, L. C. Gerstenfeld and T. A. Einhorn (2008). "Molecular mechanisms controlling bone formation during fracture healing and distraction osteogenesis." *Journal of Dental Research* 87(2): 107-118.
- Alge, D. L., J. Bennett, T. Treasure, S. Voytik-Harbin, W. S. Goebel and G. Chu (2012). "Poly(propylene fumarate) reinforced dicalcium phosphate dihydrate cement composites for bone tissue engineering." *Journal of Biomedical Materials Research Part A* 100A(7): 1792-1802.
- Alsberg, E., K. W. Anderson, A. Albeiruti, R. T. Franceschi and D. J. Mooney (2001). "Cell-interactive alginate hydrogels for bone tissue engineering." *Journal of Dental Research* 80(11): 2025-2029.
- Alsberg, E., H. J. Kong, Y. Hirano, M. K. Smith, A. Albeiruti and D. J. Mooney (2003). "Regulating bone formation via controlled scaffold degradation." *Journal of Dental Research* 82(11): 903-908.
- Andric, T., L. D. Wright and J. W. Freeman (2011). "Rapid mineralization of electrospun scaffolds for bone tissue engineering." *Journal of Biomaterials Science, Polymer Edition* 22(11): 1535-1550.
- Andric, T., L. D. Wright, B. L. Taylor and J. W. Freeman (2012). "Fabrication and characterization of three-dimensional electrospun scaffolds for bone tissue engineering." *Journal of Biomedical Materials Research - Part A* 100 A(8): 2097-2105.
- Anseth, K. S., V. R. Shastri and R. Langer (1999). "Photopolymerizable degradable polyanhydrides with osteocompatibility." *Nature Biotechnology* 17(2): 156-159.
- Arpornmaeklong, P., P. Pripatnanont and N. Suwatwirote (2008). "Properties of chitosan-collagen sponges and osteogenic differentiation of rat-bone-marrow stromal cells." *International Journal of Oral and Maxillofacial Surgery* 37(4): 357-366.

- Asikainen, A. J., J. Noponen, K. Mesimäki, O. Laitinen, J. Peltola, M. Pelto, M. Kellomäki, N. Ashammakhi, C. Lindqvist and R. Suuronen (2005). "Tyrosine derived polycarbonate membrane is useful for guided bone regeneration in rabbit mandibular defects." *Journal of Materials Science: Materials in Medicine* 16(8): 753-758.
- Attawia, M. A., K. E. Uhrich, E. Botchwey, R. Langer and C. T. Laurencin (1996). "In vitro bone biocompatibility of poly(anhydride-co-imides) containing pyromellitylimidoalanine." *Journal of Orthopaedic Research* 14(3): 445-454.
- Augst, A. D., H. J. Kong and D. J. Mooney (2006). "Alginate hydrogels as biomaterials." *Macromolecular Bioscience* 6(8): 623-633.
- Azami, M., M. J. Moosavifar, N. Baheiraei, F. Moztafzadeh and J. Ai (2012). "Preparation of a biomimetic nanocomposite scaffold for bone tissue engineering via mineralization of gelatin hydrogel and study of mineral transformation in simulated body fluid." *Journal of Biomedical Materials Research - Part A* 100 A(5): 1347-1356.
- Badylak, S.F., D. O. Freytes and T. W. Gilbert (2009). "Extracellular matrix as a biological scaffold material: structure and function." *Acta Biomaterialia* 5: 1-13.
- Bae, S. E., J. Choi, Y. K. Joung, K. Park and D. K. Han (2012). "Controlled release of bone morphogenetic protein (BMP)-2 from nanocomplex incorporated on hydroxyapatite-formed titanium surface." *Journal of Controlled Release* 160(3): 676-684.
- Baldwin, S. P. and W. M. Saltzman (1998). "Materials for protein delivery in tissue engineering." *Advanced Drug Delivery Reviews* 33(1-2): 71-86.
- Balmayor, E. R., E. T. Baran, H. S. Azevedo and R. L. Reis (2012). "Injectable biodegradable starch/chitosan delivery system for the sustained release of gentamicin to treat bone infections." *Carbohydrate Polymers* 87(1): 32-39.
- Barrère, F., C. M. Van Der Valk, G. Meijer, R. A. J. Dalmeijer, K. De Groot and P. Layrolle (2003). "Osteointegration of Biomimetic Apatite Coating Applied onto Dense and Porous Metal Implants in Femurs of Goats." *Journal of Biomedical Materials Research - Part B Applied Biomaterials* 67(1): 655-665.
- Beherei, H. H., M. S. Abdel-Aal, A. A. Shaltout and A. El-Magharby (2012). "Bio-physicochemical characterization of anticancer nano-ceramic polymer scaffold for bone grafting." *Der Pharma Chemica* 4(1): 544-551.
- Beherei, H. H., A. El-Magharby and M. S. Abdel-Aal (2011). "Preparation and characterization of novel antibacterial nano-ceramic-composites for bone grafting." *Der Pharma Chemica* 3(6): 10-27.

- Benghuzzi, H., M. Tucci, G. Russell, A. Ragab, M. Graves and J. Conflitti (2006). "Targeted sustained delivery of tobramycin at the site of a femoral osteotomy." *Biomedical Sciences Instrumentation* 42: 530-535.
- Bergman, K., T. Engstrand, J. Hilborn, D. Ossipov, S. Piskounova and T. Bowden (2009). "Injectable cell-free template for bone-tissue formation." *Journal of Biomedical Materials Research Part A* 91A(4): 1111-1118.
- Bhakta, G., B. Rai, Z. X. H. Lim, J. H. Hui, G. S. Stein, A. J. van Wijnen, V. Nurcombe, G. D. Prestwich and S. M. Cool (2012). "Hyaluronic acid-based hydrogels functionalized with heparin that support controlled release of bioactive BMP-2." *Biomaterials* 33(26): 6113-6122.
- Bhardwaj, N. and S. C. Kundu (2012). "Chondrogenic differentiation of rat MSCs on porous scaffolds of silk fibroin/chitosan blends." *Biomaterials* 33(10): 2848-2857.
- Bil, M., J. Ryszkowska, P. Woźniak, K. J. Kurzydłowski and M. Lewandowska-Szumieł (2010). "Optimization of the structure of polyurethanes for bone tissue engineering applications." *Acta Biomaterialia* 6(7): 2501-2510.
- Biondi, M., F. Ungaro, F. Quaglia and P. A. Netti (2008). "Controlled drug delivery in tissue engineering." *Advanced Drug Delivery Reviews* 60(2): 229-242.
- Bloemers, F. W., J. P. Stahl, M. R. Sarkar, W. Linhart, U. Rueckert and B. W. Wippermann (2004). "Bone Substitution and Augmentation in Trauma Surgery with a Resorbable Calcium Phosphate Bone Cement." *European Journal of Trauma* 30(1): 17-22.
- Bormann, K. H., M. M. Suarez-Cunqueiro, B. Sinikovic, A. Kampmann, C. von See, F. Tavassol, T. Binger, M. Winkler, N. C. Gellrich and M. Rücker (2012). "Dentin as a suitable bone substitute comparable to  $\beta$ -TCP-an experimental study in mice." *Microvascular Research* 84(2): 116-122.
- Budiraharjo, R., K. G. Neoh, E. T. Kang and A. Kishen (2010). "Bioactivity of novel carboxymethyl chitosan scaffold incorporating MTA in a tooth model." *International Endodontic Journal* 43(10): 930-939.
- Burg, K. J. L., S. Porter and J. F. Kellam (2000). "Biomaterial developments for bone tissue engineering." *Biomaterials* 21(23): 2347-2359.
- Cahill, S., S. Lohfeld and P. E. McHugh (2009). "Finite element predictions compared to experimental results for the effective modulus of bone tissue engineering scaffolds fabricated by selective laser sintering." *Journal of Materials Science: Materials in Medicine* 20(6): 1255-1262.
- Calvo-Guirado, J. L., G. Gómez-Moreno, J. Guardia, A. Ortiz-Ruiz, A. Piatelli, A. Barone, J. M. Martínez-González, L. Meseguer-Olmo, L. López-Marí and C. B.

Dorado (2012). "Biological response to porcine xenograft implants: An experimental study in rabbits." *Implant Dentistry* 21(2): 112-117.

Cao, H., L. B. Chen, Y. S. Liu, H. Xiu and H. Wang (2012). "Poly-D, L-lactide and levofloxacin-blended beads: A sustained local releasing system to treat osteomyelitis." *Journal of Applied Polymer Science* 124(5): 3678-3684.

Caridade, S. G., E. G. Merino, G. M. Luz, N. M. Alves and J. F. Mano (2010). "Bioactivity and viscoelastic characterization in physiological simulated conditions of chitosan/Bioglass® composite membranes." *Materials Science Forum* 636-637: 26-30.

Chakraborti, M., J. Jackson, D. Plackett, S. Gilchrist and H. Burt (2012). "The application of layered double hydroxide clay (LDH)-poly(lactide-co-glycolic acid) (PLGA) film composites for the controlled release of antibiotics." *Journal of Materials Science: Materials in Medicine* 23(7): 1705-1713.

Chen, F., S. Chen, K. Tao, X. Feng, Y. Liu, D. Lei and T. Mao (2004). "Marrow-derived osteoblasts seeded into porous natural coral to prefabricate a vascularised bone graft in the shape of a human mandibular ramus: experimental study in rabbits." *British Journal of Oral and Maxillofacial Surgery* 42(6): 532-537.

Chen, L., Z. He, B. Chen, Y. Zhao, W. Sun, Z. Xiao, J. Zhang, M. Yang, Z. Gao and J. Dai (2009). "Direct chemical cross-linking of platelet-derived growth factor-BB to the demineralized bone matrix improves cellularization and vascularization." *Biomacromolecules* 10(12): 3193-3198.

Chen, L., C. Zhu, D. Fan, B. Liu, X. Ma, Z. Duan and Y. Zhou (2011). "A human-like collagen/chitosan electrospun nanofibrous scaffold from aqueous solution: Electrospun mechanism and biocompatibility." *Journal of Biomedical Materials Research - Part A* 99 A(3): 395-409.

Chen, S. H., X. L. Wang, X. H. Xie, L. Z. Zheng, D. Yao, D. P. Wang, Y. Leng, G. Zhang and L. Qin (2012). "Comparative study of osteogenic potential of a composite scaffold incorporating either endogenous bone morphogenetic protein-2 or exogenous phytomolecule icaritin: An in vitro efficacy study." *Acta Biomaterialia* 8(8): 3128-3137.

Chen, W., H. Zhou, M. Tang, M. D. Weir, C. Bao and H. H. Xu (2012). "Gas-foaming calcium phosphate cement scaffold encapsulating human umbilical cord stem cells." *Tissue engineering. Part A* 18(7-8): 816-827.

Chen, X., Y.-Y. Qi, L.-L. Wang, Z. Yin, G.-L. Yin, X.-H. Zou and H.-W. Ouyang (2008). "Ligament regeneration using a knitted silk scaffold combined with collagen matrix." *Biomaterials* 29(27): 3683-3692.

Chen, Y. Y., C. P. Jiang and C. C. Chen (2012). Development of bio-rapid prototyping system for fabricating bone scaffold using thermal-sensitive biopolymer. 488-489: 985-990.

Chiang, Z. C., S. H. Yu, A. C. Chao and G. C. Dong (2012). "Preparation and characterization of dexamethasone-immobilized chitosan scaffold." *Journal of Bioscience and Bioengineering* 113(5): 654-660.

Clarke, B. (2008). "Normal bone anatomy and physiology." *Clinical Journal of the American Society of Nephrology : CJASN* 3 Suppl 3: S131-139.

Clyne, T. W., A. E. Markaki and J. C. Tan (2005). "Mechanical and magnetic properties of metal fibre networks, with and without a polymeric matrix." *Composites Science and Technology* 65(15-16 SPEC. ISS.): 2492-2499.

Costa-Pinto, A. R., R. L. Reis and N. M. Neves (2011). "Scaffolds based bone tissue engineering: The role of chitosan." *Tissue Engineering - Part B: Reviews* 17(5): 331-347.

Costa-Pinto Ar Fau - Salgado, A. J., V. M. Salgado Aj Fau - Correlo, P. Correlo Vm Fau - Sol, M. Sol P Fau - Bhattacharya, P. Bhattacharya M Fau - Charbord, R. L. Charbord P Fau - Reis, N. M. Reis Rl Fau - Neves and N. M. Neves (2008). "Adhesion, proliferation, and osteogenic differentiation of a mouse mesenchymal stem cell line (BMC9) seeded on novel melt-based chitosan/polyester 3D porous scaffolds." *Tissue Engineering Part:A* 14(6): 1049-1057.

Cui, Y., Y. Liu, Y. Cui, X. Jing, P. Zhang and X. Chen (2009). "The nanocomposite scaffold of poly(lactide-co-glycolide) and hydroxyapatite surface-grafted with l-lactic acid oligomer for bone repair." *Acta Biomaterialia* 5(7): 2680-2692.

De la Riva, B., C. Nowak, E. Sánchez, A. Hernández, M. Schulz-Siegmund, M. K. Pec, A. Delgado and C. Évora (2009). "VEGF-controlled release within a bone defect from alginate/chitosan/PLA-H scaffolds." *European Journal of Pharmaceutics and Biopharmaceutics* 73(1): 50-58.

De la Riva, B., E. Sánchez, A. Hernández, R. Reyes, F. Tamimi, E. López-Cabarcos, A. Delgado and C. vora (2010). "Local controlled release of VEGF and PDGF from a combined brushite-chitosan system enhances bone regeneration." *Journal of Controlled Release* 143(1): 45-52.

De Oliveira, A. A. R., S. M. De Carvalho, M. De Fátima Leite, R. L. Oréfice and M. De Magalhães Pereira (2012). "Development of biodegradable polyurethane and bioactive glass nanoparticles scaffolds for bone tissue engineering applications." *Journal of Biomedical Materials Research - Part B Applied Biomaterials* 100 B(5): 1387-1396.

Dee, K. C. and R. Bizios (1996). "Mini-review: Proactive biomaterials and bone tissue engineering." *Biotechnology and Bioengineering* 50(4): 438-442.

Demers, C., C. Reggie Hamdy, K. Corsi, F. Chellat, M. Tabrizian and L. Yahia (2002). "Natural coral exoskeleton as a bone graft substitute: A review." *Bio-Medical Materials and Engineering* 12(1): 15-35.

Deng, X. L., G. Sui, M. L. Zhao, G. Q. Chen and X. P. Yang (2007). "Poly(L-lactic acid)/hydroxyapatite hybrid nanofibrous scaffolds prepared by electrospinning." *Journal of Biomaterials Science, Polymer Edition* 18(1): 117-130.

Diab, T., E. M. Pritchard, B. A. Uhrig, J. D. Boerckel, D. L. Kaplan and R. E. Guldberg (2012). "A silk hydrogel-based delivery system of bone morphogenetic protein for the treatment of large bone defects." *Journal of the Mechanical Behavior of Biomedical Materials* 11: 123-131.

Dinarvand, P., E. Seyedjafari, A. Shafiee, A. Babaei Jandaghi, A. Doostmohammadi, M. H. Fathi, S. Farhadian and M. Soleimani (2011). "New approach to bone tissue engineering: Simultaneous application of hydroxyapatite and bioactive glass coated on a poly(L-lactic acid) scaffold." *ACS Applied Materials and Interfaces* 3(11): 4518-4524.

Dorj, B., J. H. Park and H. W. Kim (2012). "Robocasting chitosan/nanobioactive glass dual-pore structured scaffolds for bone engineering." *Materials Letters* 73: 119-122.

Duarte, A. R. C., J. F. Mano and R. L. Reis (2009). "Preparation of chitosan scaffolds loaded with dexamethasone for tissue engineering applications using supercritical fluid technology." *European Polymer Journal* 45(1): 141-148.

Duggal, S., K. B. Frønsdal, K. Szöke, A. Shahdadfar, J. E. Melvik and J. E. Brinchmann (2009). "Phenotype and gene expression of human mesenchymal stem cells in alginate scaffolds." *Tissue Engineering - Part A* 15(7): 1763-1773.

Dyondi, D., T. J. Webster and R. Banerjee (2011). Development of a dual growth factor loaded biodegradable hydrogel and its evaluation on osteoblast differentiation in vitro.

Eiselt, P., K. Y. Lee and D. J. Mooney (1999). "Rigidity of two-component hydrogels prepared from alginate and poly(ethylene glycol)-diamines." *Macromolecules* 32(17): 5561-5566.

Ekaputra, A. K., Y. Zhou, S. M. Cool and D. W. Hutmacher (2009). "Composite electrospun scaffolds for engineering tubular bone grafts." *Tissue Engineering - Part A* 15(12): 3779-3788.

El-Tahlawy, K. and S. M. Hudson (2006). "Chitosan: Aspects of fiber spinnability." *Journal of Applied Polymer Science* 100(2): 1162-1168.

Eppley, B. L., W. S. Pietrzak and M. W. Blanton (2005). "Allograft and alloplastic bone substitutes: A review of science and technology for the craniomaxillofacial surgeon." *Journal of Craniofacial Surgery* 16(6): 981-989.

Erol, M. M., V. Mouriño, P. Newby, X. Chatzistavrou, J. A. Roether, L. Hupa and A. R. Boccaccini (2012). "Copper-releasing, boron-containing bioactive glass-based scaffolds coated with alginate for bone tissue engineering." *Acta Biomaterialia* 8(2): 792-801.

Eshraghi, S. and S. Das (2012). "Micromechanical finite-element modeling and experimental characterization of the compressive mechanical properties of polycaprolactone-hydroxyapatite composite scaffolds prepared by selective laser sintering for bone tissue engineering." *Acta Biomaterialia* 8(8): 3138-3143.

Farrell, E., F. J. O'Brien, P. Doyle, J. Fischer, I. Yannas, B. A. Harley, B. O'Connell, P. J. Prendergast and V. A. Campbell (2006). "A collagen-glycosaminoglycan scaffold supports adult rat mesenchymal stem cell differentiation along osteogenic and chondrogenic routes." *Tissue Engineering* 12(3): 459-468.

Fedorovich, N. E., J. Alblas, W. E. Hennink, F. C. Öner and W. J. A. Dhert (2011). "Organ printing: the future of bone regeneration?" *Trends in Biotechnology* 29(12): 601-606.

Feng, W., L. Fu, J. Liu and D. Li (2012). "The expression and distribution of xenogeneic targeted antigens on porcine bone tissue." *Transplantation Proceedings* 44(5): 1419-1422.

Flick, L. M., J. M. Weaver, M. Ulrich-Vinther, F. Abuzzahab, X. Zhang, W. C. Dougall, D. Anderson, R. J. O'Keefe and E. M. Schwarz (2003). "Effects of receptor activator of NF $\kappa$ B (RANK) signaling blockade on fracture healing." *Journal of Orthopaedic Research* 21(4): 676-684.

Florczyk, S. J., D. J. Kim, D. L. Wood and M. Zhang (2011). "Influence of processing parameters on pore structure of 3D porous chitosan-alginate polyelectrolyte complex scaffolds." *Journal of Biomedical Materials Research - Part A* 98 A(4): 614-620.

Floren, M., S. Spilimbergo, A. Motta and C. Migliaresi (2011). "Porous poly(D,L-lactic acid) foams with tunable structure and mechanical anisotropy prepared by supercritical carbon dioxide." *Journal of Biomedical Materials Research Part B: Applied Biomaterials* 99B(2): 338-349.

Fu, Q., E. Saiz and A. P. Tomsia (2011). "Direct ink writing of highly porous and strong glass scaffolds for load-bearing bone defects repair and regeneration." *Acta Biomaterialia* 7(10): 3547-3554.

Galjour, C., S. Dzugan, M. Graves, H. Benghuzzi, G. Russell, M. Tucci and A. Tsao (2005). "Stimulation of fracture healing by continuous delivery of demineralized

bone matrix proteins and tobramycin." *Biomedical Sciences Instrumentation* 41: 122-127.

Gattás-Asfura, K. M. and C. L. Stabler (2009). "Chemoselective cross-linking and functionalization of alginate via Staudinger ligation." *Biomacromolecules* 10(11): 3122-3129.

Gomes, M. E., H. S. Azevedo, A. R. Moreira, V. Ellä, M. Kellomäki and R. L. Reis (2008). "Starch–poly( $\epsilon$ -caprolactone) and starch–poly(lactic acid) fibre-mesh scaffolds for bone tissue engineering applications: structure, mechanical properties and degradation behaviour." *Journal of Tissue Engineering and Regenerative Medicine* 2(5): 243-252.

Grynpas, M. D. and S. Omelon (2007). "Transient precursor strategy or very small biological apatite crystals?" *Bone* 41(2): 162-164.

Guelcher, S. A., K. V. Brown, B. Li, T. Guda, B. H. Lee and J. C. Wenke (2011). "Dual-purpose bone grafts improve healing and reduce infection." *Journal of Orthopaedic Trauma* 25(8): 477-482.

Guillemin, G., J. L. Patat, J. Fournie and M. Chetail (1987). "The use of coral as a bone graft substitute." *Journal of Biomedical Materials Research* 21(5): 557-567.

Guo, Z., H. Li, W. Guan, B. Xue and C. Zhou (2012). Preparation of mineralized electrospun PCL/gelatin scaffolds via double diffusion system. 512-515: 1740-1745.

Hacking, S. A., E. J. Harvey, M. Tanzer, J. J. Krygier and J. D. Bobyn (2003). "Acid-etched microtexture for enhancement of bone growth into porous-coated implants." *Journal of Bone and Joint Surgery - Series B* 85(8): 1182-1189.

Hafeman, A. E., B. Li, T. Yoshii, K. Zienkiewicz, J. M. Davidson and S. A. Guelcher (2008). "Injectable biodegradable polyurethane scaffolds with release of platelet-derived growth factor for tissue repair and regeneration." *Pharmaceutical Research* 25(10): 2387-2399.

Hall, K. K., K. M. Gattás-Asfura and C. L. Stabler (2011). "Microencapsulation of islets within alginate/poly(ethylene glycol) gels cross-linked via Staudinger ligation." *Acta Biomaterialia* 7(2): 614-624.

He, C., F. Zhang, L. Cao, W. Feng, K. Qiu, Y. Zhang, H. Wang, X. Mo and J. Wang (2012). "Rapid mineralization of porous gelatin scaffolds by electrodeposition for bone tissue engineering." *Journal of Materials Chemistry* 22(5): 2111-2119.

Healey, J. H., P. A. Zimmerman, J. M. McDonnell and J. M. Lane (1990). "Percutaneous bone marrow grafting of delayed union and nonunion in cancer patients." *Clinical Orthopaedics and Related Research* (256): 280-285.

Heath, D. E., J. J. Lannutti and S. L. Cooper (2010). "Electrospun scaffold topography affects endothelial cell proliferation, metabolic activity, and morphology." *Journal of Biomedical Materials Research - Part A* 94(4): 1195-1204.

Hench, L. L. (1999). *An Introduction to Bioceramics*. Singapore, World Scientific

Hou, J., J. Wang, L. Cao, X. Qian, W. Xing, J. Lu and C. Liu (2012). "Segmental bone regeneration using rhBMP-2-loaded collagen/chitosan microspheres composite scaffold in a rabbit model." *Biomedical Materials* 7(3): 035002.

Hsu, S. H., T. B. Huang, S. J. Cheng, S. Y. Weng, C. L. Tsai, C. S. Tseng, D. C. Chen, T. Y. Liu, K. Y. Fu and B. L. Yen (2011). "Chondrogenesis from human placenta-derived mesenchymal stem cells in three-dimensional scaffolds for cartilage tissue engineering." *Tissue Engineering - Part A* 17(11-12): 1549-1560.

Hu, Y., S. R. Winn, I. Krajbich and J. O. Hollinger (2003). "Porous polymer scaffolds surface-modified with arginine-glycine-aspartic acid enhance bone cell attachment and differentiation in vitro." *Journal of Biomedical Materials Research - Part A* 64(3): 583-590.

Huang, X. and C. S. Brazel (2003). "Analysis of burst release of proxiphylline from poly(vinyl alcohol) hydrogels." *Chemical Engineering Communications* 190(4): 519-532.

Huang, Z., B. Yu, Q. Feng and S. Li (2011). "Modification of an injectable chitosan scaffold by blending with NaHCO<sub>3</sub> to improve cytocompatibility." *Polymers and Polymer Composites* 19(9): 781-787.

Hunziker, E. B., L. Enggist, A. Küffer, D. Buser and Y. Liu (2012). "Osseointegration: The slow delivery of BMP-2 enhances osteoinductivity." *Bone* 51(1): 98-106.

Irineu, J. A. F., T. C. O. Marsi, T. G. Santos, E. J. Corat, F. R. Marciano and A. O. Lobo (2012). "Efficient method to produce biomineralized nanohydroxyapatite/vertically aligned multiwalled carbon nanotube scaffolds." *Materials Letters* 79: 166-169.

Isikli, C., V. Hasirci and N. Hasirci (2012). "Development of porous chitosan-gelatin/hydroxyapatite composite scaffolds for hard tissue-engineering applications." *Journal of Tissue Engineering and Regenerative Medicine* 6(2): 135-143.

Jeon, J. H., M. V. Thomas and D. A. Puleo (2007). "Bioerodible devices for intermittent release of simvastatin acid." *International Journal of Pharmaceutics* 340(1-2): 6-12.

Jeon, O., C. Powell, L. D. Solorio, M. D. Krebs and E. Alsberg (2011). "Affinity-based growth factor delivery using biodegradable, photocrosslinked heparin-alginate hydrogels." *Journal of Controlled Release* 154(3): 258-266.

Jeong, B., Y. H. Bae and S. W. Kim (2000). "Drug release from biodegradable injectable thermosensitive hydrogel of PEG–PLGA–PEG triblock copolymers." *Journal of Controlled Release* 63(1–2): 155-163.

Ji, J., X. Yuan, Z. Xia, P. Liu and J. Chen (2010). "Porous  $\beta$ -tricalcium phosphate composite scaffold reinforced by  $K_2HPO_4$  and gelatin." *Key Engineering Materials* 434-435: 620-623.

John, Ł., M. Bałtrukiewicz, P. Sobota, R. Brykner, Ł. Cwynar-Zajac and P. Dziegiel (2012). "Non-cytotoxic organic-inorganic hybrid bioscaffolds: An efficient bedding for rapid growth of bone-like apatite and cell proliferation." *Materials Science and Engineering C* 32(7): 1849-1858.

Kai, D., M. P. Prabhakaran, B. Stahl, M. Eblenkamp, E. Wintermantel and S. Ramakrishna (2012). "Mechanical properties and in vitro behavior of nanofiberhydrogel composites for tissue engineering applications." *Nanotechnology* 23(9).

Kailasanathan, C., N. Selvakumar and V. Naidu (2012). "Structure and properties of titania reinforced nano-hydroxyapatite/gelatin bio-composites for bone graft materials." *Ceramics International* 38(1): 571-579.

Kanczler, J. M., P. J. Ginty, L. White, N. M. P. Clarke, S. M. Howdle, K. M. Shakesheff and R. O. C. Oreffo (2010). "The effect of the delivery of vascular endothelial growth factor and bone morphogenic protein-2 to osteoprogenitor cell populations on bone formation." *Biomaterials* 31(6): 1242-1250.

Kao, L. H., H. K. Lin, F. J. Chuang and W. T. Hsu (2012). "Electrospun hierarchical cancellous-bone-like microstructures composed of a crystalline  $TiO_2$  nanonet." *Materials Letters* 82: 64-66.

Karageorgiou, V. and D. Kaplan (2005). "Porosity of 3D biomaterial scaffolds and osteogenesis." *Biomaterials* 26(27): 5474-5491.

Karakeçili, A. and A. Arıkan (2012). "Preparation of chitosan-nanohydroxyapatite composite scaffolds by a supercritical  $CO_2$  assisted process." *Polymer Composites* 33(7): 1215-1223.

Katsanevakis, E., X. Wen, D. Shi and N. Zhang (2010). "Biom mineralization of polymer scaffolds." *Key Engineering Materials* 441: 269-295.

Katz, J., N. Mukherjee, R. R. Cobb, P. Bursac and A. York-Ely (2009). "Incorporation and immunogenicity of cleaned bovine bone in a sheep model." *Journal of Biomaterials Applications* 24(2): 159-174.

Keaveny, T. M., E. F. Morgan, G. L. Niebur and O. C. Yeh (2001). "Biomechanics of trabecular bone." *Annual Review of Biomedical Engineering* 3: 307-333.

- Kempen, D. H. R., L. Lu, A. Heijink, T. E. Hefferan, L. B. Creemers, A. Maran, M. J. Yaszemski and W. J. A. Dhert (2009). "Effect of local sequential VEGF and BMP-2 delivery on ectopic and orthotopic bone regeneration." *Biomaterials* 30(14): 2816-2825.
- Khan, S. N., F. P. Cammisa Jr, H. S. Sandhu, A. D. Diwan, F. P. Girardi and J. M. Lane (2005). "The biology of bone grafting." *The Journal of the American Academy of Orthopaedic Surgeons* 13(1): 77-86.
- Kim, H.-W., Y.-H. Koh, L.-H. Li, S. Lee and H.-E. Kim (2004). "Hydroxyapatite coating on titanium substrate with titania buffer layer processed by sol-gel method." *Biomaterials* 25(13): 2533-2538.
- Kim, J., I. S. Kim, T. H. Cho, K. B. Lee, S. J. Hwang, G. Tae, I. Noh, S. H. Lee, Y. Park and K. Sun (2007). "Bone regeneration using hyaluronic acid-based hydrogel with bone morphogenic protein-2 and human mesenchymal stem cells." *Biomaterials* 28(10): 1830-1837.
- Kim, J., M. H. R. Magno, H. Waters, B. A. Doll, S. McBride, P. Alvarez, A. Darr, A. Vasanthi, J. Kohn and J. O. Hollinger (2012). "Bone regeneration in a rabbit critical-sized calvarial model using tyrosine-derived polycarbonate scaffolds." *Tissue Engineering - Part A* 18(11-12): 1132-1139.
- Kim, J., S. McBride, B. Tellis, P. Alvarez-Urena, Y. H. Song, D. D. Dean, V. L. Sylvia, H. Elgandy, J. Ong and J. O. Hollinger (2012). "Rapid-prototyped PLGA/ $\beta$ -TCP/hydroxyapatite nanocomposite scaffolds in a rabbit femoral defect model." *Biofabrication* 4(2).
- Kim, J. Y., J. Y. Choi, J. H. Jeong, E. S. Jang, A. S. Kim, S. G. Kim, H. Y. Kweon, Y. Y. Jo and J. H. Yeo (2010). "Low molecular weight silk fibroin increases alkaline phosphatase and type I collagen expression in MG63 cells." *BMB Reports* 43(1): 52-56.
- Kim, S., Y. Kang, C. A. Krueger, M. Sen, J. B. Holcomb, D. Chen, J. C. Wenke and Y. Yang (2012). "Sequential delivery of BMP-2 and IGF-1 using a chitosan gel with gelatin microspheres enhances early osteoblastic differentiation." *Acta Biomaterialia* 8(5): 1768-1777.
- Kim, S. S., M. Sun Park, O. Jeon, C. Yong Choi and B. S. Kim (2006). "Poly(lactide-co-glycolide)/hydroxyapatite composite scaffolds for bone tissue engineering." *Biomaterials* 27(8): 1399-1409.
- Knaut, J. Z. and K. A. M. Creber (1997). "Coagulation rate studies of spinnable chitosan solutions." *Journal of Applied Polymer Science* 66(1): 117-127.
- Kokubo, T. (1991). "Bioactive glass ceramics: properties and applications." *Biomaterials* 12(2): 155-163.

- Kokubo, T. and H. Takadama (2006). "How useful is SBF in predicting in vivo bone bioactivity?" *Biomaterials* 27(15): 2907-2915.
- Kong, L., Y. Gao, G. Lu, Y. Gong, N. Zhao and X. Zhang (2006). "A study on the bioactivity of chitosan/nano-hydroxyapatite composite scaffolds for bone tissue engineering." *European Polymer Journal* 42(12): 3171-3179.
- Kreeger, P. K., J. W. Deck, T. K. Woodruff and L. D. Shea (2006). "The in vitro regulation of ovarian follicle development using alginate-extracellular matrix gels." *Biomaterials* 27(5): 714-723.
- Kumar, G., M. S. Waters, T. M. Farooque, M. F. Young and C. G. Simon (2012). "Freeform fabricated scaffolds with roughened struts that enhance both stem cell proliferation and differentiation by controlling cell shape." *Biomaterials* 33(16): 4022-4030.
- Kundu, B., S. K. Nandi, S. Roy, N. Dandapat, C. Soundrapandian, S. Datta, P. Mukherjee, T. K. Mandal, S. Dasgupta and D. Basu (2012). "Systematic approach to treat chronic osteomyelitis through ceftriaxone-sulbactam impregnated porous  $\beta$ -tri calcium phosphate localized delivery system." *Ceramics International* 38(2): 1533-1548.
- Kwan, M. D., M. A. Sellmyer, N. Quarto, A. M. Ho, T. J. Wandless and M. T. Longaker (2011). "Chemical control of FGF-2 release for promoting calvarial healing with adipose stem cells." *Journal of Biological Chemistry* 286(13): 11307-11313.
- Lai, H. L., A. Abu'Khalil and D. Q. M. Craig (2003). "The preparation and characterisation of drug-loaded alginate and chitosan sponges." *International Journal of Pharmaceutics* 251(1-2): 175-181.
- Langer, R. and J. P. Vacanti (1993). "Tissue engineering." *Science* 260(5110): 920-926.
- Laschke, M. W., A. Strohe, M. D. Menger, M. Alini and D. Eglin (2010). "In vitro and in vivo evaluation of a novel nanosize hydroxyapatite particles/poly(ester-urethane) composite scaffold for bone tissue engineering." *Acta Biomaterialia* 6(6): 2020-2027.
- Laursen, T. (2004). "Clinical pharmacological aspects of growth hormone administration." *Growth hormone & IGF research : official journal of the Growth Hormone Research Society and the International IGF Research Society* 14(1): 16-44.
- Lawrie, G., I. Keen, B. Drew, A. Chandler-Temple, L. Rintoul, P. Fredericks and L. Grøndahl (2007). "Interactions between alginate and chitosan biopolymers characterized using FTIR and XPS." *Biomacromolecules* 8(8): 2533-2541.

Leach, J. B. and C. E. Schmidt (2005). "Characterization of protein release from photocrosslinkable hyaluronic acid-polyethylene glycol hydrogel tissue engineering scaffolds." *Biomaterials* 26(2): 125-135.

Lee, D. W., Y. P. Yun, K. Park and S. E. Kim (2012). "Gentamicin and bone morphogenic protein-2 (BMP-2)-delivering heparinized-titanium implant with enhanced antibacterial activity and osteointegration." *Bone* 50(4): 974-982.

Lee, H. J., S. H. Ahn and G. H. Kim (2012). "Three-dimensional collagen/alginate hybrid scaffolds functionalized with a drug delivery system (DDS) for bone tissue regeneration." *Chemistry of Materials* 24(5): 881-891.

Lee Hy Fau - Jin, G.-Z., U. S. Jin Gz Fau - Shin, J.-H. Shin Us Fau - Kim, H.-W. Kim Jh Fau - Kim and H. W. Kim (2012). "Novel porous scaffolds of poly(lactic acid) produced by phase-separation using room temperature ionic liquid and the assessments of biocompatibility." *Journal of Materials Science: Materials in Medicine* 23(5): 1271-1279.

Lee, J. Y., J. E. Choo, Y. S. Choi, J. B. Park, D. S. Min, S. J. Lee, H. K. Rhyu, I. H. Jo, C. P. Chung and Y. J. Park (2007). "Assembly of collagen-binding peptide with collagen as a bioactive scaffold for osteogenesis in vitro and in vivo." *Biomaterials* 28(29): 4257-4267.

Lee, K. Y., J. A. Rowley, P. Eiselt, E. M. Moy, K. H. Bouhadir and D. J. Mooney (2000). "Controlling mechanical and swelling properties of alginate hydrogels independently by cross-linker type and cross-linking density." *Macromolecules* 33(11): 4291-4294.

Lee, Y. T., B. Y. Yu, H. J. Shao, C. H. Chang, Y. M. Sun, H. C. Liu, S. M. Hou and T. H. Young (2011). "Effects of the Surface Characteristics of Nano-Crystalline and Micro-Particle Calcium Phosphate/Chitosan Composite Films on the Behavior of Human Mesenchymal Stem Cells In Vitro." *Journal of Biomaterials Science, Polymer Edition* 22(17): 2369-2388.

Lei, B., K. H. Shin, D. Y. Noh, I. H. Jo, Y. H. Koh, W. Y. Choi and H. E. Kim (2012). "Nanofibrous gelatin-silica hybrid scaffolds mimicking the native extracellular matrix (ECM) using thermally induced phase separation." *Journal of Materials Chemistry* 22(28): 14133-14140.

Leonor, I. B., M. T. Rodrigues, M. E. Gomes and R. L. Reis (2011). "In situ functionalization of wet-spun fibre meshes for bone tissue engineering." *Journal of Tissue Engineering and Regenerative Medicine* 5(2): 104-111.

Leukers, B., H. Gülkan, S. H. Irsen, S. Milz, C. Tille, M. Schieker and H. Seitz (2005). "Hydroxyapatite scaffolds for bone tissue engineering made by 3D printing." *Journal of Materials Science: Materials in Medicine* 16(12): 1121-1124.

- Leung, L. H. and H. E. Naguib (2012). "Characterization of the viscoelastic properties of poly( $\epsilon$ -caprolactone)–hydroxyapatite microcomposite and nanocomposite scaffolds." *Polymer Engineering & Science* 52(8): 1649-1660.
- Levine, B. R., S. Sporer, R. A. Poggie, C. J. Della Valle and J. J. Jacobs (2006). "Experimental and clinical performance of porous tantalum in orthopedic surgery." *Biomaterials* 27(27): 4671-4681.
- Lewis, G. (1997). "Properties of acrylic bone cement: State of the art review." *Journal of Biomedical Materials Research* 38(2): 155-182.
- Li, B., K. V. Brown, J. C. Wenke and S. A. Guelcher (2010). "Sustained release of vancomycin from polyurethane scaffolds inhibits infection of bone wounds in a rat femoral segmental defect model." *Journal of Controlled Release* 145(3): 221-230.
- Li, B., L. Li and C. Zhou (2012). Bio-inspired fabrication of polymer composite scaffolds with chitosan network inside the pore channels. 140: 38-42.
- Li, C., C. Vepari, H. J. Jin, H. J. Kim and D. L. Kaplan (2006). "Electrospun silk-BMP-2 scaffolds for bone tissue engineering." *Biomaterials* 27(16): 3115-3124.
- Lin, L. L., W. J. Wang, J. F. Zhang and M. L. Fang (2011). "Biomechanical numerical simulation of bone tissue engineering scaffolds." *Advanced Materials Research* 213: 306-310.
- Lindhorst, D., F. Tavassol, C. Von See, P. Schumann, M. W. Laschke, Y. Harder, K. H. Bormann, H. Essig, H. Kokemüller, A. Kampmann, A. Voss, R. Mülhaupt, M. D. Menger, N. C. Gellrich and M. Rucker (2010). "Effects of VEGF loading on scaffold-confined vascularization." *Journal of Biomedical Materials Research - Part A* 95(3 A): 783-792.
- Lipowiecki, M., M. Ryvolova, A. Tottosi, S. Naher and D. Brabazon (2012). "Permeability of rapid prototyped artificial bone scaffold structures." *Advanced Materials Research* 445: 607-612.
- Liu, X., G. J. Pettway, L. K. McCauley and P. X. Ma (2007). "Pulsatile release of parathyroid hormone from an implantable delivery system." *Biomaterials* 28(28): 4124-4131.
- Liu, X.-M., L.-D. Quan, J. Tian, Y. Alnouti, K. Fu, G. Thiele and D. Wang (2008). "Synthesis and Evaluation of a Well-defined HPMA Copolymer–Dexamethasone Conjugate for Effective Treatment of Rheumatoid Arthritis." *Pharmaceutical Research* 25(12): 2910-2919.
- Lo H., P. M. S., Leong K.W. (1995). "Fabrication of controlled release biodegradable foams by phase separation." *Tissue Engineering* 1(1): 15-28.

- Lovekamp J. J., D. T. Simionescu, J. J. Mercuri, B. Zubiare, M. S. Sacks and N. R. Vyavahare (2006). "Stability and function of glycosamineglycans in porcine bioprosthetic heart valves." *Biomaterials* 27: 1507-1518.
- Lu, H., N. Kawazoe, T. Kitajima, Y. Myoken, M. Tomita, A. Umezawa, G. Chen and Y. Ito (2012). "Spatial immobilization of bone morphogenetic protein-4 in a collagen-PLGA hybrid scaffold for enhanced osteoinductivity." *Biomaterials* 33(26): 6140-6146.
- Lu, X. and Y. Leng (2005). "Theoretical analysis of calcium phosphate precipitation in simulated body fluid." *Biomaterials* 26(10): 1097-1108.
- Luo, C., L. Li, J. Li, G. Yang, S. Ding, W. Zhi, J. Weng and S. Zhou (2012). "Modulating cellular behaviors through surface nanoroughness." *Journal of Materials Chemistry* 22(31): 15654-15664.
- Madhumathi, K., N. S. Binulal, H. Nagahama, H. Tamura, K. T. Shalumon, N. Selvamurugan, S. V. Nair and R. Jayakumar (2009). "Preparation and characterization of novel  $\beta$ -chitin-hydroxyapatite composite membranes for tissue engineering applications." *International Journal of Biological Macromolecules* 44(1): 1-5.
- Malheiro, V. N., S. G. Caridade, N. M. Alves and J. F. Mano (2010). "New poly( $\epsilon$ -caprolactone)/chitosan blend fibers for tissue engineering applications." *Acta Biomaterialia* 6(2): 418-428.
- Mandal, B. B., A. Grinberg, E. S. Gil, B. Panilaitis and D. L. Kaplan (2012). "High-strength silk protein scaffolds for bone repair." *Proceedings of the National Academy of Sciences of the United States of America* 109(20): 7699-7704.
- Mao, J., L. Zhao, K. de Yao, Q. Shang, G. Yang and Y. Cao (2003). "Study of novel chitosan-gelatin artificial skin in vitro." *Journal of Biomedical Materials Research Part A* 64A(2): 301-308.
- Martins, A., S. Chung, A. J. Pedro, R. A. Sousa, A. P. Marques, R. L. Reis and N. M. Neves (2009). "Hierarchical starch-based fibrous scaffold for bone tissue engineering applications." *Journal of Tissue Engineering and Regenerative Medicine* 3(1): 37-42.
- Mathews, S., P. K. Gupta, R. Bhonde and S. Totey (2011). "Chitosan enhances mineralization during osteoblast differentiation of human bone marrow-derived mesenchymal stem cells, by upregulating the associated genes." *Cell proliferation* 44(6): 537-549.
- Mathieu, L. M., T. L. Mueller, P. E. Bourban, D. P. Pioletti, R. Müller and J. A. E. Månson (2006). "Architecture and properties of anisotropic polymer composite scaffolds for bone tissue engineering." *Biomaterials* 27(6): 905-916.

- Mehrabanian, M. and M. Nasr-Esfahani (2011). "HA/nylon 6,6 porous scaffolds fabricated by salt-leaching/solvent casting technique: effect of nano-sized filler content on scaffold properties." *International Journal of Nanomedicine* 6: 1651-1659.
- Meinel, L., R. Fajardo, S. Hofmann, R. Langer, J. Chen, B. Snyder, G. Vunjak-Novakovic and D. Kaplan (2005). "Silk implants for the healing of critical size bone defects." *Bone* 37(5): 688-698.
- Miyazaki, T., H. M. Kim, T. Kokubo, C. Ohtsuki, H. Kato and T. Nakamura (2002). "Mechanism of bonelike apatite formation on bioactive tantalum metal in a simulated body fluid." *Biomaterials* 23(3): 827-832.
- Mooney, D. J., D. F. Baldwin, N. P. Suh, J. P. Vacanti and R. Langer (1996). "Novel approach to fabricate porous sponges of poly(d,l-lactic-co-glycolic acid) without the use of organic solvents." *Biomaterials* 17(14): 1417-1422.
- Morgan, S. M., S. Tilley, S. Perera, M. J. Ellis, J. Kanczler, J. B. Chaudhuri and R. O. C. Oreffo (2007). "Expansion of human bone marrow stromal cells on poly-(dl-lactide-co-glycolide) (PDLLGA) hollow fibres designed for use in skeletal tissue engineering." *Biomaterials* 28(35): 5332-5343.
- Mouriño, V. and A. R. Boccaccini (2010). "Bone tissue engineering therapeutics: Controlled drug delivery in three-dimensional scaffolds." *Journal of the Royal Society Interface* 7(43): 209-227.
- Mozafari, M., F. Moztarzadeh, M. Rabiee, M. Azami, S. Maleknia, M. Tahriri, Z. Moztarzadeh and N. Nezafati (2010). "Development of macroporous nanocomposite scaffolds of gelatin/bioactive glass prepared through layer solvent casting combined with lamination technique for bone tissue engineering." *Ceramics International* 36(8): 2431-2439.
- Mroz, T. E., E. L. Lin, M. C. Summits, J. R. Bianchi, J. E. Keesling Jr, M. Roberts, C. T. Vangsness Jr and J. C. Wang (2006). "Biomechanical analysis of allograft bone treated with a novel tissue sterilization process." *Spine Journal* 6(1): 34-39.
- Murphy, C. M., M. G. Haugh and F. J. O'Brien (2010). "The effect of mean pore size on cell attachment, proliferation and migration in collagen-glycosaminoglycan scaffolds for bone tissue engineering." *Biomaterials* 31(3): 461-466.
- Nageeb, M., S. R. Nouh, K. Bergman, N. B. Nagy, D. Khamis, M. Kisiel, T. Engstrand, J. Hilborn and M. K. Marei (2012). "Bone engineering by biomimetic injectable hydrogel." *Molecular Crystals and Liquid Crystals* 555: 177-188.
- Oh, S. H., S. G. Kang, E. S. Kim, S. H. Cho and J. H. Lee (2003). "Fabrication and characterization of hydrophilic poly(lactic-co-glycolic acid)/poly(vinyl alcohol) blend cell scaffolds by melt-molding particulate-leaching method." *Biomaterials* 24(22): 4011-4021.

Oliveira, A. L., L. Sun, H. J. Kim, X. Hu, W. Rice, J. Kluge, R. L. Reis and D. L. Kaplan (2012). "Aligned silk-based 3-D architectures for contact guidance in tissue engineering." *Acta Biomaterialia* 8(4): 1530-1542.

Oliveira, J. M., S. A. Costa, I. B. Leonor, P. B. Malafaya, J. F. Mano and R. L. Reis (2009). "Novel hydroxyapatite/carboxymethylchitosan composite scaffolds prepared through an innovative "autocatalytic" electroless coprecipitation route." *Journal of Biomedical Materials Research - Part A* 88(2): 470-480.

Oliveira Jt Fau - Correlo, V. M., P. C. Correlo Vm Fau - Sol, A. R. Sol Pc Fau - Costa-Pinto, P. B. Costa-Pinto Ar Fau - Malafaya, A. J. Malafaya Pb Fau - Salgado, M. Salgado Aj Fau - Bhattacharya, P. Bhattacharya M Fau - Charbord, N. M. Charbord P Fau - Neves, R. L. Neves Nm Fau - Reis and R. L. Reis (2008). "Assessment of the suitability of chitosan/polybutylene succinate scaffolds seeded with mouse mesenchymal progenitor cells for a cartilage tissue engineering approach." *Tissue Engineering Part:A* 14(10): 1651-1661.

Olszta, M. J., X. Cheng, S. S. Jee, R. Kumar, Y. Y. Kim, M. J. Kaufman, E. P. Douglas and L. B. Gower (2007). "Bone structure and formation: A new perspective." *Materials Science and Engineering R: Reports* 58(3-5): 77-116.

Oonishi, H., H. Oonishi Jr, S. Mizokawa, H. Ohashi, M. Ueno and M. Iwamoto (2012). 29 to 24 year-clinical results of total hip arthroplasty cemented with HA by interface bioactive bone cement (IBBC). 493-494: 366-369.

Osathanon, T., C. M. Giachelli and M. J. Somerman (2009). "Immobilization of alkaline phosphatase on microporous nanofibrous fibrin scaffolds for bone tissue engineering." *Biomaterials* 30(27): 4513-4521.

Padmanabhan, S. K., M. Carrozzo, F. Gervaso, F. Scalera, A. Sannino and A. Licciulli (2012). "Mechanical performance and in vitro studies of hydroxyapatite/wollastonite scaffold for bone tissue engineering." *Key Engineering Materials* 493-494: 855-860.

Park, J. W., H. J. Ko, J. H. Jang, H. Kang and J. Y. Suh (2012). "Increased new bone formation with a surface magnesium-incorporated deproteinized porcine bone substitute in rabbit calvarial defects." *Journal of Biomedical Materials Research - Part A* 100 A(4): 834-840.

Park, Y. J., K. H. Kim, J. Y. Lee, Y. Ku, S. J. Lee, B. M. Min and C. P. Chung (2006). "Immobilization of bone morphogenetic protein-2 on a nanofibrous chitosan membrane for enhanced guided bone regeneration." *Biotechnology and Applied Biochemistry* 43(1): 17-24.

Pattnaik, S., S. Nethala, A. Tripathi, S. Saravanan, A. Moorthi and N. Selvamurugan (2011). "Chitosan scaffolds containing silicon dioxide and zirconia nano particles for bone tissue engineering." *International Journal of Biological Macromolecules* 49(5): 1167-1172.

Paul, D. R. (1968). "Diffusion during the coagulation step of wet-spinning." *Journal of Applied Polymer Science* 12(3): 383-402.

Peter, M., N. S. Binulal, S. Soumya, S. V. Nair, T. Furuike, H. Tamura and R. Jayakumar (2010). "Nanocomposite scaffolds of bioactive glass ceramic nanoparticles disseminated chitosan matrix for tissue engineering applications." *Carbohydrate Polymers* 79(2): 284-289.

Petite, H., V. Viateau, W. Bensaïd, A. Meunier, C. De Pollak, M. Bourguignon, K. Oudina, L. Sedel and G. Guillemin (2000). "Tissue-engineered bone regeneration." *Nature Biotechnology* 18(9): 959-963.

Place, E. S., L. Rojo, E. Gentleman, J. P. Sardinha and M. M. Stevens (2011). "Strontium-and zinc-alginate hydrogels for bone tissue engineering." *Tissue Engineering - Part A* 17(21-22): 2713-2722.

Prosdocimi, M. and C. Bevilacqua (2012). "Exogenous hyaluronic acid and wound healing: An updated vision." *Panminerva Medica* 54(2): 129-135.

Puppi, D., A. M. Piras, F. Chiellini, E. Chiellini, A. Martins, I. B. Leonor, N. Neves and R. Reis (2011). "Optimized electro- and wet-spinning techniques for the production of polymeric fibrous scaffolds loaded with bisphosphonate and hydroxyapatite." *Journal of Tissue Engineering and Regenerative Medicine* 5(4): 253-263.

Qi, X., J. Ye and Y. Wang (2009). "Alginate/poly (lactic-co-glycolic acid)/calcium phosphate cement scaffold with oriented pore structure for bone tissue engineering." *Journal of Biomedical Materials Research - Part A* 89(4): 980-987.

Rada, T., T. C. Santos, A. P. Marques, V. M. Correlo, A. M. Frias, A. G. Castro, N. M. Neves, M. E. Gomes and R. L. Reis (2012). "Osteogenic differentiation of two distinct subpopulations of human adipose-derived stem cells: An in vitro and in vivo study." *Journal of Tissue Engineering and Regenerative Medicine* 6(1): 1-11.

Rahaman, M. N., X. Liu and T. S. Huang (2011). "Advances in Bioceramics and Porous Ceramics." New Jersey, USA: John Wiley & Sons Inc.

Ramay, H. R. R. and M. Zhang (2004). "Biphasic calcium phosphate nanocomposite porous scaffolds for load-bearing bone tissue engineering." *Biomaterials* 25(21): 5171-5180.

Ramírez-Fernández, M. P., J. L. Calvo-Guirado, R. Arcesio Delgado-Ruiz, J. E. Maté-Sánchez del Val, G. Gómez-Moreno and J. Guardia (2011). "Experimental model of bone response to xenografts of bovine origin (Endobon®): A radiological and histomorphometric study." *Clinical Oral Implants Research* 22(7): 727-734.

Rath, S. N., G. Pryymachuk, O. A. Bleiziffer, C. X. F. Lam, A. Arkudas, S. T. B. Ho, J. P. Beier, R. E. Horch, D. W. Hutmacher and U. Kneser (2011). "Hyaluronan-based

heparin-incorporated hydrogels for generation of axially vascularized bioartificial bone tissues: In vitro and in vivo evaluation in a PLDLLA-TCP-PCL-composite system." *Journal of Materials Science: Materials in Medicine* 22(5): 1279-1291.

Re'em, T., O. Tsur-Gang and S. Cohen (2010). "The effect of immobilized RGD peptide in macroporous alginate scaffolds on TGF $\beta$ 1-induced chondrogenesis of human mesenchymal stem cells." *Biomaterials* 31(26): 6746-6755.

Reichert, J. C., A. Heymer, A. Berner, J. Eulert and U. Nöth (2009). "Fabrication of polycaprolactone collagen hydrogel constructs seeded with mesenchymal stem cells for bone regeneration." *Biomedical Materials* 4(6).

Remuñán-López, C. and R. Bodmeier (1997). "Mechanical, water uptake and permeability properties of crosslinked chitosan glutamate and alginate films." *Journal of Controlled Release* 44(2-3): 215-225.

Rhim, J.-W. (2004). "Physical and mechanical properties of water resistant sodium alginate films." *LWT - Food Science and Technology* 37(3): 323-330.

Rijcken, C. J. F., O. Soga, W. E. Hennink and C. F. v. Nostrum (2007). "Triggered destabilisation of polymeric micelles and vesicles by changing polymers polarity: An attractive tool for drug delivery." *Journal of Controlled Release* 120(3): 131-148.

Rodrigues, A. I., M. E. Gomes, I. B. Leonor and R. L. Reis (2011). "In vitro evaluation of osteoconductive starch based scaffolds under dynamic conditions." *Bioengineering*: 1-7.

Rodrigues, C. V. M., P. Serricella, A. B. R. Linhares, R. M. Guerdes, R. Borojevic, M. A. Rossi, M. E. L. Duarte and M. Farina (2003). "Characterization of a bovine collagen-hydroxyapatite composite scaffold for bone tissue engineering." *Biomaterials* 24(27): 4987-4997.

Rubert, M., M. Monjo, S. P. Lyngstadaas and J. M. Ramis (2012). "Effect of alginate hydrogel containing polyproline-rich peptides on osteoblast differentiation." *Biomedical Materials (Bristol)* 7(5).

Rungsiyanont, S., N. Dhanesuan, S. Swadison and S. Kasugai (2012). "Evaluation of biomimetic scaffold of gelatin-hydroxyapatite crosslink as a novel scaffold for tissue engineering: Biocompatibility evaluation with human PDL fibroblasts, human mesenchymal stromal cells, and primary bone cells." *Journal of Biomaterials Applications* 27(1): 47-54.

Ryszkowska, J. L., M. Auguścik, A. Sheikh and A. R. Boccaccini (2010). "Biodegradable polyurethane composite scaffolds containing Bioglass® for bone tissue engineering." *Composites Science and Technology* 70(13): 1894-1908.

- Sachlos, E. and J. T. Czernuszka (2003). "Making tissue engineering scaffolds work. Review: the application of solid freeform fabrication technology to the production of tissue engineering scaffolds." *European Cells and Materials* 5: 29-39; discussion 39.
- Saha, S. and S. Pal (1984). "Mechanical properties of bone cement: A review." *Journal of Biomedical Materials Research* 18(4): 435-462.
- Salgado, A. J., O. P. Coutinho and R. L. Reis (2004). "Novel Starch-Based Scaffolds for Bone Tissue Engineering: Cytotoxicity, Cell Culture, and Protein Expression." *Tissue Engineering* 10(3-4): 465-474.
- Samavedi, S., C. Olsen Horton, S. A. Guelcher, A. S. Goldstein and A. R. Whittington (2011). "Fabrication of a model continuously graded co-electrospun mesh for regeneration of the ligament-bone interface." *Acta Biomaterialia* 7(12): 4131-4138.
- Santos, M. I., S. Fuchs, M. E. Gomes, R. E. Unger, R. L. Reis and C. J. Kirkpatrick (2007). "Response of micro- and macrovascular endothelial cells to starch-based fiber meshes for bone tissue engineering." *Biomaterials* 28(2): 240-248.
- Sargeant, T. D., M. O. Guler, S. M. Oppenheimer, A. Mata, R. L. Satcher, D. C. Dunand and S. I. Stupp (2008). "Hybrid bone implants: Self-assembly of peptide amphiphile nanofibers within porous titanium." *Biomaterials* 29(2): 161-171.
- Schliephake, H. (2002). "Bone growth factors in maxillofacial skeletal reconstruction." *International Journal of Oral Maxillofacial Surgery* 31(5): 469-484.
- Schindeler, A., M. M. McDonald, P. Bokko and D. G. Little (2008). "Bone remodeling during fracture repair: The cellular picture." *Seminars in Cell and Developmental Biology* 19(5): 459-466.
- Schliephake, H., C. Bötel, A. Förster, B. Schwenzer, J. Reichert and D. Scharnweber (2012). "Effect of oligonucleotide mediated immobilization of bone morphogenic proteins on titanium surfaces." *Biomaterials* 33(5): 1315-1322.
- Schneiders, W., C. Rentsch, S. Rehberg, S. Rein, H. Zwipp and S. Rammelt (2012). "Effect of chondroitin sulfate on osteogenetic differentiation of human mesenchymal stem cells." *Materials Science and Engineering C* 32(7): 1926-1930.
- Sellgren, K. L. and T. Ma (2012). "Perfusion conditioning of hydroxyapatite–chitosan–gelatin scaffolds for bone tissue regeneration from human mesenchymal stem cells." *Journal of Tissue Engineering and Regenerative Medicine* 6(1): 49-59.
- Sharaf, B., C. B. Faris, H. Abukawa, S. M. Susarla, J. P. Vacanti, L. B. Kaban and M. J. Troulis (2012). "Three-dimensionally printed polycaprolactone and  $\beta$ -tricalcium phosphate scaffolds for bone tissue engineering: an in vitro study." *Journal of oral and maxillofacial surgery : official journal of the American Association of Oral and Maxillofacial Surgeons* 70(3): 647-656.

- Shi, J., X. Zhang, Y. Pi, J. Zhu, C. Zhou and Y. Ao (2012). "Nanopolymers delivery of the bone morphogenetic protein-4 plasmid to mesenchymal stem cells promotes articular cartilage repair in vitro and in vivo." *Journal of Nanomaterials* 2012.
- Shiraishi, N., T. Anada, Y. Honda, T. Masuda, K. Sasaki and O. Suzuki (2010). "Preparation and characterization of porous alginate scaffolds containing various amounts of octacalcium phosphate (OCP) crystals." *Journal of Materials Science: Materials in Medicine* 21(3): 907-914.
- Silverman, L. D., L. Lukashova, O. T. Herman, J. M. Lane and A. L. Boskey (2007). "Release of gentamicin from a tricalcium phosphate bone implant." *Journal of Orthopaedic Research* 25(1): 23-29.
- Skedros, J. G., R. D. Bloebaum, K. N. Bachus, T. M. Boyce and B. Constantz (1993). "Influence of mineral content and composition on graylevels in backscattered electron images of bone." *Journal of Biomedical Materials Research* 27(1): 57-64.
- Skinner, H. C. W. (2005). "Biomaterials." *Mineralogical Magazine* 69(5): 621-641.
- Son, J. S., M. Appleford, J. L. Ong, J. C. Wenke, J. M. Kim, S. H. Choi and D. S. Oh (2011). "Porous hydroxyapatite scaffold with three-dimensional localized drug delivery system using biodegradable microspheres." *Journal of Controlled Release* 153(2): 133-140.
- Spoerke, E. D., N. G. Murray, H. Li, L. C. Brinson, D. C. Dunand and S. I. Stupp (2005). "A bioactive titanium foam scaffold for bone repair." *Acta Biomaterialia* 1(5): 523-533.
- Strobel, C., N. Bormann, A. Kadow-Romacker, G. Schmidmaier and B. Wildemann (2011). "Sequential release kinetics of two (gentamicin and BMP-2) or three (gentamicin, IGF-I and BMP-2) substances from a one-component polymeric coating on implants." *Journal of Controlled Release* 156(1): 41-49.
- Strobel, L., S. Rath, A. Maier, J. Beier, A. Arkudas, P. Greil, R. Horch and U. Kneser (2012). "Induction of bone formation in biphasic calcium phosphate scaffolds by bone morphogenetic protein-2 and primary osteoblasts." *Journal of Tissue Engineering and Regenerative Medicine*.
- Su, Y., Q. Su, W. Liu, M. Lim, J. R. Venugopal, X. Mo, S. Ramakrishna, S. S. Al-Deyab and M. El-Newehy (2012). "Controlled release of bone morphogenetic protein 2 and dexamethasone loaded in core-shell PLLACL-collagen fibers for use in bone tissue engineering." *Acta Biomaterialia* 8(2): 763-771.
- Suárez-González, D., K. Barnhart, E. Saito, R. Vanderby, S. J. Hollister and W. L. Murphy (2010). "Controlled nucleation of hydroxyapatite on alginate scaffolds for stem cell-based bone tissue engineering." *Journal of Biomedical Materials Research Part A* 95A(1): 222-234.

Sultana, N. and M. Wang (2012). "PHBV/PLLA-based composite scaffolds fabricated using an emulsion freezing/freeze-drying technique for bone tissue engineering: Surface modification and in vitro biological evaluation." *Biofabrication* 4(1).

Tai, B. C. U., C. Du, S. Gao, A. C. A. Wan and J. Y. Ying (2010). "The use of a polyelectrolyte fibrous scaffold to deliver differentiated hMSCs to the liver." *Biomaterials* 31(1): 48-57.

Takagi, G., M. Miyamoto, S. Tara, I. Takagi, H. Takano, M. Yasutake, Y. Tabata and K. Mizuno (2011). "Controlled-release basic fibroblast growth factor for peripheral artery disease: Comparison with autologous bone marrow-derived stem cell transfer." *Tissue Engineering - Part A* 17(21-22): 2787-2794.

Tam, S. K., J. Dusseault, S. Polizu, M. Ménard, J.-P. Hallé and L. H. Yahia (2005). "Physicochemical model of alginate-poly-L-lysine microcapsules defined at the micrometric/nanometric scale using ATR-FTIR, XPS, and ToF-SIMS." *Biomaterials* 26(34): 6950-6961.

Tamimi, F., Z. Sheikh and J. Barralet (2012). "Dicalcium phosphate cements: Brushite and monetite." *Acta Biomaterialia* 8(2): 474-487.

Tanase, C. E., M. I. Popa and L. Verestiuc (2011). "Biomimetic bone scaffolds based on chitosan and calcium phosphates." *Materials Letters* 65(11): 1681-1683.

Tao, C., Y. Chen and Y. Q. Zhong (2012). "RGD-modified polylactide-co-glycolic acid tissue engineering scaffolds for bone regeneration: An advance." *Academic Journal of Second Military Medical University* 33(1): 95-98.

Thanyaphoo, S. and J. Kaewsrichan (2012). "Synthesis and evaluation of novel glass ceramics as drug delivery systems in osteomyelitis." *Journal of Pharmaceutical Sciences* 101(8): 2870-2882.

Tong, H. W., M. Wang and W. W. Lu (2012). "Electrospinning and evaluation of PHBV-based tissue engineering scaffolds with different fibre diameters, surface topography and compositions." *Journal of Biomaterials Science, Polymer Edition* 23(6): 779-806.

Tsai, W. B., Y. R. Chen, W. T. Li, J. Y. Lai and H. L. Liu (2012). "RGD-conjugated UV-crosslinked chitosan scaffolds inoculated with mesenchymal stem cells for bone tissue engineering." *Carbohydrate Polymers* 89(2): 379-387.

Tsaih, M. L. and R. H. Chen (1999). "Effects of Ionic Strength and pH on the Diffusion Coefficients and Conformation of Chitosans Molecule in Solution." *Journal of Applied Polymer Science* 73(10): 2041-2050.

Tsurushima, H., A. Marushima, K. Suzuki, A. Oyane, Y. Sogo, K. Nakamura, A. Matsumura and A. Ito (2010). "Enhanced bone formation using hydroxyapatite ceramic coated with fibroblast growth factor-2." *Acta Biomaterialia* 6(7): 2751-2759.

Tunc, Y., N. Hasirci and K. Ulubayram (2012). "Synthesis of emulsion-templated acrylic-based porous polymers: From brittle to elastomeric." *Soft Materials* 10(4): 449-461.

Turco, G., E. Marsich, F. Bellomo, S. Semeraro, I. Donati, F. Brun, M. Grandolfo, A. Accardo and S. Paoletti (2009). "Alginate/hydroxyapatite biocomposite for bone ingrowth: A trabecular structure with high and isotropic connectivity." *Biomacromolecules* 10(6): 1575-1583.

Tuzlakoglu, K., C. M. Alves, J. F. Mano and R. L. Reis (2004). "Production and Characterization of Chitosan Fibers and 3-D Fiber Mesh Scaffolds for Tissue Engineering Applications." *Macromolecular Bioscience* 4(8): 811-819.

Tuzlakoglu, K., I. Pashkuleva, M. T. Rodrigues, M. E. Gomes, G. H. Van Lenthe, R. Müller and R. L. Reis (2010). "A new route to produce starch-based fiber mesh scaffolds by wet spinning and subsequent surface modification as a way to improve cell attachment and proliferation." *Journal of Biomedical Materials Research - Part A* 92(1): 369-377.

Tuzlakoglu, K. and R. L. Reis (2007). "Formation of bone-like apatite layer on chitosan fiber mesh scaffolds by a biomimetic spraying process." *Journal of Materials Science: Materials in Medicine* 18(7): 1279-1286.

Tuzlakoglu K Fau - Santos, M. I., N. Santos Mi Fau - Neves, R. L. Neves N Fau - Reis and R. L. Reis "Design of nano- and microfiber combined scaffolds by electrospinning of collagen onto starch-based fiber meshes: a man-made equivalent of natural extracellular matrix." *Tissue Engineering Part:A* 17(3): 463-473.

Urabe, K., M. Itoman, Y. Toyama, Y. Yanase, Y. Iwamoto, H. Ohgushi, M. Ochi, Y. Takakura, Y. Hachiya, H. Matsuzaki, Y. Matsusue and S. Mori (2007). "Current trends in bone grafting and the issue of banked bone allografts based on the fourth nationwide survey of bone grafting status from 2000 to 2004." *Journal of Orthopaedic Science* 12(6): 520-525.

Valenzuela, F., C. Covarrubias, C. Martínez, P. Smith, M. Díaz-Dosque and M. Yazdani-Pedram (2012). "Preparation and bioactive properties of novel bone-repair bionanocomposites based on hydroxyapatite and bioactive glass nanoparticles." *Journal of Biomedical Materials Research - Part B Applied Biomaterials* 100 B(6): 1672-1682.

Vallet-Regí, M., M. Colilla and B. González (2011). "Medical applications of organic-inorganic hybrid materials within the field of silica-based bioceramics." *Chemical Society Reviews* 40(2): 596-607.

- Van der Pol, U., L. Mathieu, S. Zeiter, P. E. Bourban, P. Y. Zambelli, S. G. Pearce, L. P. Bouré and D. P. Pioletti (2010). "Augmentation of bone defect healing using a new biocomposite scaffold: An in vivo study in sheep." *Acta Biomaterialia* 6(9): 3755-3762.
- Vasile, E., L. M. Popescu, R. M. Piticescu, A. Burlacu and T. Buruiana (2012). "Physico-chemical and biocompatible properties of hydroxyapatite based composites prepared by an innovative synthesis route." *Materials Letters* 79: 85-88.
- Venkatesan, J., B. Ryu, P. N. Sudha and S. K. Kim (2012). "Preparation and characterization of chitosan-carbon nanotube scaffolds for bone tissue engineering." *International Journal of Biological Macromolecules* 50(2): 393-402.
- Vitale-Brovarone, C., G. Ciapetti, E. Leonardi, N. Baldini, O. Bretcanu, E. Verné and F. Baino (2011). "Resorbable glass-ceramic phosphate-based scaffolds for bone tissue engineering: Synthesis, properties, and in vitro effects on human marrow stromal cells." *Journal of Biomaterials Applications* 26(4): 465-489.
- Wahl, D. A., E. Sachlos, C. Liu and J. T. Czernuszka (2007). "Controlling the processing of collagen-hydroxyapatite scaffolds for bone tissue engineering." *Journal of Materials Science: Materials in Medicine* 18(2): 201-209.
- Wang, C., Y. Xue, K. Lin, J. Lu, J. Chang and J. Sun (2012). "The enhancement of bone regeneration by a combination of osteoconductivity and osteostimulation using  $\beta$ -CaSiO<sub>3</sub>/ $\beta$ -Ca<sub>3</sub>(PO<sub>4</sub>)<sub>2</sub> composite bioceramics." *Acta Biomaterialia* 8(1): 350-360.
- Wang, G., Z. Lu, D. Dwarte and H. Zreiqat (2012). "Porous scaffolds with tailored reactivity modulate in-vitro osteoblast responses." *Materials Science and Engineering C* 32(7): 1818-1826.
- Wang, J., Y. B. Li, Y. Zuo, W. H. Yang and L. Zhang (2008). "Preparation and characterization of nano-hydroxyapatite/silk fibroin porous scaffold composite." *Gongneng Cailiao/Journal of Functional Materials* 39(10): 1714-1716+1719.
- Wang, L., Y. Zuo, Q. Zou and Y. B. Li (2011). "Effect of composition on physical-chemical properties and biological properties of hydroxyapatite/aliphatic polyurethane scaffolds for bone tissue engineering." *Gaodeng Xuexiao Huaxue Xuebao/Chemical Journal of Chinese Universities* 32(10): 2453-2459.
- Wang, Q., Z. Dong, Y. Du and J. F. Kennedy (2007). "Controlled release of ciprofloxacin hydrochloride from chitosan/polyethylene glycol blend films." *Carbohydrate Polymers* 69(2): 336-343.
- Wehrhan, F., K. Amann, A. Molenberg, R. Lutz, F. W. Neukam and K. A. Schlegel (2012). "PEG matrix enables cell-mediated local BMP-2 gene delivery and increased bone formation in a porcine critical size defect model of craniofacial bone regeneration." *Clinical Oral Implants Research* 23(7): 805-813.

- Wei, G., Q. Jin, W. V. Giannobile and P. X. Ma (2007). "The enhancement of osteogenesis by nano-fibrous scaffolds incorporating rhBMP-7 nanospheres." *Biomaterials* 28(12): 2087-2096.
- Wei, G. and P. X. Ma (2004). "Structure and properties of nano-hydroxyapatite/polymer composite scaffolds for bone tissue engineering." *Biomaterials* 25(19): 4749-4757.
- Weiner, S. and H. D. Wagner (1998). "The material bone: Structure-mechanical function relations." *Annual Review of Materials Science* 28(1): 271-298.
- Wen, C. E., M. Mabuchi, Y. Yamada, K. Shimojima, Y. Chino and T. Asahina (2001). "Processing of biocompatible porous Ti and Mg." *Scripta Materialia* 45(10): 1147-1153.
- Wen, C. E., Y. Yamada, K. Shimojima, Y. Chino, T. Asahina and M. Mabuchi (2002). "Processing and mechanical properties of autogenous titanium implant materials." *Journal of Materials Science: Materials in Medicine* 13(4): 397-401.
- Wernike, E., M. O. Montjovent, Y. Liu, D. Wismeijer, E. B. Hunziker, K. A. Siebenrock, W. Hofstetter and F. M. Klenke (2010). "Vegf incorporated into calcium phosphate ceramics promotes vascularisation and bone formation in vivo." *European Cells and Materials* 19: 30-40.
- Williams, J. M., A. Adewunmi, R. M. Schek, C. L. Flanagan, P. H. Krebsbach, S. E. Feinberg, S. J. Hollister and S. Das (2005). "Bone tissue engineering using polycaprolactone scaffolds fabricated via selective laser sintering." *Biomaterials* 26(23): 4817-4827.
- Wilson, C. E., J. D. De Bruijn, C. A. Van Blitterswijk, A. J. Verbout and W. J. A. Dhert (2004). "Design and fabrication of standardized hydroxyapatite scaffolds with a defined macro-architecture by rapid prototyping for bone-tissue-engineering research." *Journal of Biomedical Materials Research - Part A* 68(1): 123-132.
- Wise, E. R., S. Maltsev, M. E. Davies, M. J. Duer, C. Jaeger, N. Loveridge, R. C. Murray and D. G. Reid (2007). "The organic-mineral interface in bone is predominantly polysaccharide." *Chemistry of Materials* 19(21): 5055-5057.
- Wu, F., J. Wei, C. Liu, B. O'Neill and Y. Ngothai (2012). "Fabrication and properties of porous scaffold of zein/PCL biocomposite for bone tissue engineering." *Composites Part B: Engineering* 43(5): 2192-2197.
- Wu, J., G. H. Wang, H. Zhang, Y. P. Wu, Y. C. Lv, J. S. Liu, J. K. Ma and J. Zhu (2011). "Chondrogenic ability of bone marrow mesenchymal stem cells in alginate and collagen sponge." *Biomaterials* 32(2): 474-476: 1935-1938.

Wu, T., X. Hua, Z. He, X. Wang, X. Yu and W. Ren (2012). "The bactericidal and biocompatible characteristics of reinforced calcium phosphate cements." *Biomedical Materials* 7(4).

Xia, Y., F. Mei, Y. Duan, Y. Gao, Z. Xiong, T. Zhang and H. Zhang (2012). "Bone tissue engineering using bone marrow stromal cells and an injectable sodium alginate/gelatin scaffold." *Journal of Biomedical Materials Research - Part A* 100 A(4): 1044-1050.

Xiao, S. J., M. Textor, N. D. Spencer and H. Sigrist (1998). "Covalent attachment of cell-adhesive, (Arg-Gly-Asp)-containing peptides to titanium surfaces." *Langmuir* 14(19): 5507-5516.

Xu, Y. and Y. Du (2003). "Effect of molecular structure of chitosan on protein delivery properties of chitosan nanoparticles." *International Journal of Pharmaceutics* 250(1): 215-226.

Xu, Y., C. Zhan, L. Fan, L. Wang and H. Zheng (2007). "Preparation of dual crosslinked alginate-chitosan blend gel beads and in vitro controlled release in oral site-specific drug delivery system." *International Journal of Pharmaceutics* 336(2): 329-337.

Xue, M., D. Zhou, J. Cao, H. Wang and B. Cao (2009). "Preparation and properties of the CS/AW composite as porous scaffold material." *Fuhe Cailiao Xuebao/Acta Materiae Compositae Sinica* 26(3): 127-132.

Yeo, M., H. Lee and G. Kim (2011). "Three-dimensional hierarchical composite scaffolds consisting of polycaprolactone,  $\beta$ -tricalcium phosphate, and collagen nanofibers: Fabrication, physical properties, and in vitro cell activity for bone tissue regeneration." *Biomacromolecules* 12(2): 502-510.

Yeo, M. G. and G. H. Kim (2012). "Preparation and characterization of 3D composite scaffolds based on rapid-prototyped PCL/ $\beta$ -TCP struts and electrospun PCL coated with collagen and HA for bone regeneration." *Chemistry of Materials* 24(5): 903-913.

Yilgor, P., R. A. Sousa, R. L. Reis, N. Hasirci and V. Hasirci (2010). "Effect of scaffold architecture and BMP-2/BMP-7 delivery on in vitro bone regeneration." *Journal of Materials Science: Materials in Medicine* 21(11): 2999-3008.

Yilgor, P., K. Tuzlakoglu, R. L. Reis, N. Hasirci and V. Hasirci (2009). "Incorporation of a sequential BMP-2/BMP-7 delivery system into chitosan-based scaffolds for bone tissue engineering." *Biomaterials* 30(21): 3551-3559.

Yoshikawa, H., N. Tamai, T. Murase and A. Myoui (2009). "Interconnected porous hydroxyapatite ceramics for bone tissue engineering." *Journal of the Royal Society Interface* 6(SUPPL. 3): S341-S348.

- Yoshimoto, H., Y. M. Shin, H. Terai and J. P. Vacanti (2003). "A biodegradable nanofiber scaffold by electrospinning and its potential for bone tissue engineering." *Biomaterials* 24(12): 2077-2082.
- Yuan, Y. C. B. M. H. W. O. (2011). "Deacetylation of chitosan: material characterization and in vitro evaluation via albumin adsorption and pre-osteoblastic cell cultures." *Materials* 4(8): 1399-1416.
- Yubao, L., K. Groot, J. Wijn, C. P. A. T. Klein and S. V. D. Meer (1994). "Morphology and composition of nanograde calcium phosphate needle-like crystals formed by simple hydrothermal treatment." *Journal of Materials Science: Materials in Medicine* 5(6): 326-331.
- Zanetta, M., N. Quirici, F. Demarosi, M. C. Tanzi, L. Rimondini and S. Farè (2009). "Ability of polyurethane foams to support cell proliferation and the differentiation of MSCs into osteoblasts." *Acta Biomaterialia* 5(4): 1126-1136.
- Zhang, J., C. Wang, J. Wang, Y. Qu and G. Liu (2012). "In vivo drug release and antibacterial properties of vancomycin loaded hydroxyapatite/chitosan composite." *Drug Delivery* 19(5): 264-269.
- Zhang, Q., Q. F. He, T. H. Zhang, X. L. Yu, Q. Liu and F. L. Deng (2012). "Improvement in the delivery system of bone morphogenetic protein-2: A new approach to promote bone formation." *Biomedical Materials* 7(4).
- Zhang, S., X. Zhang, Q. Cai, B. Wang, X. Deng and X. Yang (2010). "Microfibrous  $\beta$ -TCP/collagen scaffolds mimic woven bone in structure and composition." *Biomedical Materials* 5(6).
- Zhang, Y., N. Cheng, R. Miron, B. Shi and X. Cheng (2012). "Delivery of PDGF-B and BMP-7 by mesoporous bioglass/silk fibrin scaffolds for the repair of osteoporotic defects." *Biomaterials* 33(28): 6698-6708.
- Zhang, Y., W. Fan, L. Nothdurft, C. Wu, Y. Zhou, R. Crawford and Y. Xiao (2011). "In vitro and in vivo evaluation of adenovirus combined silk fibroin scaffolds for bone morphogenetic protein-7 gene delivery." *Tissue Engineering - Part C: Methods* 17(8): 789-797.
- Zhao, J., W. Han, M. Tu, S. Huan, R. Zeng, H. Wu, Z. Cha and C. Zhou (2012). "Preparation and properties of biomimetic porous nanofibrous poly(l-lactide) scaffold with chitosan nanofiber network by a dual thermally induced phase separation technique." *Materials Science and Engineering: C* 32(6): 1496-1502.
- Zhao, L., M. D. Weir and H. H. K. Xu (2010). "An injectable calcium phosphate-alginate hydrogel-umbilical cord mesenchymal stem cell paste for bone tissue engineering." *Biomaterials* 31(25): 6502-6510.

Zhong, C. and C. C. Chu (2012). "Biomimetic mineralization of acid polysaccharide-based hydrogels: Towards porous 3-dimensional bone-like biocomposites." *Journal of Materials Chemistry* 22(13): 6080-6087.

Zhou, Y., L. Xu, X. Zhang, Y. Zhao, S. Wei and M. Zhai (2012). "Radiation synthesis of gelatin/CM-chitosan/ $\beta$ -tricalcium phosphate composite scaffold for bone tissue engineering." *Materials Science and Engineering C* 32(4): 994-1000.

Zhu, C. T., Y. Q. Xu, J. Shi, J. Li and J. Ding (2010). "Liposome combined porous  $\beta$ -TCP scaffold: Preparation, characterization, and anti-biofilm activity." *Drug Delivery* 17(6): 391-398.

Zhu, Y. and S. Kaskel (2009). "Comparison of the in vitro bioactivity and drug release property of mesoporous bioactive glasses (MBGs) and bioactive glasses (BGs) scaffolds." *Microporous and Mesoporous Materials* 118(1-3): 176-182.

Zilberman, M. and J. J. Elsner (2008). "Antibiotic-eluting medical devices for various applications." *Journal of Controlled Release* 130(3): 202-215.

Zima, A., Z. Paszkiewicz, D. Siek, J. Czechowska and A. Ślósarczyk (2012). "Study on the new bone cement based on calcium sulfate and Mg, CO<sub>3</sub> doped hydroxyapatite." *Ceramics International* 38(6): 4935-4942.

Zomer Volpato, F., J. Almodóvar, K. Erickson, K. C. Popat, C. Migliaresi and M. J. Kipper (2012). "Preservation of FGF-2 bioactivity using heparin-based nanoparticles, and their delivery from electrospun chitosan fibers." *Acta Biomaterialia* 8(4): 1551-1559.

Zumstein Ma Fau - Berger, S., M. Berger S Fau - Schober, P. Schober M Fau - Boileau, R. W. Boileau P Fau - Nyffeler, M. Nyffeler R W Fau - Horn, C. A. Horn M Fau - Dahinden and C. A. Dahinden (2012). "Leukocyte- and platelet-rich fibrin (l-prf) for long-term delivery of growth factor in rotator cuff repair: review, preliminary results and future directions." *Current Pharmaceutical Biotechnology* 13(7): 1196-1206.

## APPENDIX A

### CALIBRATION CURVES

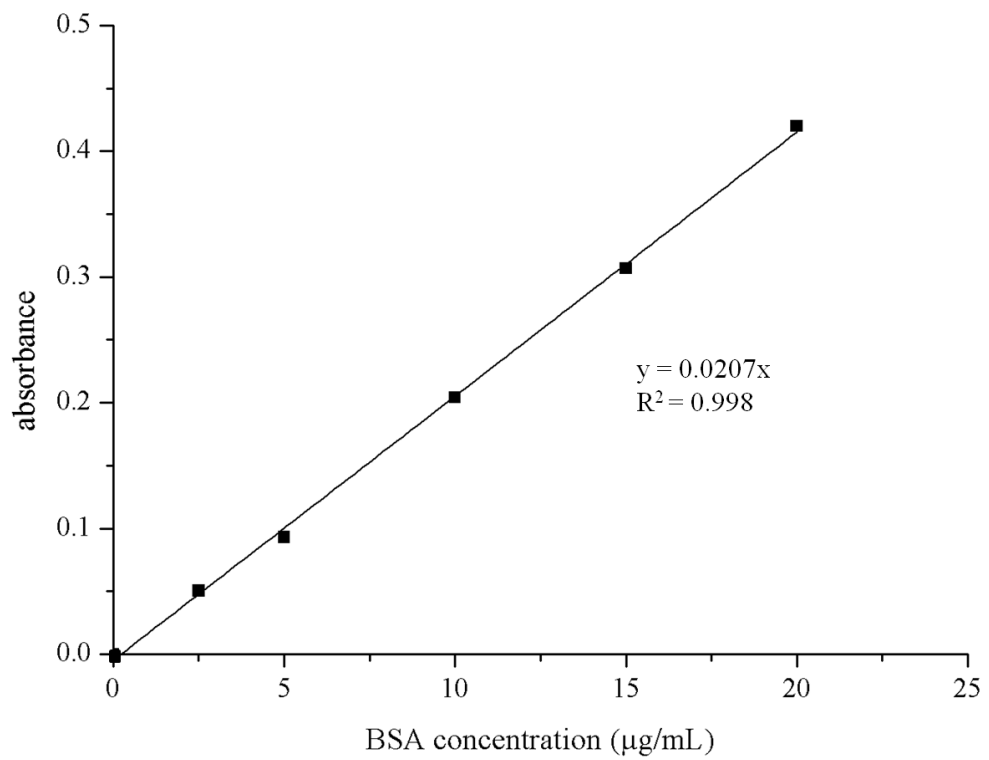


**Figure A.1.** Calibration curve of BSA concentration for Bradford Assay, microplate protocol at 595 nm.

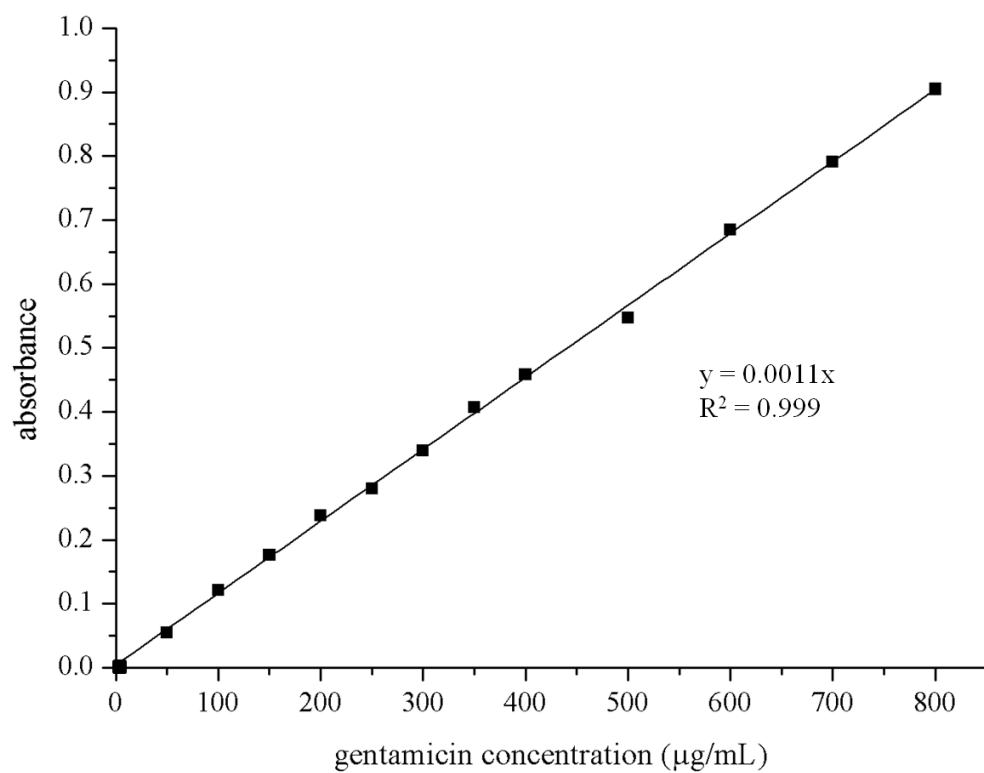


**Figure A.2.** Calibration curve of gentamicin concentration for UV-vis spectrometry at 256 nm.

## APPENDIX B

### EDX ANALYSES OF SCAFFOLDS

### INCUBATED IN SBF SOLUTION

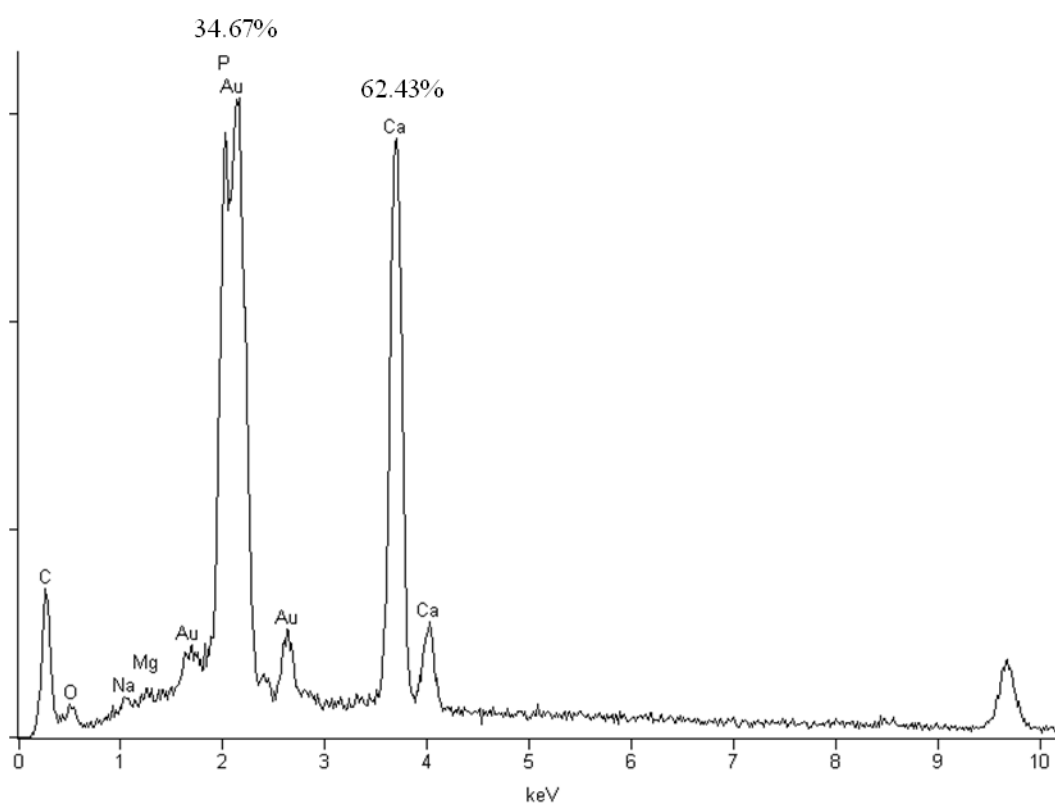


**Figure B.1.** EDX spectrum of chitosan scaffold incubated in SBF solution for 48 h.

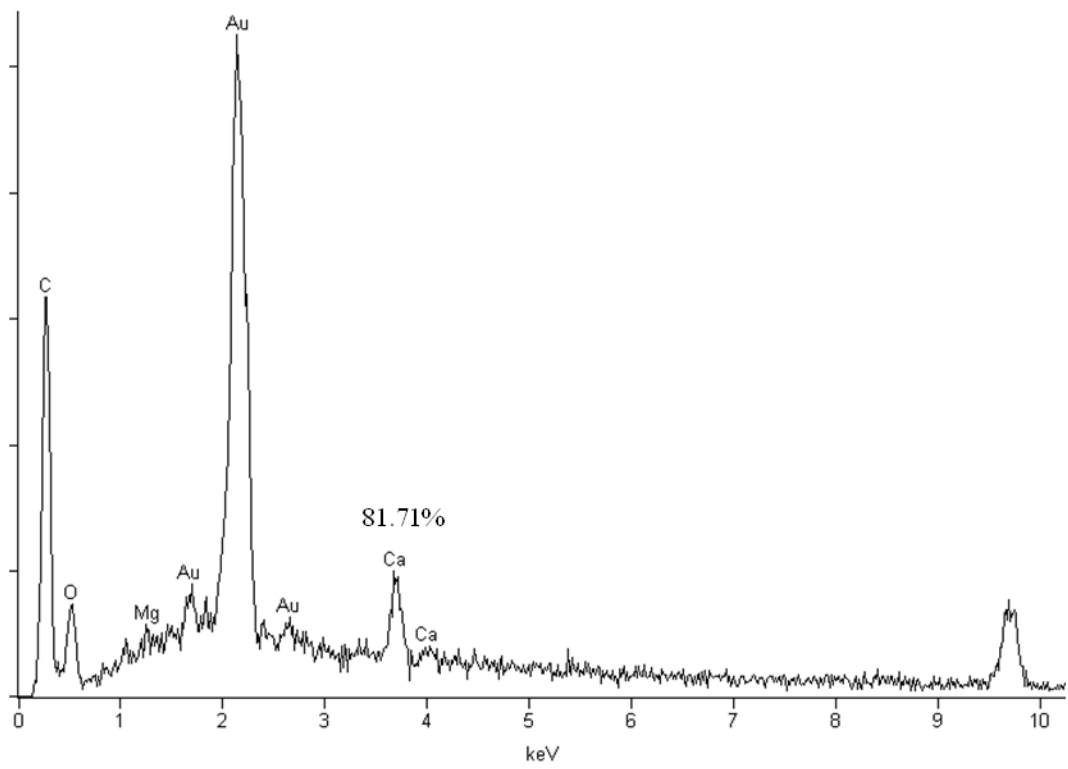


**Figure B.2.** EDX spectrum of chitosan scaffold incubated in SBF solution for 7 d.

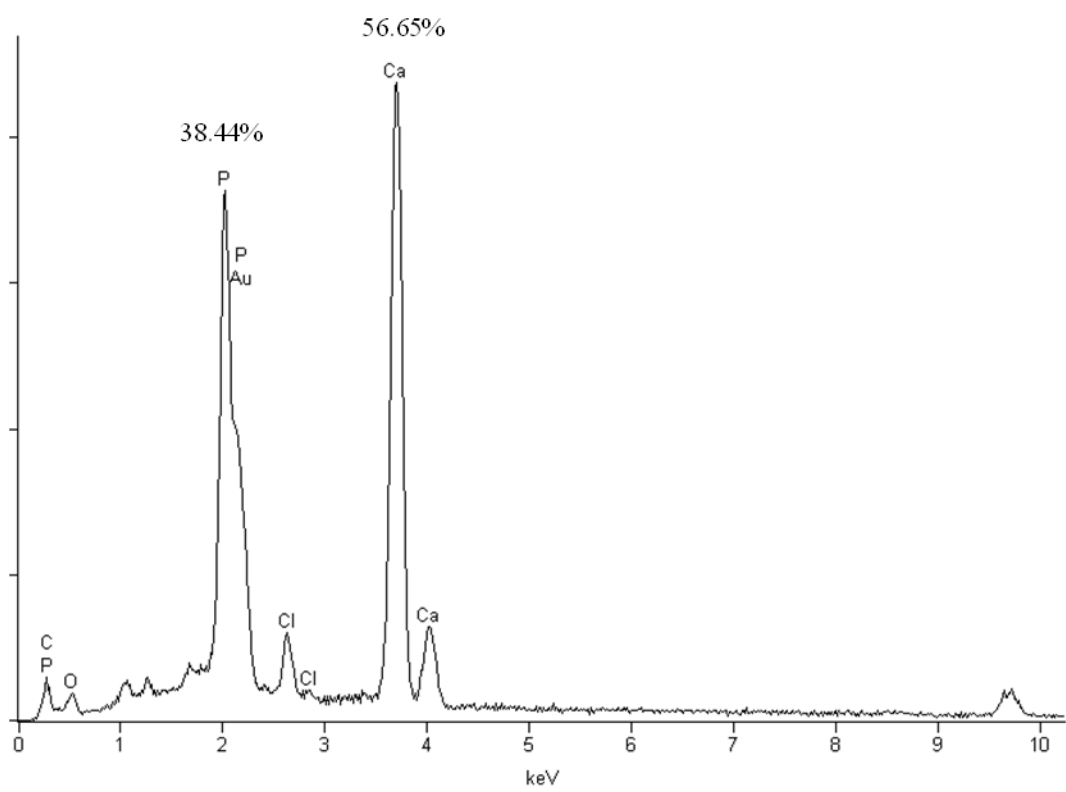


**Figure B.3.** EDX spectrum of chitosan scaffold incubated in SBF solution for 14 d.

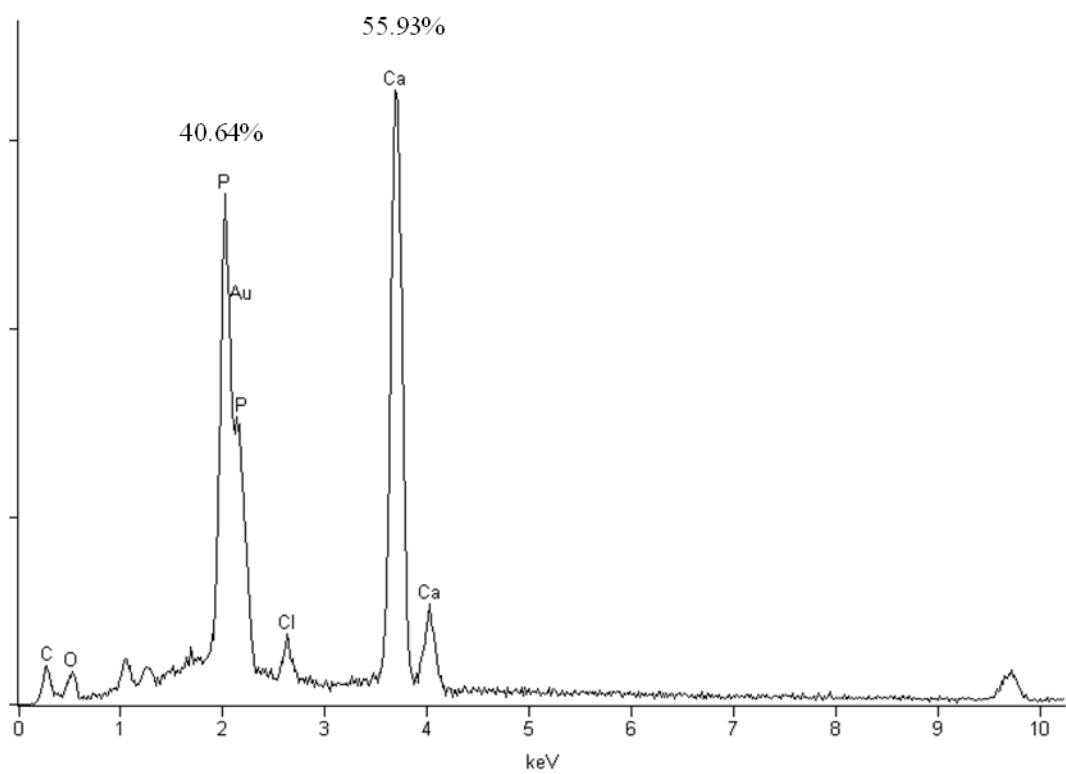


**Figure B.4.** EDX spectrum of alginate coated chitosan scaffold incubated in same SBF solution for 7 d.

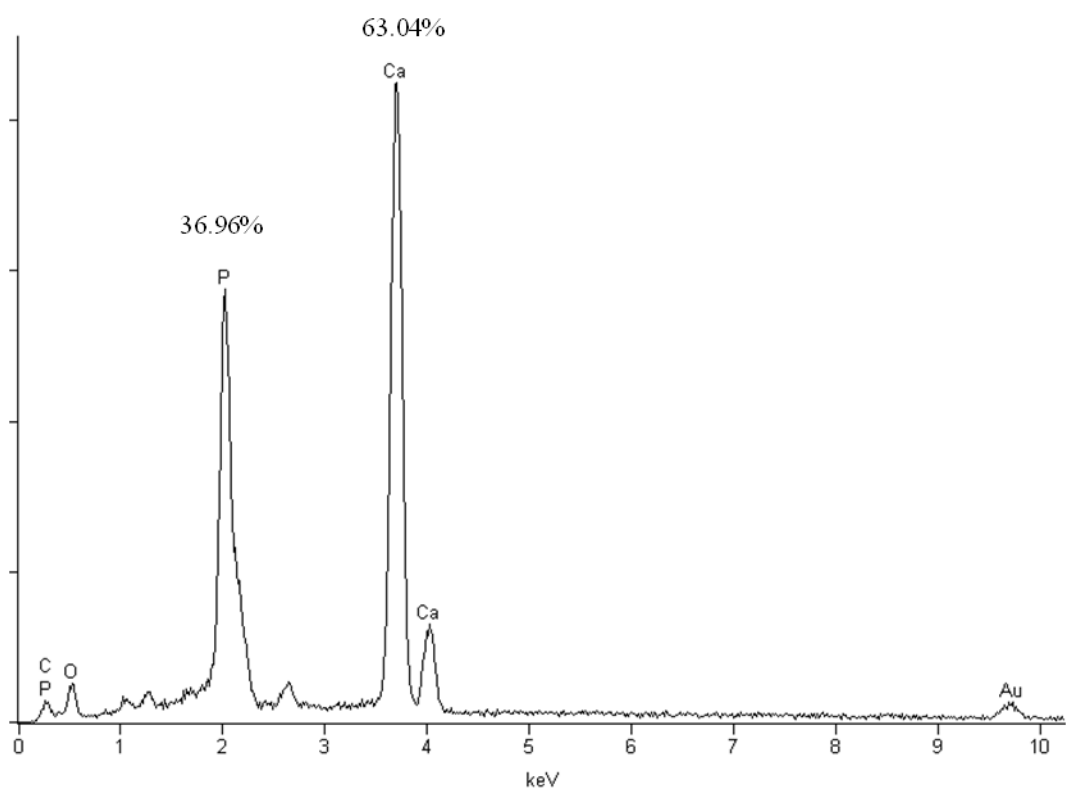


**Figure B.5.** EDX spectrum of alginate coated chitosan scaffold incubated in refreshed SBF solution for 7 d.

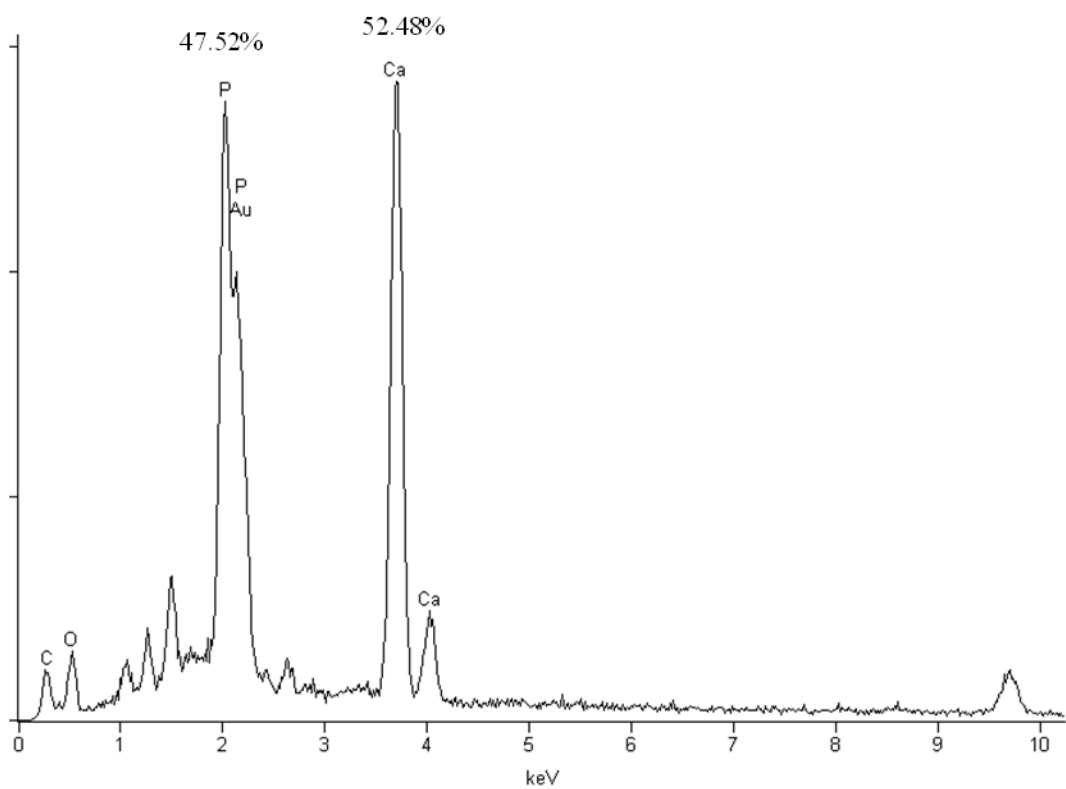


**Figure B.6.** EDX spectrum of alginate coated chitosan scaffold incubated in same SBF solution for 14 d.

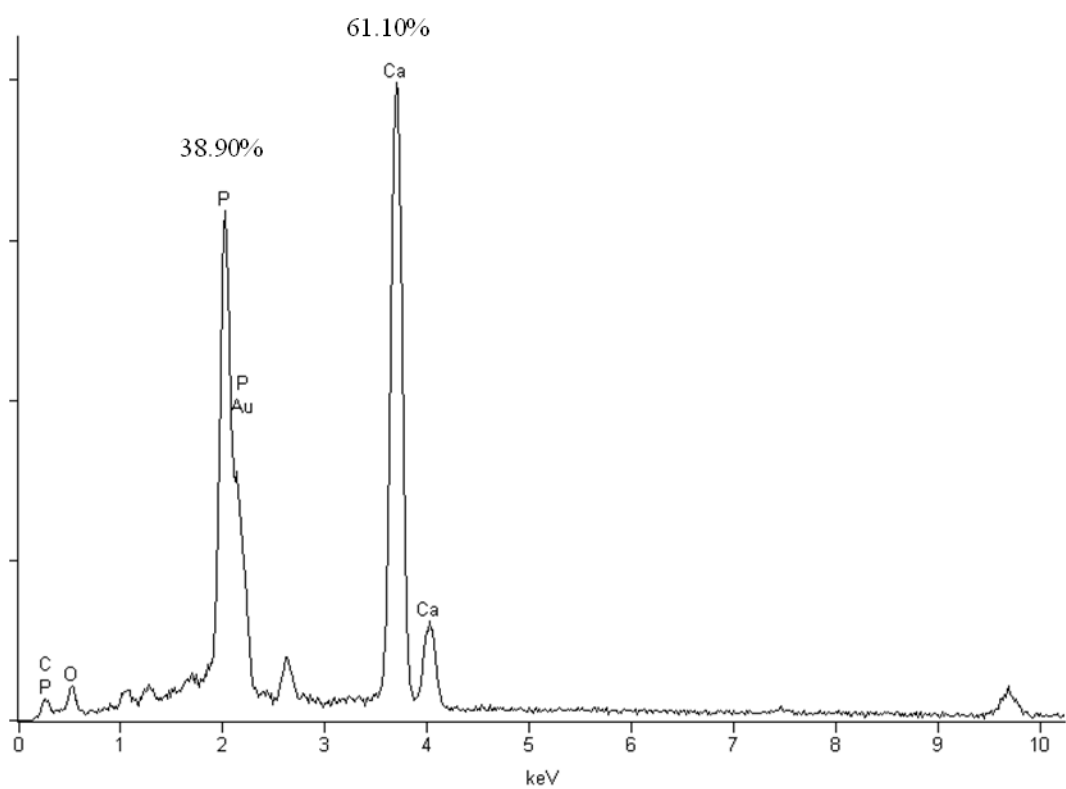


**Figure B.7.** EDX spectrum of alginate coated chitosan scaffold incubated in refreshed SBF solution for 14 d.

## APPENDIX C

### COMPRESSIVE STRESS-STRAIN CURVES OF SCAFFOLDS INCUBATED IN CULTURE MEDIUM

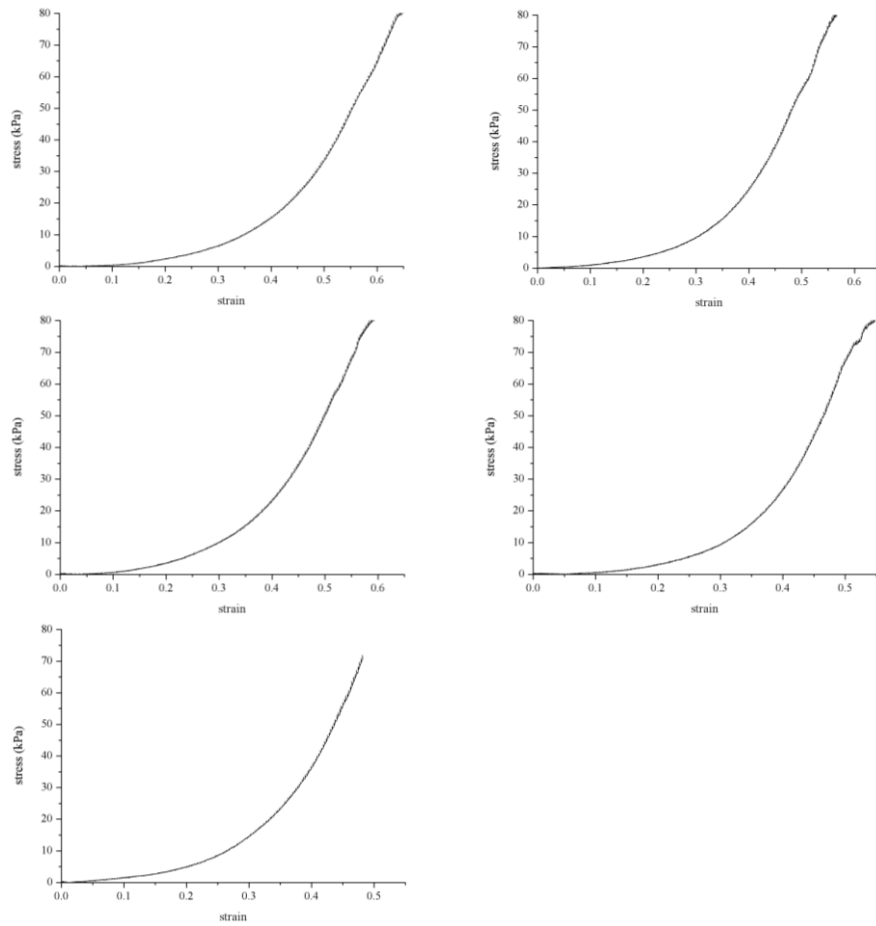


**Figure C.1.** Stress-strain curves of chitosan scaffolds incubated in DMEM, high glucose medium for 24 h.

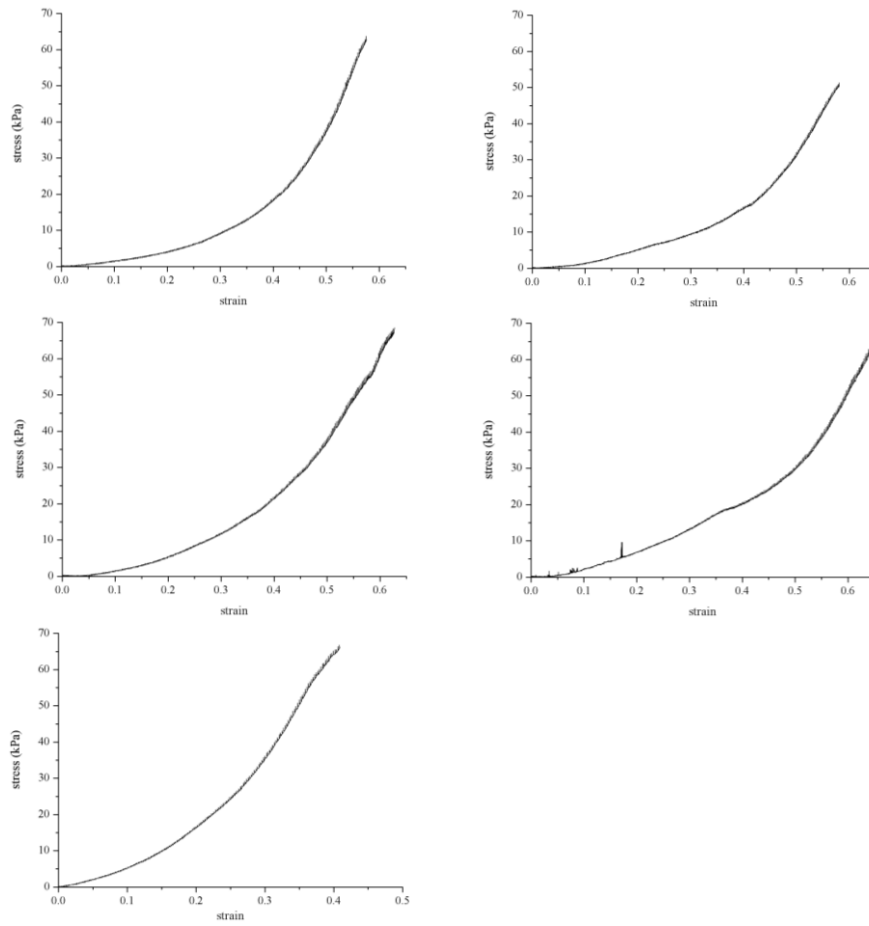


**Figure C.2.** Stress-strain curves of alginate coated chitosan scaffolds incubated in DMEM, high glucose medium for 24 h.

## APPENDIX D

### COMPRESSIVE STRESS-STRAIN CURVES OF SCAFFOLDS INCUBATED IN SBF SOLUTION

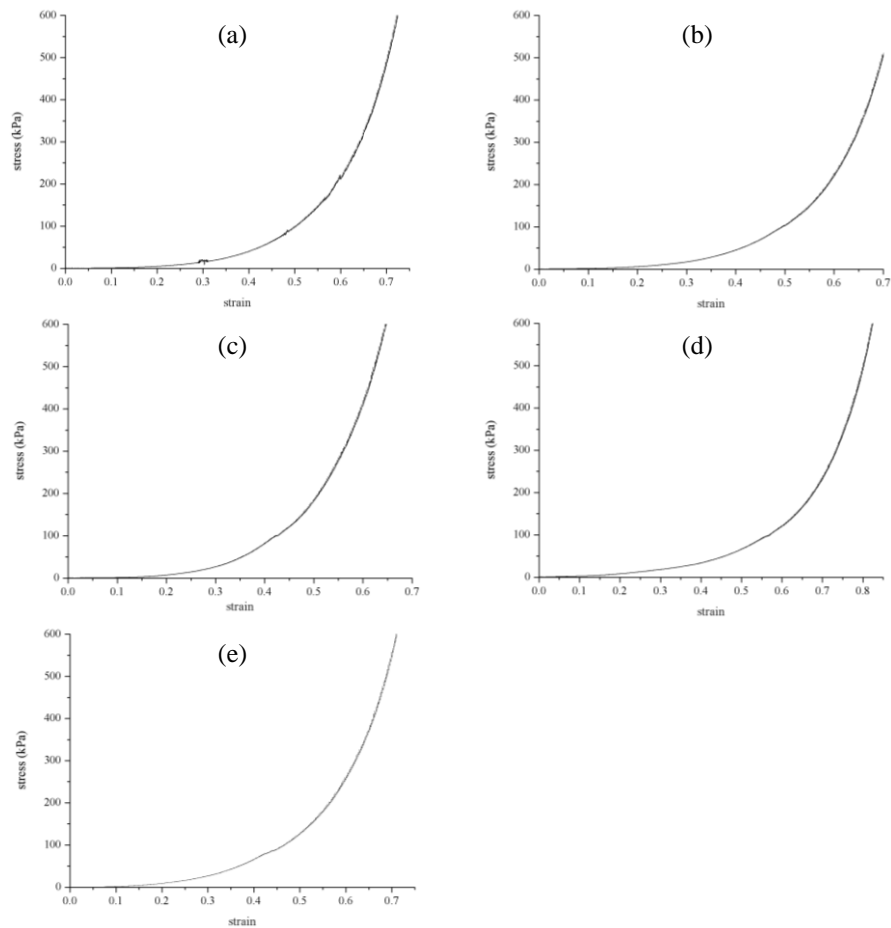


**Figure D.1.** Stress-strain curves of (a,b) chitosan and (c,d,e) alginate coated chitosan scaffolds incubated in SBF-5 solution for 48 h.

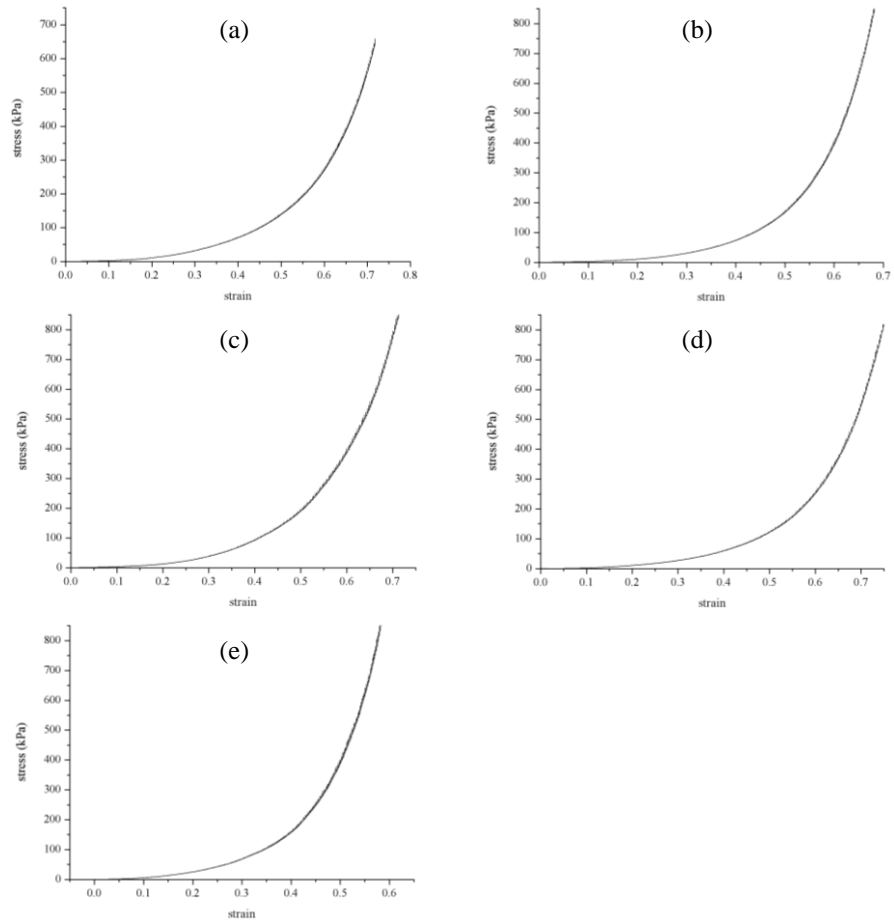


**Figure D.2.** Stress-strain curves of (a,b) chitosan and (c,d,e) alginate coated chitosan scaffolds incubated in SBF solution for 7 d.